SCHOOL OF BIOSCIENCES

TITLE:

Development of inhaled CaSR NAMs for the treatment of pulmonary disorders

DEGREE:

Master of Philosophy (Biosciences)

TIME OF PRESENTATION:

September 2021

AUTHOR:

Petar ASENOV POPOV

TABLE OF CONTENTS

ABBRE*VIA*TIONS

7TMD	Seven transmembrane domain
AA	Amino acid
AAMs	Alternatively activated macrophages (aka M2)
AHR	Airway hyperresponsiveness
AKT	Serine/threonine kinase, aka PKB
AMs	Airway macrophages
ANOVA	Analysis of variance
APC	Antigen-presenting cells
APCs	Antigen-presenting cells
ASC	Apoptosis-associated speck-like protein with a caspase-recruitment domain
ASM	Airway smooth muscle
ASMCs	Airway smooth muscle cells
ATP	Adenosine triphosphate
BCs	Basal cells
BECs	Bronchial epithelial cells
BMD	Bone mineral density
BSA	Bovine serum albumin
Ca^{2+}_i	Intracellular Ca^{2+} ion
Ca^{2+}_o	Extracellular Ca^{2+} ion
cAMP	Cyclic adenosine monophosphate
CaSR	Calcium Sensing receptor
CCP	Calciprotein colloidal particles
CCs	Club cells
CCSP	Club cell secretory protein
CGRP	Calcitonin gene-related peptide
CLR	C-type lectin-like receptor
CNS	Central nervous system
COPD	Chronic obstructive pulmonary disease
COX	Cyclooxygenases
CREB	cAMP-responsive element binding
CRTC	cAMP-regulated transcriptional coactivators
DAG	Diacylglycerol
DAMPs	Danger-associated molecular patterns
DCs	Dendritic cells
DCVs	Dense-core vesicles
DMEM	Dulbecco's modified Eagle's medium
DMSO	Dimethyl sulfoxide
ECD	Extracellular domain
ECM	Extracellular matrix

ECS	Extracellular solution
EGF	Epithelial growth factor
ERK1/2	Extracellular signal-regulated kinases 1/2
FBS	Foetal Bovine Serum
FEV	Functional expiratory volume
FRC	Functional residual capacity
Fura-2AM	Fura-2 Acetoxymethyl
FVC	Functional vital capacity
GABA	Gamma aminobutyric acid
GM-CSF	Granulocyte-macrophage colony-stimulating factor
GPCR	Guanine nucleotide-binding protein-coupled receptor
HAT	Histone acetyltransferase
HBEC	Human bronchial epithelial cells
HDAC	Histone deacetylases
HEK	Human embryonic kidney
HEPES	4-(2-hydroxyethyl)-1-piperazineethanesulfonic acid
HLFs	Human lung fibroblasts
Ig	Immunoglobin
IKK	IκB kinase
IL	Interleukine
ILC2s	T_H2 type innate lymphoid cells
ILD	Inflammatory lung disorders
IP3	Inositol 1,4,5- triphosphate
IPF	Idiopathic pulmonary fibrosis
IRAK-M	IL-1R-associated kinase-M
IκB	Inhibitor of NF-κB
LB	Loading buffer
LDH	Lactate dehydrogenase
M1	Classically- activated macrophages
M2	Alternatively- activated macrophages (aka AAMs)
MAPK	Mitogen-activated protein kinase
MHCII	Major histocompatibility complex II
MLC	Myosin light chain
MMP	Matrix metalloproteinases
mTORC	Mechanistic target of rapamycin complex
NAD	Nicotine adenine dinucleotide
NADH	Nicotine adenine dinucleotide + hydrogen
NADPH	Nicotinamide adenine dinucleotide phosphate
NAMs	Negative allosteric modulators
NCEs	New chemical entities

NEBs	Neuroepithelial bodies
NF-κB	Nuclear factor kappa-light-chain-enhancer of activated B cells
NLR	Nucleotide-binding oligomerisation domain-like receptor
NLRP3	Nucleotide-binding oligomerisation domain-like receptor family protein 3
NO	Nitric Oxide
Nrf	Nuclear factor (erythroid-derived 2)-like 2;
P2YR	Purinergic receptor
PAMPs	Pathogen-associated molecular patterns
PBS	Phosphate buffered saline
PCR	Polymerase chain reaction
PDs	Pulmonary disorders
PGE_2	Prostaglandin E2
PGH_2	Prostaglandin H_2
PHDs	Prolyl hydroxylase domain enzymes
PI	Phosphatidyl-inositol
PI3K	Phosphoinositide 3-kinase
PIP2	Phosphatidylinositol 4,5-bisphosphate
PKA	Protein kinase A
PKB	Protein kinase B
PKC	Protein kinase C
PLA2	Phospholipase A2
PLC	Phospholipase C
PNECs	Pulmonary neuroendocrine cells
PNECs	Pulmonary neuroepithelial cells
PRRs	Pattern-recognition receptors
PTH	Parathyroid hormone
qRT-PCR	Quantitative reverse transcriptase polymerase chain reaction
ROS	Reactive oxygen species
RSC	Rapid solution changer
ST2	Supressor of tumorigenicity 2
STAT	Signal transducers and activators of transcription
TGF-β	Transforming growth factor-beta
T_H2	T helper 2
TJ	Tight junction
TLR	Toll-like receptor
TNF-α	Tumour necrosis factor-alpha
TSLP	Thymic stromal lymphopoietin
UPM	Urban particulate matter
VC	Vehicle control
VFT	Venus-Flytrap-like

ABSTRACT

Asthma, chronic obstructive pulmonary disease (COPD) and idiopathic pulmonary fibrosis (IPF) are worldwide health issues. These are progressive and life-threatening lung diseases associated with chronic coughing, wheezing, difficulty breathing, and predisposing sufferers to severe illness, hospitalisation, and ultimately death. Existing therapies for these conditions offer symptomatic relief, thus reducing disease severity; however, none of the standard-of-care treatments is ubiquitously effective because they do not target the underlying pathology; as such, no treatment alters disease course.

The G protein-coupled Calcium-Sensing receptor (CaSR) was recently implicated in orchestrating inflammatory, hyperresponsive and fibrotic responses in pulmonary disorders (PD). The CaSR is expressed on most healthy lung cells and is overexpressed in cells harvested from patients with PDs (Yarova *et al.* 2015). We have recently demonstrated that CaSR NAMs - negative allosteric modulators (NAM) at the CaSR - have enormous potential as a completely novel treatment of PDs, due to their disease-modifying ability to abolish airway smooth muscle hyperresponsiveness (AHR), as well as reduce airway inflammation and remodelling. Existing CaSR NAMs were initially developed for systemic use. In collaboration with Cardiff University School of Pharmacy, we have employed computer-assisted drug design to identify, synthesise and test novel CaSR NAMs to be delivered topically for PD treatment, herein referred to as New Chemical Entities (NCEs). The goal of this project was thus to identify the most suitable NCE CaSR NAM for further pre-clinical development and clinical *in vivo* testing using safety and efficacy *in vitro* biological assays and conduct a chemical synthesis review to identify which of the NCEs exhibits an optimal lung delivery profile.

The activation of the CaSR in response to extracellular calcium ions (Ca^{2+}_o) leads to an increase in intracellular calcium ion (Ca^{2+}_i) mobilisation. This response is blunted by pre- and co-exposure with CaSR NAMs. We hypothesised that selected NCE CaSR NAM exhibits a safe and potent effect for inhibiting activation of the CaSR. NCE activity was determined by single-cell intracellular Ca^{2+} imaging carried out on HEK-CaSR cells, which are genetically modified to stably express the human CaSR. Short and long-term live-cell imaging and cytotoxicity lactate dehydrogenase (LDH) assays were performed on primary Human Bronchial Epithelial and HEK-CaSR cells. These experiments could determine the most active NCE NAMs, E1 and C4. It was also determined via long-term exposure experiments that these compounds do not directly cause cytotoxicity to Primary Human Bronchial Epithelial cells *in vitro* at concentrations of <10 μM. Owing to their ability to directly target the core of PDs, instead of alle*via*ting symptoms, NCE CaSR NAMs could provide an alternative therapy for treatment-resistant asthma and potentially extend to other pulmonary conditions, such as COPD and IPF.

Keywords: pulmonary disease, Calcium-Sensing Receptor (CaSR), negative allosteric modulators at the CaSR (CaSR NAMs), free ionised calcium (Ca^{2+}), Ca^{2+} imaging, live-cell imaging, cytotoxicity assay, human bronchial epithelial cells (HBECs)

1. INTRODUCTION

1.1. Pulmonary Anatomy and Physiology

The human respiratory system consists of the branching airways of the lungs, contained in the chest cavity, and facilitates gas exchange between the circulatory system and the external environment. The principal role of gas exchange is providing for organism metabolic needs and eliminating carbon dioxide, the main by-product of oxidative energy metabolism. The human respiratory system (***Figure 1***) consists of a conducting zone - the branching airways, and a respiratory zone, which includes the respiratory bronchioles, alveolar ducts, and alveolar sacs. Elastic fibres within the respiratory zone allow the system *elastance*, which antagonises the ability of the lungs to be *compliant* – the proportional change of volume to change in pressure. This proportional and inverse relation allows healthy lungs to return to their pre-inspiratory volumes after respiratory muscles have ceased contracting *via* passive expiration due to the pull elastic fibres have on alveoli and the higher pressure within the air-filled lungs (Neergaard 1929). The conducting airway carries air in and out of the lungs and filters, warms up and humidifies that air, which then enters the respiratory zone through the active contraction of the diaphragm and external intercostal muscles. Through branching, the airway divide 23 times and become progressively smaller, permitting the light 250g organ to have a total surface area of 75 m^2 for adequate gas exchange (Lorenz 1966). The walls of the proximal conducting airway are lined with smooth muscle, submucosal secretory glands, and ciliated pseudostratified columnar epithelial cells, acting as an effective host defence mechanism for the lungs, protecting against various environmental insults (Crystal *et al*. 2008). The smooth muscle regulates airway diameter, altering resistance and airflow by parasympathetic and sympathetic innervation (Canning and Fischer 2001). The airway epithelium, anchored to the reticular basement membrane, consists of bronchial epithelial cells (BECs), which can be classified into a ciliated, goblet (expressing *MUC5B* and *MUC5AC*), basal and club cells (CCs), tuft cells, ionocytes and neuroendocrine cells (PNECs). Secretory submucosal glands and goblet cells produce mucin glycoproteins to form a moisturising mucin layer, mobilised towards the pharynx by ciliated epithelial cells that uniformly beat towards the pharynx.

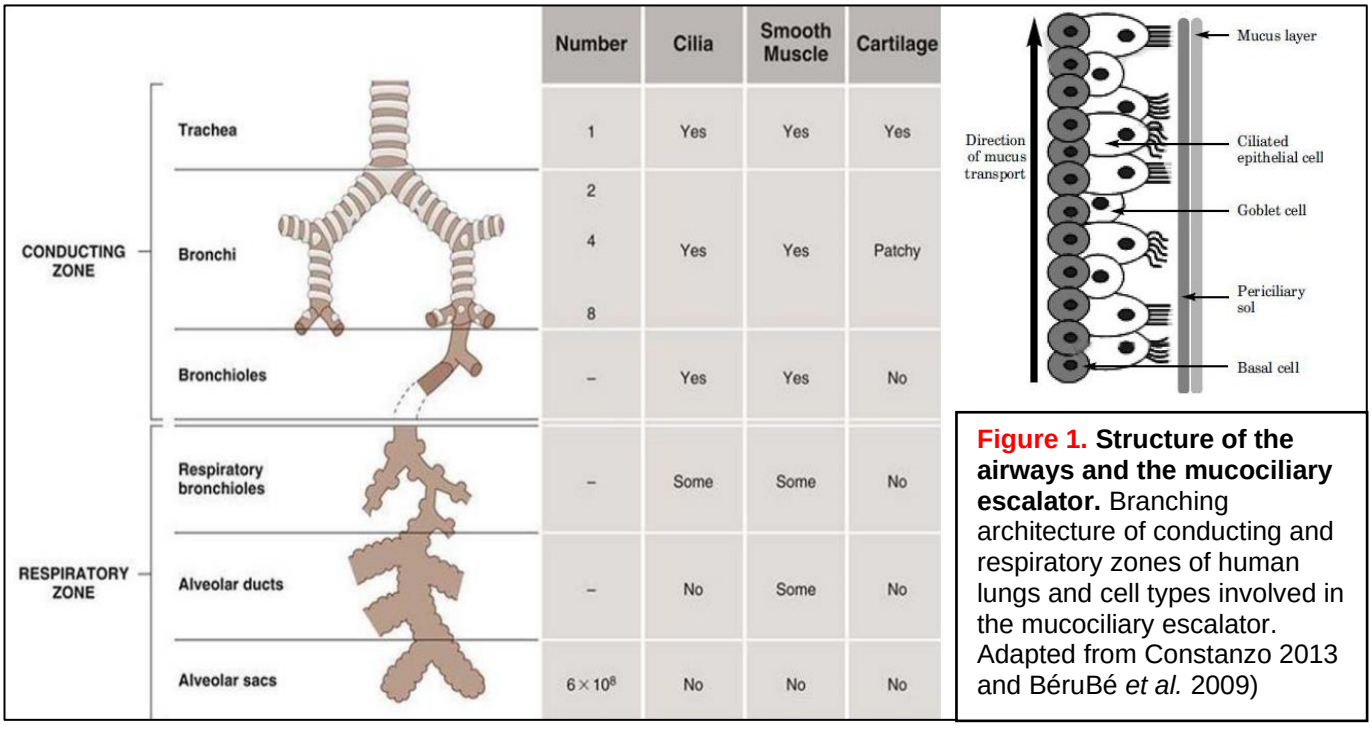

Figure 1. Structure of the airways and the mucociliary escalator. Branching architecture of conducting and respiratory zones of human lungs and cell types involved in the mucociliary escalator. Adapted from Constanzo 2013 and BéruBé *et al.* 2009)

This mucociliary escalator **(*Figure 1)*** propels excess material or contaminations out of the airway and into the gastrointestinal tract. BECs, pseudostratified in the upper airway, become more columnar and cuboidal towards the small airway, where basal, submucosal glands and goblet cell numbers decrease, but present are non-mucous secretory CCs.

The respiratory zone (parenchyma) consists of bronchioles, alveolar ducts, and pouch-like invaginations called alveoli, surrounded by a stromal endothelial capillary plexus (Hsia et al. 2016). Type I alveolar epithelial cells are thin, simple squamous cells attached to the reticular basement membrane, which share a collagen type IV-rich (Yurchenco 2010), fused basal lamina with endothelial capillary cells, allowing for gas exchange through simple diffusion between these units. Type II alveolar epithelial cells synthesise pulmonary surfactant that reduces the high surface tension within alveoli and act as progenitor cells to renew and repair type I alveolar cells (Barkauskas *et al*. 2013). The space in between is the interstitium. It contains the extracellular matrix (ECM) of elastic and collagen fibres and resident cells like lung fibroblasts (HLF) that secrete ECM and maintain the shape of alveolar sacs. HLFs also serve as bridges *via* cytoskeletal interdigitations through gaps in the basal epithelial lamina between type I and II alveolar cells, directly linking them with endothelial capillary cells, allowing for resident and adaptive immune cellular migration (Sirianni *et al.* 2003). There are no ciliated cells in the distal respiratory zone **(*Figure 2*)**, which is why the zone is also populated by resident innate alveolar macrophages (AMs) that phagocyte invaders and debris and migrate to the conducting zone and mucociliary escalator. AMs and dendritic cells (DCs) constantly sample and internalise their environment *via* CaSR-dependent and -independent constitutive micropinocytosis, allowing continuous capture of antigens, which are processed and presented to the adaptive immune system (Canton *et al*. 2016).

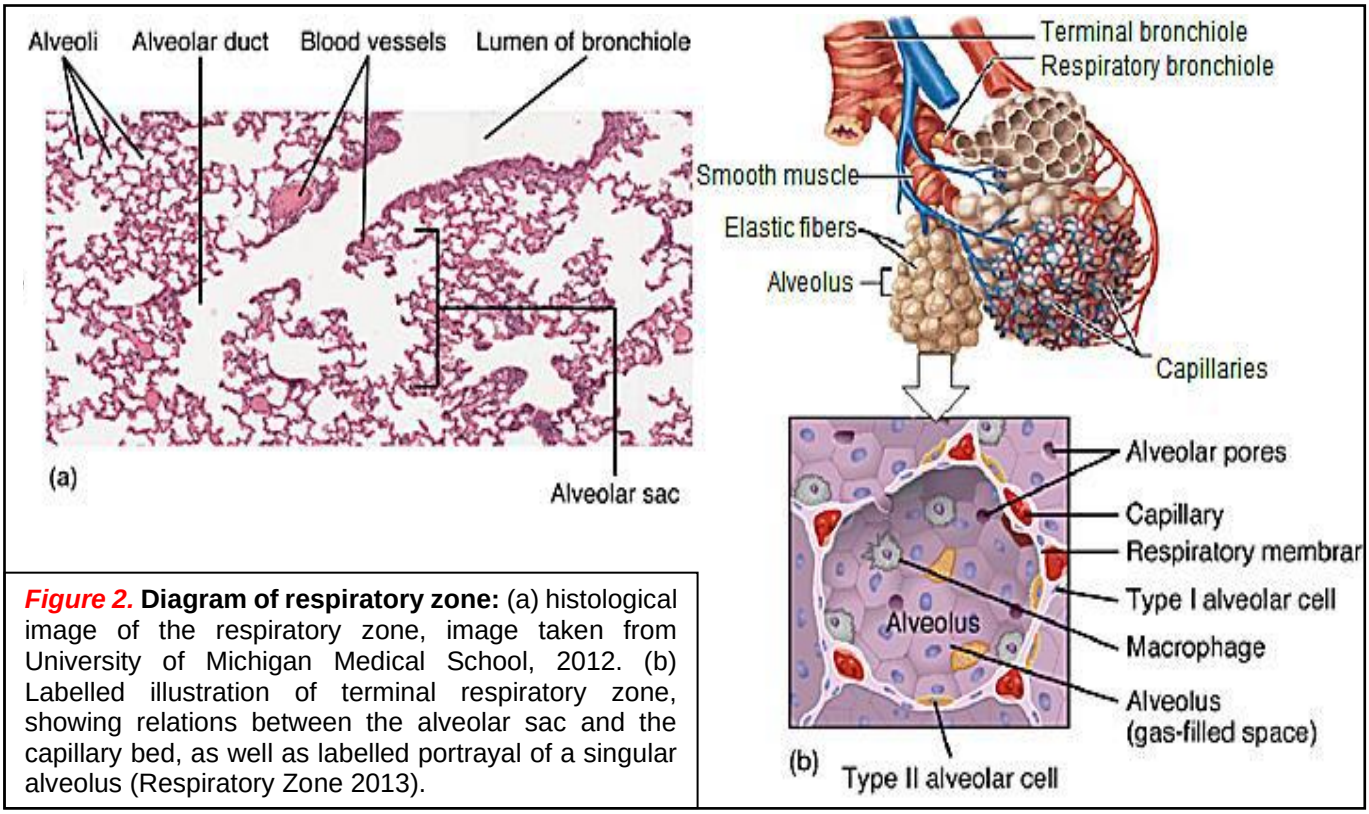

Figure 2. **Diagram of respiratory zone:** (a) histological image of the respiratory zone, image taken from University of Michigan Medical School, 2012. (b) Labelled illustration of terminal respiratory zone, showing relations between the alveolar sac and the capillary bed, as well as labelled portrayal of a singular alveolus (Respiratory Zone 2013).

Cells secrete cytokines (small, soluble proteins) to modulate inflammation, which are the non-specific, physiological responses to danger-associated molecular patterns (DAMPs) and structurally variable agonists, allergens, pathogens, toxins, and irritants (pathogen-associated molecular patterns (PAMPs). Pattern-recognition receptor (PRR)-expressing cells, like leukocytes (innate or adaptive immune cells), BECs, endothelial and other stromal cell types, detect such signals and initiate inflammatory and subsequent repair responses. Such PRRs include but are not limited to scavenger, Toll-like (TLR), nucleotide-binding oligomerisation domain-like (NLR), absent in melanoma 2-like, retinoic acid-inducible gene-I-like, C-type lectin-like (CLR) and the calcium-sensing receptor (CaSR) (Rossol *et al*. 2012). AMs **(*Figure 3*)** are the first innate immune cell type to encounter foreign particles, whereby their activity is regulated by mechanistic target of rapamycin complex 1 (mTORC1) and by cytokine granulocyte-macrophage colony-stimulating factor (GM-CSF). AMs aim to eliminate foreign particles and apoptotic cells *via* phagocytosis and efferocytosis, after which they migrate towards the conducting zone to be expelled by the mucociliary escalator. Phagocytosis causes AMs to suppress pro-inflammatory cytokines, chemokines (cytokines that coordinate leukocyte trafficking and activation), and leukotrienes by the secretion of transforming growth factor β1 (TGF-β1), prostaglandin E2 (PGE_2), and platelet-activating factor (Fadok *et al*. 1998). Aerobic glycolysis is induced in classically-activated (M1) macrophages, increasing M1 macrophage glucose uptake and converting pyruvate to lactate. M1 macrophages activate the pentose phosphate pathway, critical for generating NADPH, an electron donor essential for reduction-oxidation (redox) homeostasis and biosynthesis of oxidase. In M2, alternatively activated macrophages (AAMs), arginase-1 (Arg1) pathway is carried out, where L-ornithine is converted by ornithine decarboxylase to putrescine, which is then converted by spermidine synthase and spermine synthase to spermidine and spermine, respectively (Hussell and Bell 2014).

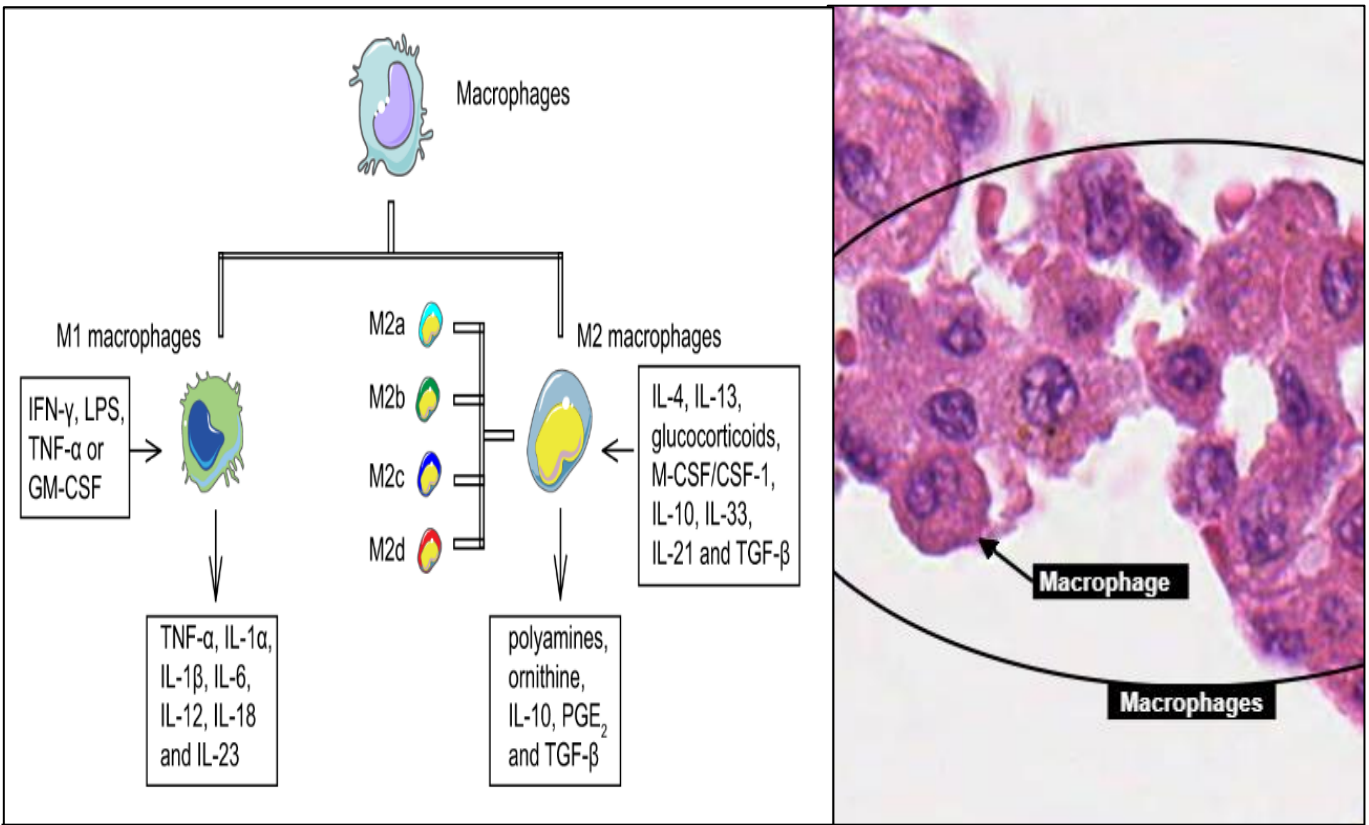

Figure 3. **AM categories, factors upregulating them and their primary secretions;** H&E section of normal human lung, macrophage colony and cell (The Human Protein Atlas 2019); adapted from Duan and Luo 2021.

The primary cells damaged by infection and inflammation in the lung are epithelial cells (Crystal et al. 2008). Following inflammation or infection resolution, barrier integrity and epithelial tissue must be restored to the standard architecture. The lung exhibits extraordinary regenerative qualities under normal wound healing conditions, carried out by the various lung stem cell and progenitor niches. Basal cells and CCs serve as progenitor cells, participate in xenobiotic metabolism, and regulate the pulmonary immune system. The primary secretion of CCs is uteroglobin (also known as blastokinin or club cell secretory protein, CCSP) and glycoproteins, lipids, and proteins providing chemical and physical protection for both pulmonary surfactant and small airway (Roth et al. 2013). CCs have a protective role by metabolising inhaled toxins using cytochrome P450 in their smooth endoplasmic reticulum. This metabolism destroys CCs as early as 24 hours after the action of a harmful factor, but due to their stem-cell niche with NEBs, CCs are rebuilt after approximately 30 days (Roth *et al*. 2013). PNECs are intrapulmonary sensors acting as part of the diffuse neuroendocrine system. PNECs are present as individual cells but are predominantly located at bifurcation points in human lung bronchioles, forming clusters called neuroepithelial bodies (NEBs) **(*Figure 4*)**. CN X vagal nerve fibres mainly innervate NEBs from cell bodies in the brainstem and the nodose ganglion, communicating pulmonary chemosensing and respiratory stretch (Adriaensen *et al*. 1998). Several vagal nerves interact with NEBs, including Na/K, ATPase, vesicular glutamate transporters, calbindin-D (28k) or P2X2/3 nerves (Adriaensen *et al*. 2006). These myelinated afferent nerves lose their myelin sheaths next to NEBs, then branch and protrude into the epithelium. Unmyelinated non-vagal calcitonin gene-related peptide (CGRP) nerve fibres originating from dorsal root ganglia from thoracic vertebrae T1 to T6 contact the basal pole of pulmonary NEBs. PNECs express and secrete 5-HT in response to hypoxia in a Ca^{2+}-mediated, dose-dependent way (Lauweryns *et al*. 1977).

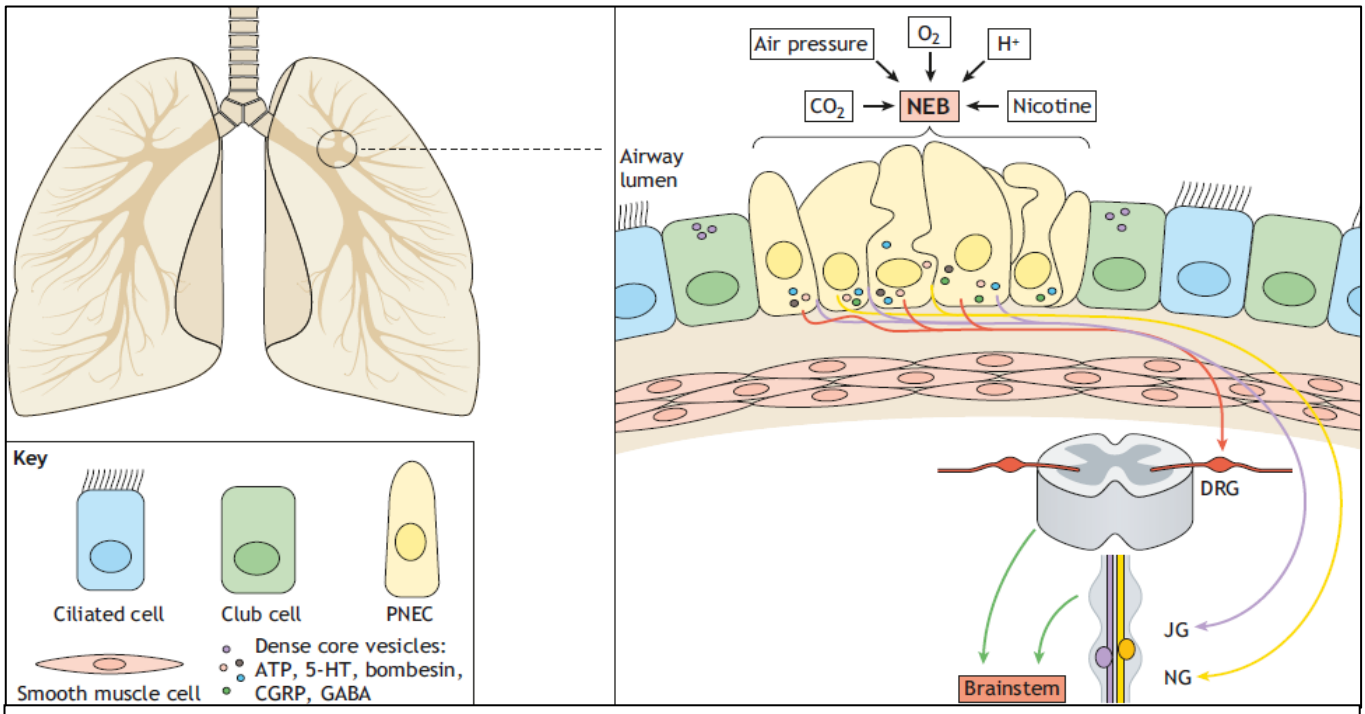

Figure 4. **Pulmonary neuroendocrine cells (PNECs), neuroepithelial bodies (NEBs) and their innervation.** In the mammalian lung, PNECs cluster at airway bifurcation sites (circled), forming NEBs, innervated by vagus (CN X) myelinated afferent nerves fibres (yellow and purple) and unmyelinated non-vagal immunoreactive nerve fibres (orange). NEBs can sense changes in mechanical forces and chemo stimuli like CO2, air pressure, O2, H^+ ions and nicotine, signal this information to the brainstem, and activate reactions. ATP, adenosine triphosphate; CGRP, calcitonin gene-related peptide; GABA, gamma-aminobutyric acid; JG, jugular ganglion; NG, nodose ganglion; 5-HT, serotonin. (Noguchi *et al.* 2020).

1.2. Pulmonary pathophysiology

Pulmonary disorders (PDs) like asthma, chronic obstructive pulmonary disorder (COPD) and idiopathic pulmonary fibrosis (IPF) are global health problems and leading causes of premature death and suffering (Marciniuk *et al.* 2017). COPD and asthma are generally underpinned by chronic inflammation of the lungs, leading to chronic airway remodelling, and asthma is characterised by airway hyperresponsiveness (AHR). Existing therapies only target symptoms, as disease aetiology is not fully understood; however, it is known that repeated exposure to stimuli such as allergens (Hernández-Ramírez *et al.* 2020), pollutants (Matthews *et al.* 2016), and viruses (Wark *et al.* 2001) are the primary risk factors for PD exacerbation. Current treatments for COPD and asthma include corticosteroids to reduce airway inflammation and bronchodilators to increase airway diameter by relaxing constricted ASM cells (ASMCs). Chronic oral corticosteroid use can lead to corticosteroid resistance and complications such as growth suppression in children, osteoporosis, hyperglycaemia, and pancreatitis. Chronic corticosteroid use can also cause haematologic, immunologic, adrenal, or hepatic insufficiencies (Buchman 2001) and increased prevalence of pneumonia in COPD patients (Niederman 2018). No currently existing treatment directly targets the hallmark of asthma, AHR (Corrigan 2020). In addition, the aetiology of COPD and IPF is presently unknown. Thus, there is an urgent need for novel therapeutics addressing the root cause of PDs.

The airway epithelium in the conducting and respiratory zone plays an essential frontline role in immune response regulations against exogenous stimuli (Vareille *et al.* 2011). Injured or apoptotic cells release cellular components into extracellular space – DAMPs, like ATP or Ca^{2+}_{o} (Rossol *et al.* 2012), but also reactive oxygen species (ROS), enzymes, protease inhibitors, permeable peptides, recruiting the innate immune system **(Figure 5)**.

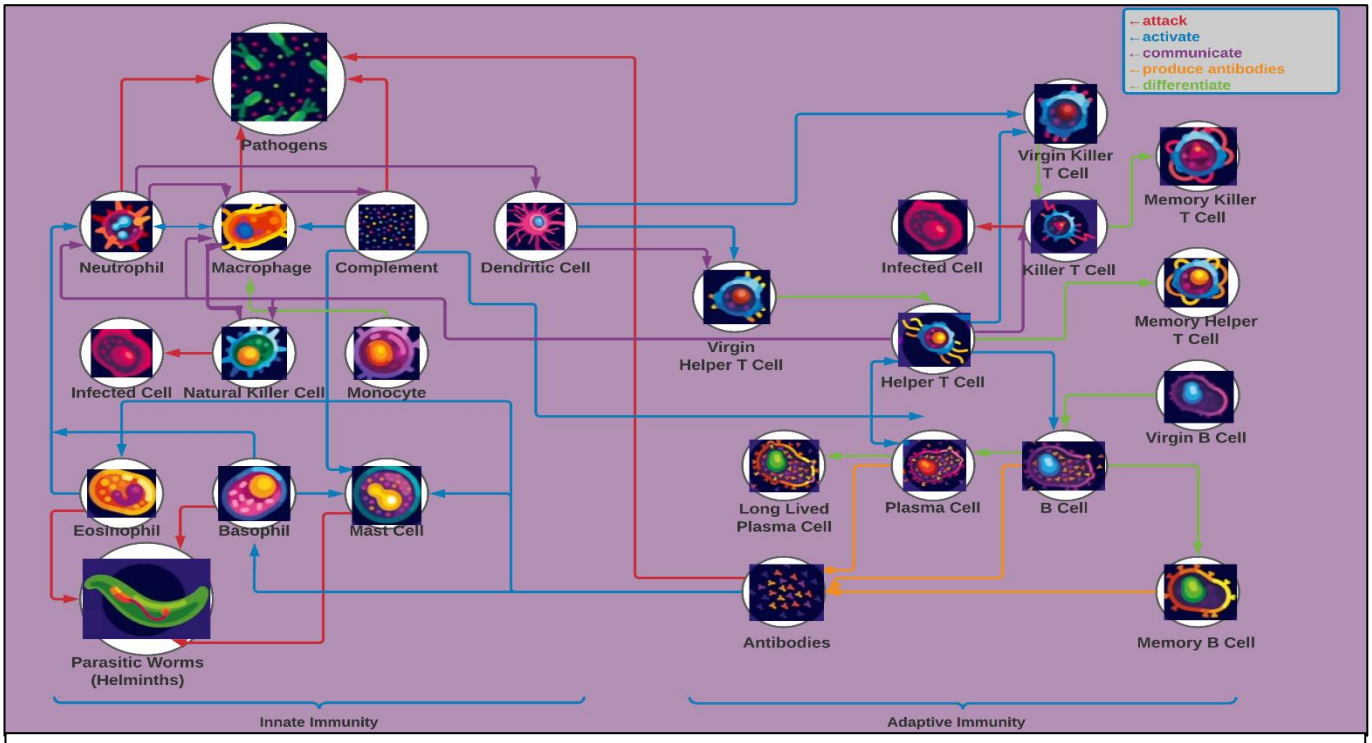

Figure 5. **Diagrammatic simplification of immune cell types, their activity and coordination.** The first line of defence against pathogens are innate immune cells like macrophages, eosinophils and neutrophils. These attack the invading cells, however incomplete removal of hostile cells calls for the adaptive immune system via the activation of different cell types by APCs. Adapted from Dettmer 2021.

AMs are responsible for most pro-inflammatory cytokines and chemokines, including IL-1β, IL-6, IFNs, IL-8, TNFα, NO, CCL5, GM-CSF, macrophage inflammatory protein, and others (Kolli *et al*. 2014). The primary antigen-presenting cells (APCs) that are crucial for the induction of adaptive immune responses are AMs and mature dendritic cells (DCs), the primary antigen-presenting cells (APCs). DCs cooperate with other activated APC granulocytes (Tang *et al.* 2010) *via* major histocompatibility complex II (MHCII) to present antigens to naïve T-cells within lymph nodes. Antigen presentation leads to T-cell differentiation into effector leukocyte T helper (T_H2) cells (Yoshimoto *et al.* 2009), promoting immunoglobin (Ig)E from B helper cells and driving inflammation *via* cytokine release of IL-13 and IL-5 (Venkayya *et al.* 2002). The human Ig(E) antibody cross-links to and upregulates the expression of the high-affinity Fcε receptor on antigen-presenting cells (APC) granulocytes like basophils and mast cells, activating them (Yamaguchi *et al.* 1997). Secretion of alarmins, neuropeptides (GABA, CGRP, substance P, bombesin) and lipids (prostaglandins and leukotrienes) can directly activate Type 2 innate lymphoid cells (ILC2s) towards inflammatory ST-2-expressing ILC2s, which produce high levels of T_H2 type cytokines like IL-4, IL-5, IL-9, IL-13 and GM-CSF. Pro-inflammatory T_H2 cells and ILC2 migrate to the site of infection to mediate immune responses *via* lysis of damaged cells, following exocytosis of granules containing perforin and granzyme from cytotoxic T cells and by TNF receptor family-dependent apoptosis/phagocytosis following recognition of these cells by antibodies (Licona-Limón et al. 2013).

Congenital or acquired defective macrophage phagocytosis is a hallmark of PDs, like asthma (Huynh *et al*. 2005), COPD (Hodge *et al*. 2003) and IPF (Morimoto *et al*. 2012), which defective phagocytosis might promote imbalanced oxidative/antioxidative processes. While irritancy or barrier dysfunction persists, pro-inflammatory signals continue and further damage the epithelium; thus, the repair process is integral to resolving inflammation. As seen in **Figure 6**, DAMP- and PAMP- mediated PRR activation is facilitated through TLRs, TNFs, GPCRs, NLRs and CLRs that activate nuclear transcription factor NF-κB, MAP kinases and IFNγ response priming immune system NOD-like receptor family protein 3 (NLRP3) inflammasome (Coll *et al*. 2016). Critical in the immune response is OX40, a TNF transmembrane protein that binds to adaptor proteins tumour necrosis factor receptor-associated factor (TRAF) 2,3 and 5, priming the inflammasome by activating the NF-κB1 pathway through signalling cascades PI3K (PI-3-kinase)/PKB (protein kinase B/Akt) (Baum *et al*. 1994). Canonically this priming step is followed by a second signal, initiating NLRP3 oligomerisation, which through its adapter molecule ASC (apoptosis-associated speck-like protein with a caspase-recruitment domain) causes dimerisation of caspase-1 and caspase-8, activating them. Active caspases are essential in the recruitment of neutrophils and the secretion of inflammatory cytokines *via* inducing the proteolytic expression of IL-1β and cytokine IL-18 (Yeretssian *et al*. 2008), as well as cleavage of Gasdermin-D, causing pyroptosis (LaRock and Cookson 2013). NLRP3 activation *via* lymphocyte activating factor IL-1 receptor (IL-1R) activation polarises AMs towards pro-inflammatory functions and facilitates the recruitment of further immunomodulatory cells involved in injury. IL-1R signalling function within epithelial and immune cells leads to the upregulated secretion of alarmins – IL-33, Thymic stromal lymphopoietin (TSLP) and IL-25 (Saenz *et al.* 2008), GM-CSF (Guilliams *et al*. 2013), and TNF-α.

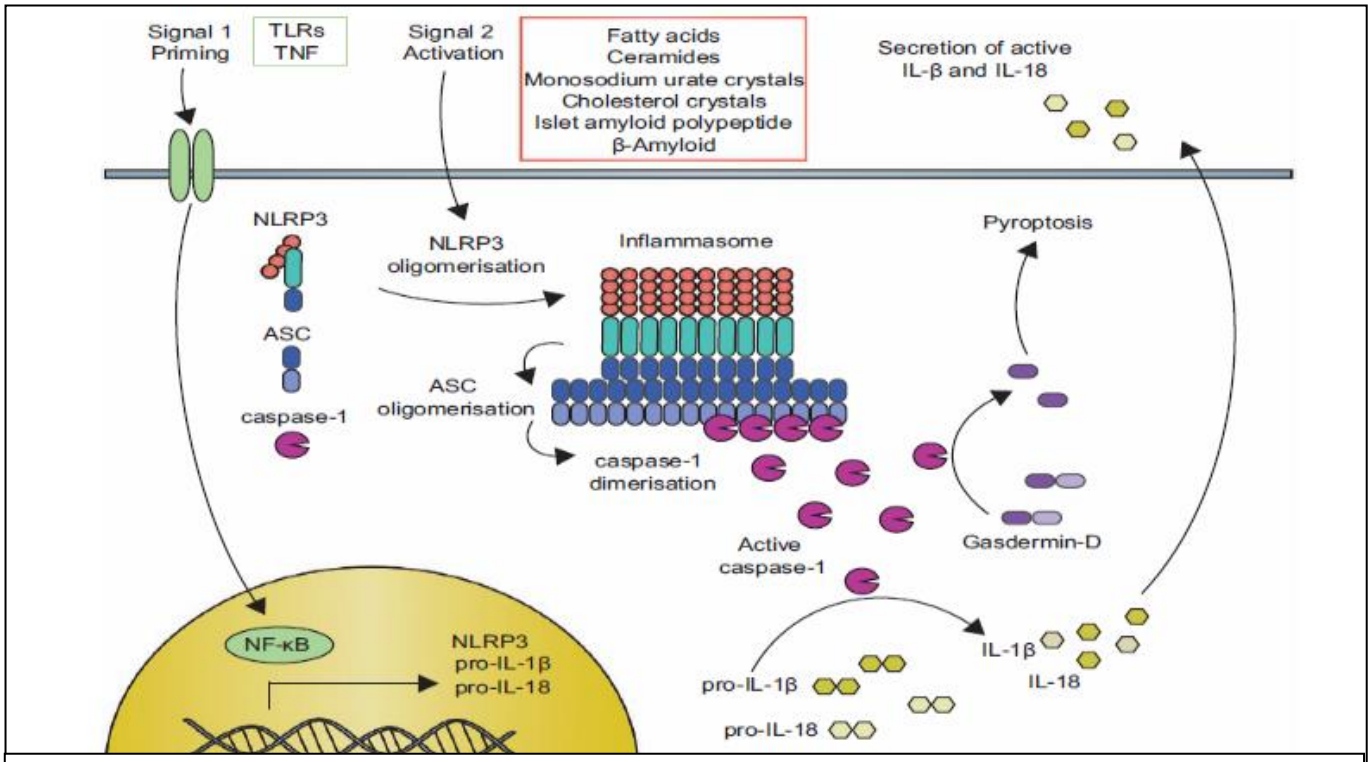

Figure 6. **The canonical NLRP3 inflammasome signalling pathway**. Canonical NLRP3 inflammasome requires a priming signal, such as toll-like receptor or TNF receptor activation, that activates NF-κB, inducing NLRP3 and pro-IL-1β transcription and modification. A second NLRP3-specific activation then initiates NLRP3 oligomerization and causes the apoptosis-associated speck-like protein with a caspase-recruitment domain (ASC) to form large prion-like oligomers. ASC dimerizes caspase-1, activating it, which then goes on to processes pro-IL-1β and pro-IL-18 and secrete their active mature forms. **Figure** from Coll *et al.* 2016.

1.3. Asthma

Over 340 million people worldwide have asthma, a chronic PD associated with wheezing, shortness of breath (dyspnea), chest tightness, and coughing. The fundamental abnormality associated with asthma is the altered immune system response to allergens, AHR to seemingly benign stimuli, such as cold air, urban particulate matter (UPM) or exercise, constricting the airway, reducing airway diameter and thus increasing resistance. AHR is defined as lowering the threshold for responsiveness to external stimuli and the ease of narrowing the airway *via* ASM constriction response to bronchoconstrictive challenges (Brannan and Lougheed 2012). ASM cell constricting forces and the elasticity of the parenchyma are the primary driving factors for airway diameter regulation. Eosinophilic infiltration causes major basic protein release, driving allergic asthma inflammatory remodelling (Boulet *et al.* 2000) and is correlated with AHR (Kay 2005). Inflammation, by causing swelling of the airway lining with oedema, dramatically amplifies the obstruction caused by a given degree of smooth muscle contraction (Yarova *et al*. 2021). New blood vessel creation (neoangiogenesis) and vasodilation occur in areas of persistent inflammation, allowing further inflammatory cell infiltration ASMCs and HLF migration to the airway and distal lung tissues. ***Figure 7*** presents the remodelling of the asthmatic airway, characterised by: epithelial barrier dysfunction (Heijink *et al.* 2020); smooth muscle hypertrophy and hyperplasia (Johnson *et al.* 2001); sub-mucosal gland and goblet cell hypertrophy/hyperplasia (Ordoñez *et al.* 2001), and irreversible reduction of lumen size due to reticular basement membrane fibrosis *via* deposition of type I, III, V and VI collagen, instead of type IV (Palmans *et al.* 2002).

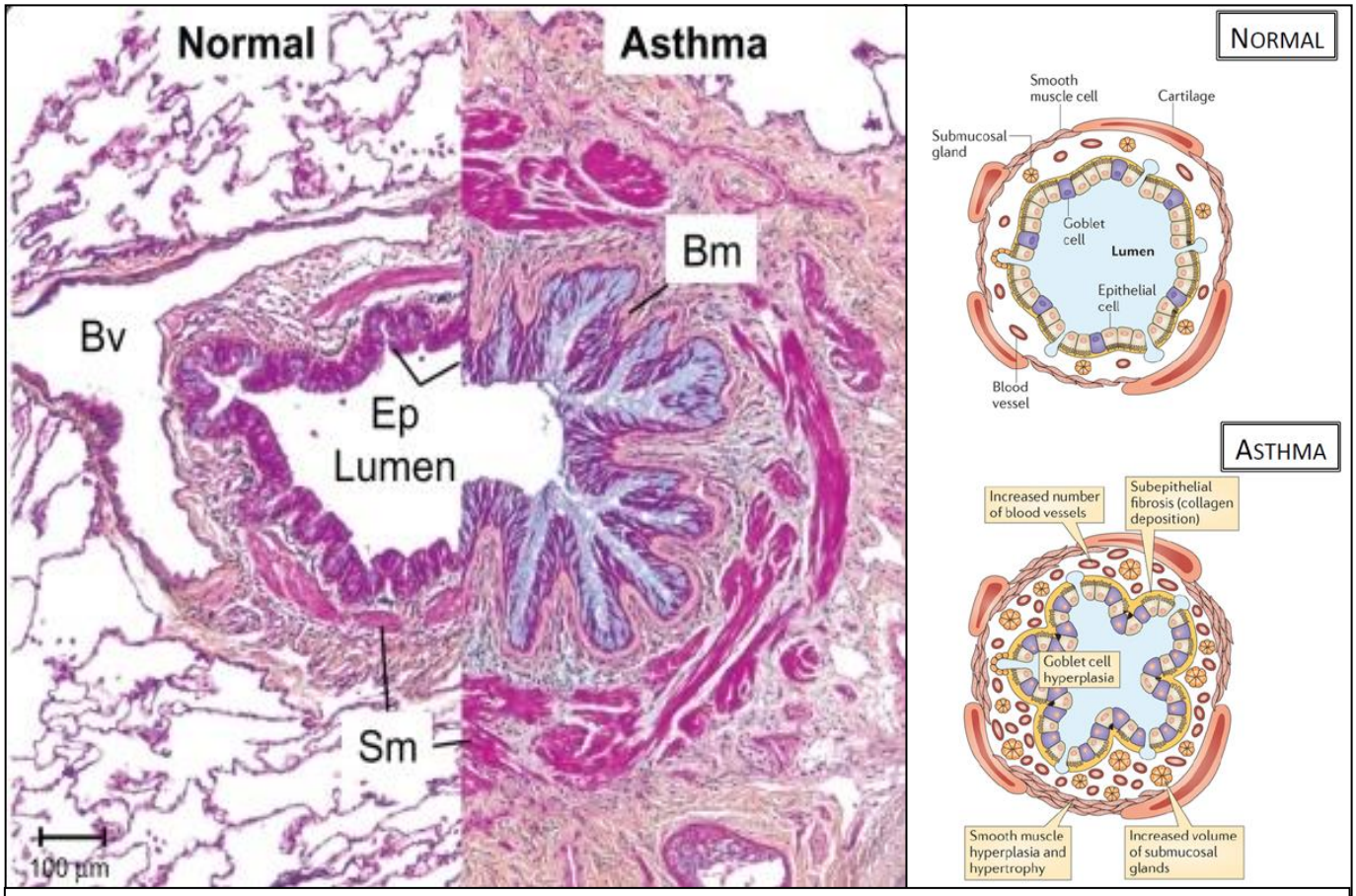

Figure 7. **Asthma airway structural remodelling.** Movat's pentachrome stain of normal and severely asthmatic lungs, showing smooth muscle (Sm) volume increase, mucous hyperplasia and hypersecretion (blue), significant basement membrane (Bm) thickening, changes supported by neoangeogenesis; (Wadsworth *et al.* 2011).

Central to cell death and inflammation in asthma is the lymphocyte activating factor IL-1 receptor (IL-1R) (Monie and Bryant 2015), which can be activated by canonical and direct (Gaidt and Hornung 2017) inflammasome activation that drives alarmin secretion ***(Figure 8)***. IL-1β and IL-1α have overlapping roles directed at T_H2 cells differentiation for immune response hyperactivation and allergic airway inflammation in the asthma model (Qi *et al*. 2016). TGF-β, which correlates with PD severity (Hung et al. 2018), is a major fibrotic cytokine that promotes ECM deposition by HLFs and is a crucial mediator of allergen-driven eosinophil recruitment to the lung (Saito *et al*. 2018). TGF-β is directly controlled by the epithelial alarmins – IL-33 (Denney *et al*. 2015), TSLP (Cai *et al*. 2019) and IL-25 (Gregory *et al*. 2012). HLFs are responsible for tissue repair and wound healing; however, in PD, inflammatory signalling pathways cause HLFs to deposit pathologic ECM protein of collagen I, fibronectin, laminins, and others, which promote cell adhesion and airway remodelling (Scaffidi *et al.* 2001). Additionally, asthmatic HLFs are hyperproliferative and transform into myofibroblasts (Johnson *et al.* 2006). Indeed, TGF-β is the most potent inducer of these α-SMA-expressing myofibroblasts, which cause subepithelial fibrosis *via* cytoskeletal contraction of surrounding ECM (Fernandes *et al*. 2006) and production of collagen I, III, IV and V (Hinz 2007) and thus lead to collagenosis. The number of myofibroblasts is increased in the lung parenchyma of asthmatics (Boser *et al*. 2017). Eosinophils, in turn, drive pulmonary fibrosis *via* further upregulation of TGF-β and platelet-derived growth factors, further inducing myofibroblasts, thus increasing contractility, migration and proliferation of ASMCs (Kardas *et al*. 2020).

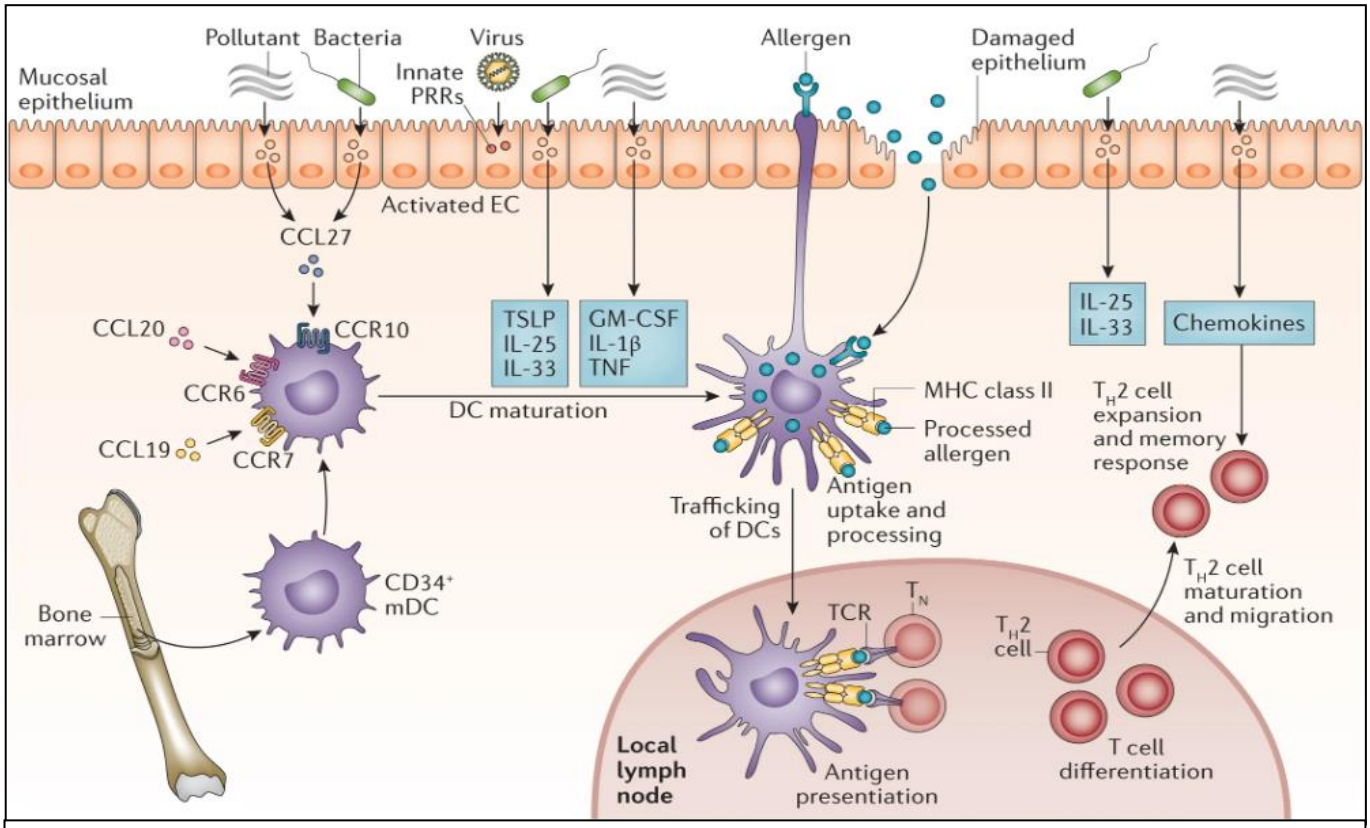

Figure 8. ***Alarmin-induced airway inflammation and remodelling.*** DAMPs and PAMPs cause BECs to secrete alarmins (IL-33/TSLP/IL-25), releasing T_H2-type cytokines (IL-4/IL-5/IL-13) from ILC2s, promote T_H2-type T cell development, local switching of B cells/plasma cells to IgE production. Image from (Corrigan 2020).

IL-25 activity, promoted at least partially through TGF-β family signalling molecule activin A (Gregory *et al.* 2012), increased alarmin secretion of IL-33 and TSLP, resulting in increased lung eosinophilic and T_H2 cell recruitment and increased secretion of IL-4, IL-5 and IL-13. IL-25 activity results in goblet cell hyperplasia, mucous hyperproduction, neoangiogenesis and fibroblast collagen deposition (Gregory *et al.* 2012), as well as inflammation-independent AHR (Ballantyne *et al.* 2007). The alarmin IL-33 drives inflammation as it binds to the suppression of tumorigenicity 2 (ST2) receptor-expressing cells, activating T_H2 cells, ILC2s, DCs, basophils and mast cells *via* mitogen-activated protein kinases (MAPK) and NF-κB pathways (Schmitz *et al.* 2005). IL-33 directly promotes HLF activity (Schmitz *et al.* 2005), recruits further granulocytes to the inflammation site, and causes these cells to upregulate secretion of pro-inflammatory factors IL-1β (Cho *et al.* 2012), IL-4, IL-5, IL-9, IL-13, and TNF-α cytokines. TLR4- (Hammad *et al.* 2009) and TLR2- (Lv *et al.* 2018) dependent epithelial-derived TSLP secretion has been reported to induce the expression of OX40 ligand in dendritic cells (DCs), driving T_H2 cell differentiation, inhibiting anti-inflammatory IL-10 secretion and promoting TNF-α production (Ito *et al*. 2005). Cytokine IL-4 is primarily secreted by activated basophils (van Panhuys *et al.* 2011) and is a crucial mediator of eosinophilic infiltration (Cohn *et al.* 1998), alternative activation macrophages. It also prompts local B lymphocyte cells to secrete immunoglobin (Ig)E (Coffman *et al.* 1988). IL-9 (Temann *et al.* 1998) and IL-5 (Louahed *et al.* 2001) synergistically promote eosinophilic infiltration and mast cell hyperplasia, respectively, and IL-13 (upregulated by alarmin IL-25) promotes mucous hypersecretion and AHR (Walter *et al.* 2001). Thus, the chronic overreaction of asthmatic lungs to irritants and stimuli stands upstream of alarmin release, leading to the pathophysiological outcomes associated with asthma ***(Figure 9).***

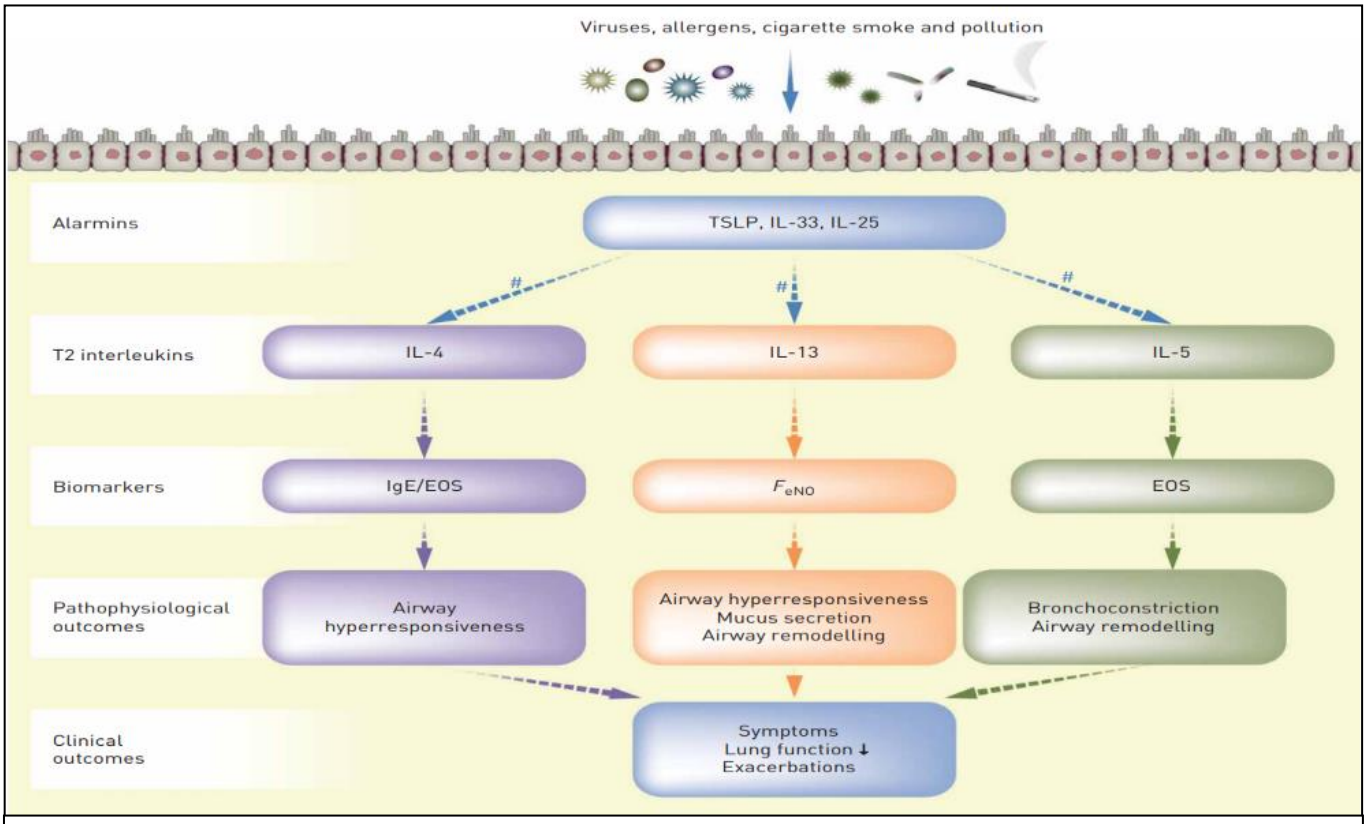

Figure 9. **Alarmins in type 2 inflammation, their clinical biomarkers and pathophysiological implications in asthma.** #: upregulated, EOS: eosinophils, F_{eNO}: fractional exhaled nitric oxide. (Porsbjerg *et al.* 2020)

1.3.1. Current treatment options

The gold standard treatment of chronic asthma is the combination of daily inhaled corticosteroids with long-acting bronchodilators. Inhaled treatments are potent and fast-acting, causing minor systemic side effects compared to orally delivered treatments. In the most severe cases, chronic high inhaled glucocorticoid doses are combined with oral glucocorticoids and sometimes with a third modifier like anti-IgE, anti-leukotriene agents, or theophylline. Even combination therapies become ineffective in asthma cases with distal pulmonary inflammation, extensive ECM remodelling, and glucocorticoid receptor mutations (caused by long-term medication use) (Fraga Righetti 2014). Hernandez et al. in 2015 presented a therapeutic attempt to block multiple cytokines upstream in the overall cascade, such as blocking the IL-1 receptor through its antagonist (anakinra), which was shown to be effective in reducing IL1β, IL-6 and IL-8 levels significantly and had no serious adverse effects. However, as summarised by Porsbjerg *et al.* 2020, currently available biological therapies are anti-immunoglobulin (Ig)E, anti-IL-5, anti-IL-5Rα and anti-IL-4Rα monoclonal antibodies (blocking the IL-4 and IL-13 pathways), which decrease exacerbation rates in study populations by only 50%. No currently existing treatment directly targets AHR, and ten % of people with asthma do not respond to corticosteroids. Corticosteroids reduce asthma symptoms not by targeting AHR but by reducing infiltration of the airway with inflammatory cells, reducing oedema and swelling of the airway mucosa, and enhancing the effects of bronchodilators, thus increasing airway diameter (Corrigan 2020). Asthma pathogenesis is underpinned by a dysbalance of the ratio of all pathways involved. Due to the immense number of different cytokines involved and the redundancy between them, blocking individual or multiple asthma-related pathways would lead to unsatisfactory results.

1.3.2. The role of calcium in asthma

Elevated [Ca^{2+}_i] in the lung is a fundamental aspect of airway smooth muscle asthma pathophysiology and is responsible for enhanced bronchoconstriction and long-term effects that result in airway remodelling and ECM component deposition (Yarova *et al.* 2015). In allergic asthma, irritants such as smoke, viruses and allergens cause the release of eosinophilic polycations, which bind to and activate the CaSR on pulmonary cells, increasing Ca^{2+}_i mobilisation (Quinn et al. 1997, Yarova *et al.* 2015). NLRP3 has also been shown not to require priming, whereby activation of G-protein (guanine nucleotide-binding protein)-coupled GPRC6A and Calcium-Sensing Receptor (activated by Ca^{2+}_o, polyamines and other ligands) directly activate the NLRP inflammasome *via* the phosphatidyl-inositol (PI)/Ca^{2+} pathway (Rossol *et al.* 2012). Our group, led by Professor Riccardi, has shown that activation of the CaSR leads to inflammatory-independent AHR in asthma, which in turn promotes CaSR overexpression and overactivation, driving the pathogenesis of airway inflammation and remodelling, shown in pre-clinical models of PDs (Yarova *et al.* 2015). Using murine asthma surrogates and cultured human asthmatic smooth muscle cells, we have recently presented evidence consistent with the hypothesis that AHR in human asthma reflects an abnormal expression of the CaSR. Small molecule CaSR negative allosteric modulators (NAMs) safely abolish AHR and airway inflammation (Yarova *et al.* 2015, Yarova *et al.* 2020).

1.4. Chronic Obstructive Pulmonary Disorder (COPD)

COPD is not a disorder of the smooth muscle but is a combination of two conditions – chronic bronchitis and emphysema. According to World Health Organisation, in 2019 3.23 million people died from COPD, making it the third most common cause of death worldwide (Marciniuk et al. 2017). Cigarette smoking is the most prevalent reason – 80-85% of COPD cases are smoking-related; however, only 15-25% of all smokers develop the disease. Thus, a genetic predisposition, like α1-antitrypsin deficiency (Carrell and Lomas 2002), or epigenetic changes, must be driving COPD development. The remaining cases are occupational exposure to coal dust, cadmium, pollution and biomass burning (Diette et al. 2012). Emphysema is a disorder in which alveoli have become partially unattached by the destruction of the alveolar septa, leading to permanent enlargement of the airspaces (Taraseviciene-Stewart 2006). Radial traction of bronchioles becomes reduced due to loss of elastic recoil, restricting alveolar expansion and decreasing O_2 saturation of haemoglobin during the pulmonary cycle. There are two types of emphysema: 95% of cases are centracinar, involving the central/proximal acini parts, and panacinar – destruction involves the lower lobes of respiratory bronchioles and is usually characteristic of patients with α1-antitrypsin deficiency (Carrell and Lomas 2002). The symptoms of emphysema are dyspnea, cough, hypoxemia, hypercapnia and cor pulmonale. Emphysema is also associated with increased mucus production, which, coupled with air entrapment and hyperinflation, ultimately causes an increase in Functional Residual Capacity (FRC) and a decrease in Functional Vital Capacity (FVC) (Lee et al. 2007). Dynamic compression occurs when intrathoracic pressure is greater than alveolar pressure due to a collapse of the bronchial wall, increasing airway resistance and altering standard lung mechanics (Robins 1983). Pulmonary capillaries are lost, there is altered compliance of the lungs, and a loss of elasticity, all of which cause hypoventilation and hypercapnia.

Chronic bronchitis is a chronic inflammation of the bronchial wall by environmental irritants or infection. Mucus is accumulated in the airway by the hypertrophy of mucous glands and excessive production of viscous mucous, thus highly increasing resistance within the airway. Cilia become unable to move, thus immobilising the "mucous escalator" (Hogg and Timens 2009). As well as the obvious pulmonary difficulties caused by mucous, this environment is also prime grounds for further secondary infection by bacteria. The combined effects of chronic bronchitis (bronchial oedema, mucosal hypersecretion and bacterial colonisation of the airway) and emphysema (destruction of the alveolar septa and loss of elastic recoil of bronchial walls) cause airway obstruction, air entrapment within alveoli, and a loss of surface for gas exchange ***(Figure 10)***. Irreversible airspace enlargement distal to the terminal bronchiole *via* the alveolar septal structures destruction leads to loss of elastic recoil, making the respiratory system more compliant, turning exhalation into an active process. COPD manifests in abnormal inflammatory responses within the lungs to xenobiotics. Irritants cause the release of growth factors by resident epithelial cells, such as TGF-β and fibroblast growth factor, which lead to fibroblast proliferation and subsequent airway diameter reduction through fibrosis and inflammation (Oliveira *et al.* 2015).

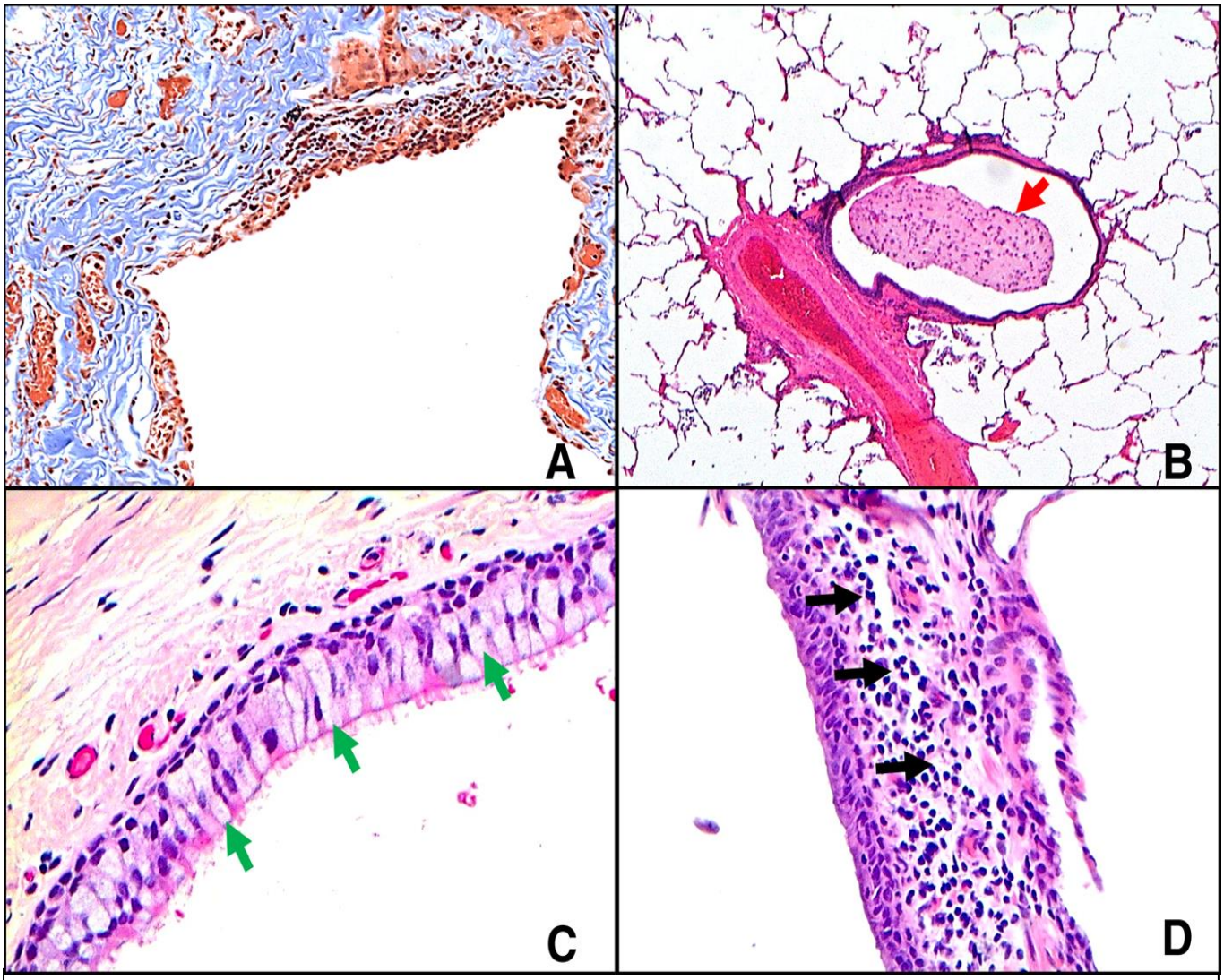

Figure 10. **COPD histological slides of small airway disease. (A)** Masson's trichrome (10X) slide of aberrant wound repair and fibrotic remodelling with resulting thickened airway wall and excessive collagen bundle deposition (blue). **(B, C and D)** H&E stains of terminal bronchiole and endothelial capillary vessel, red arrow points to intra-luminal mucous plug (2X), green arrows pointing to increased goblet cells in airway mucosa (20X), and black arrows indicate the increased inflammatory cell count in COPD patient bronchiole. Adapted from (Higham *et al*. 2019)

Upregulation of many pro-inflammatory genes is caused by the overexpression of NF-κB, brought about by the degradation of its inhibitor, IκBα. IκBα degradation allows NF-κB to reach the nuclei of cells and change gene transcription, upregulating macrophage and neutrophil proteolytic functions. NF-κB activity inhibits protease repair mechanisms in a transcriptional cascade, leading to disease progression (Oliveira *et al.* 2015). There is a clear dose-response relationship between the amount smoked and the decline in respiratory and systemic function, especially in patients diagnosed with COPD (Esquivel *et al.* 2014, Kamiide *et al.* 2015, Krüger *et al.* 2015). Smoking has been long correlated with an increase in goblet cells in the distal human airway and a reduction in club cells (Lumsden *et al*. 1984), whereby the sputum of smokers has higher quantities of NF-κB than that of non-smokers (Caramori 2003) due to increased IκBα degradation.

Macrophages and neutrophils contribute to the overall oxidative imbalance by forcing epithelial apoptosis through reactive oxygen species release and inactivating tissue inhibitors of metalloproteinases (TIMPS) and α-1 antitrypsin (Oliveira *et al.* 2015). Matrix metalloproteinases (MMPs) and α-1 antitrypsin are involved in the degradation of collagen and elastin, meaning that lowered expression of their inhibitors allows the increased activity of these proteinases. A driving factor for COPD progression is oxidative damage to Nuclear factor (erythroid-derived 2)-like 2 (Nrf2), responsible for cellular antioxidant activity (Jaiswal 2004), causing a disbalance that leads to oxidative damage to histone deacetylase 2 (HDAC2) complex. HDAC2 carries out defensive anti-inflammatory responses, the degradation of which leads to corticosteroid resistance and disease progression (Adenuga *et al.* 2010).

Macrophage activation causes the release of proinflammatory cytokines and chemokines that force an influx of more macrophage cells within the respiratory zone (Oliveira *et al.* 2015). Degradation leaves behind cytokine-secreting apoptotic cell fragments, causing an influx of more inflammatory cells. These inflammatory infiltrates attempt to perform their phagocytotic function and carry the fragments to the mucociliary escalator within the conducting airway. Still, with increased proteolytic expression and defective phagocytosis, as seen in COPD, macrophages further damage the area in a continuous self-feeding cycle (Oliveira *et al.* 2015). Inflammation induces goblet cell hyperplasia and damages the mucociliary "escalator" *via* ciliated cell death, reducing the overall beat of ciliated cells, causing the inability to outflow the highly increased mucous produced, which further reduces airway diameter through mucous plugging (BéruBé *et al.* 2009). Thus, implying an auto-immune component to the disease, with defence mechanism cells causing damage instead (Lee *et al.* 2007), (Taraseviciene-Stewart *et al.* 2006). Thus, COPD pathophysiology (**Figure 11**) consists of inflammation, mucous plugging, and apoptosis of epithelial and endothelial pulmonary cells, followed by abnormal repair, which presents as airway fibrotic remodelling, alveolar destruction and airspace enlargement. Such conditions cause the respiratory system to become increasingly compliant due to loss of elasticity, reducing surface area for gas exchange, and increasing the prevalence of comorbidities, like pneumonia and other acute exacerbations.

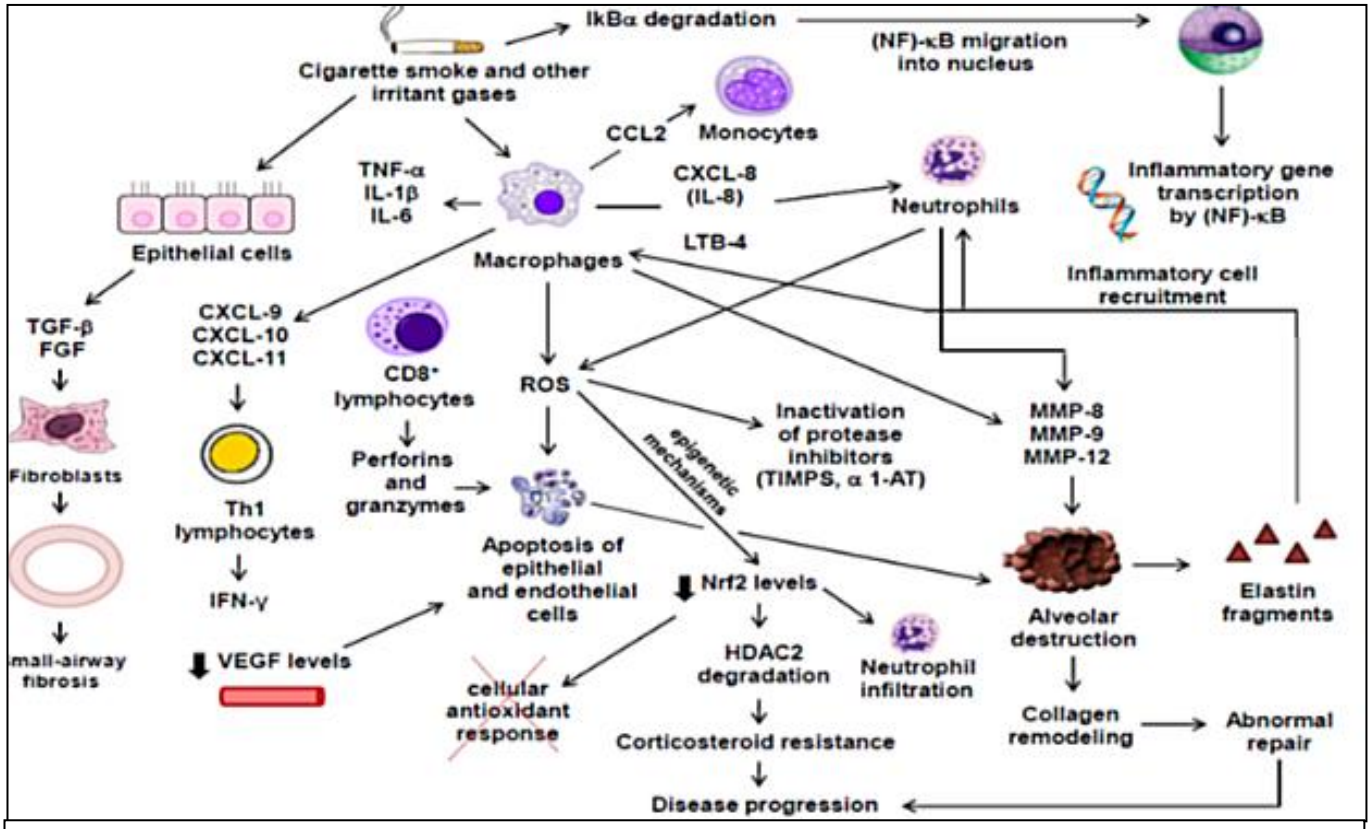

Figure 11. **COPD Pathophysiology.** IkBα -inhibitory protein κBα, NF-κB, factor nuclear kappa B, CXCL and microtubule-associated protein 1 light chain 3lc – chemokines; MMP – matrix metalloproteinases, TIMPS – tissue inhibitors of metalloproteinases, ROS – reactive oxidative species, HDAC2 – histone deacetylase-2; IFN-γ – interferon gamma; IL-1β – interleukin 1β; IL-6 – interleukin 6; LTB-4 – leukotriene B4; Nrf – nuclear factor (erythroid-derived 2)-like 2; TGF-β – transforming growth factor beta, TNF-α – tumour necrosis factor- alpha; VEGF – vascular endothelial growth factor. **Figure** from (Oliveira *et al*. 2015).

1.4.1. Current treatment options

COPD is confirmed by a history check and spirometry - if FEV1:FVC < 70%; if FEV1 <80%, and if FEV1 is more reduced than FVC, there is insufficient delivery of O_2 to working tissues. Smoking cessation is the only proven disease-modifying intervention; however, as summarised by Riley and Sciurba in 2019, short-acting Bronchodilators like β2-Agonists (salbutamol and terbutaline) that relax smooth muscle and Anti-Cholinergic Drugs (ipratropium), which block bronchoconstriction, provide temporary relief. Long-acting Bronchodilators, like β2-Agonists and Anti-Cholinergic drugs, have greater affinity & slower rate of dissociation and combination Inhalers (Symbicort), which are long-acting β2-Agonists with corticosteroids, offer a 30% reduction in exacerbations (Cazzola and Donner 2000). Oral medications like methylxanthines (theophylline) offer cAMP stimulation of β-adrenoreceptors (Barr et al. 2003); PDE-4 inhibitors (roflumilast) offer exacerbation reduction (Vlahos and Bozinovski 2014), and mucolytics (N-acetylcysteine) reduce mucus viscosity and can also reduce exacerbations (Sadowska et al. 2006). CaSR NAM NPS2143 decreased mucous overproduction in cigarette smoke extract-stimulated human lung cells. The NAM significantly reduced the expression of MUC5AC, MMP-9 and proinflammatory cytokines such as IL-6 and TNF- α (Lee *et al*. 2016). CaSR NAM NPS89636 attenuated inflammation in the guinea pig COPD model by inhaling lipopolysaccharide, specifically leukocyte and neutrophil infiltration within LPS-treated animals (Yarova *et al*. 2016). CaSR NAM treatment also reduced interstitial wall thickening, suggesting that this drug class represents a novel treatment option for COPD.

1.5. Idiopathic Pulmonary Fibrosis (IPF)

Chronic interstitial disease is brought about by an imbalance of inflammation and repair that results in fibrosis, reducing the compliance and volume of the lungs. Common symptoms include shortness and rapidity of breath, crackling at the end of a breath, acute exacerbations (like asthma attacks) and eventually cyanosis. Risk factors include smoking, pollutants, particle exposure, viral infections, and genetic predispositions to IPF, where 3-20% of cases are thought to be familial (ATS 2000). An imbalance of profibrotic and antifibrotic mediators is a hallmark of IPF: during the healing process, excess ECM is deposited. Particles, viruses and irritants cause the activation of the immune response. As long as the irritant remains, the inflammatory process continues. Occupational fibrotic diseases (Silicosis siderosis, coal worker's pneumoconiosis) are driven by dust particles that macrophages cannot digest, causing them to necrose and release pro-fibrotic enzymes (Zhang et al. 2018). Myofibroblasts are the central fibrotic cells, and their persistent activation causes fibre deposition. The honeycomb cysts form from the excessive alveolar type 2 mutant/stressed cells that aggregate together, a situation exacerbated by potential excess mucous and fibrous deposition (Sgalla *et al*. 2018). Damage to the distal respiratory epithelium typically results in the surfactant-producing alveolar type 2 cells renewing and replacing the lost alveolar type 1 cells, the respiratory cells (Barkausus and Noble 2014). Telomere-related loss of alveolar type 2 cells' ability to repair and maintain alveolar structure leads to their proliferation and dysfunctional differentiation to goblet cells, leading to a positive feedback loop that maintains a TGF-β-induced chronic irregular lung wound healing (Camelo et al. 2014). In ineffective healing, chronic irritation causes disease progression in IPF patients, progressively increasing lung hypoxia and mechanical stiffness, causing NEBs to over-proliferate, secrete pro-fibrotic factors, and direct club cells in their niche to differentiate into goblet cells (Wolffs *et al*. 2020). Additionally, a viral infection can enhance IPF symptoms and presentation, augmenting the fibrotic response in established IPF (McMilan *et al.* 2008). Mutations affecting the telomerase or the length of telomeres have been shown to cause early epithelial stem cell senescence, reducing the ability of the epithelia to repair. Cronkite *et al.* 2008 found that 25% of sporadic and 37% of IPF patients possessed telomere lengths below the tenth percentile. Armanios *et al.* 2007 found that 8% of subjects had mutations in essential telomerase genes. *TERT/TERC* mutations can cause shortened telomeres, which means earlier cell death and more repair and aberrance. *SP-A* and *SP-C* mutations alter surfactant properties, making alveolar collapse more likely and affecting gas exchange. *MUC5B* single nucleotide polymorphisms cause an increase in mucous production. Polymorphisms in most cytokines and profibrotic molecules like TGF- β1 and MMPs can also cause PF.

An FEV-FVC ratio greater than 80% indicates PF. Less air is expelled quickly due to the reduced compliance of the lungs, making inspiration more challenging. Other lung function tests, like exercise stress tests or arterial blood gas tests, can monitor the efficacy of the lungs. Echocardiograms can detect an increased pressure in the right side of the heart, indicating lung deficiency. X-rays can show fibrosis in some cases, though not those in earlier stages of IPF. High-resolution CT scans ***(Figure 12)*** can determine severity through the diffusing capacity of CO_2 and the degree of fibrosis (Lynch *et al.* 2005). Biopsies may also be used, although Hunninghake *et al.* (2001) describe their use only as necessary should imaging and clinical results fail to be conclusive.

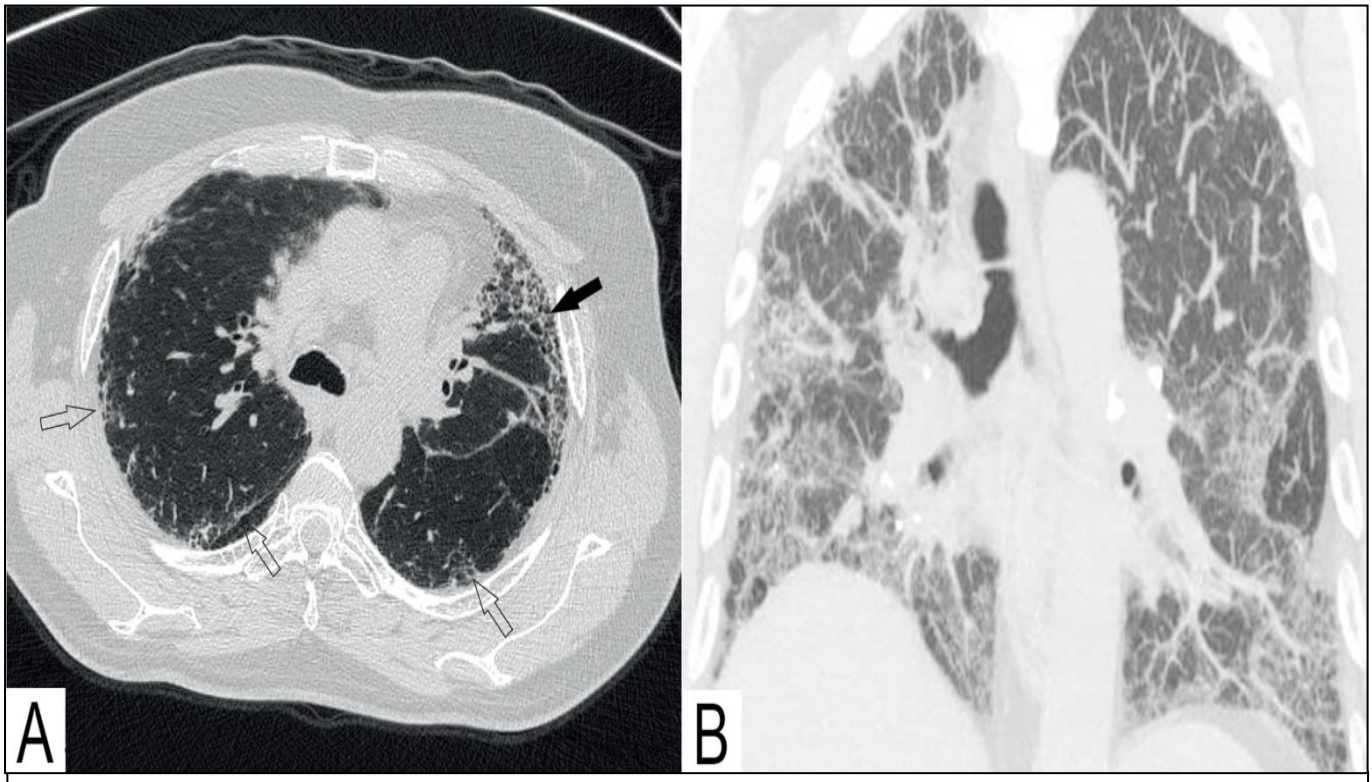

Figure 12. **CT scan of IPF showcasing usual interstitial pneumonia-pattern**. Axial section **(A)** showcases lung remodelling and fibrosis (no-fill arrows) and distal lung honeycombing (black arrows) and coronal section **(B)** contains characteristic heterogenous fibrosis, as well as the lung base honeycombing. Images adapted from (Hart *et al*. 2016) and (Smith *et al*. 2013).

1.5.1 Current treatment options

Oxygen therapy and pulmonary rehabilitation can treat all forms of PF. Oxygen therapy can augment the low oxygen concentrations in the blood even over 15 hours a day, but this can be restrictive despite its apparent efficacy. Rehabilitation can build up the diaphragm and accessory respiratory muscles to be more efficient and use available oxygen. Transplantation is partially effective, with median survival being 4.5 years (Kistler *et al.* 2014).

Prednisolone was used as a reference agent in a study by Oku *et al.* 2008**,** where it failed to suppress IPF induced with bleomycin in mice. It suppresses inflammatory oedema and several inflammatory cytokines; however, the mice bleomycin model has been criticised as it does not cause progressive fibrosis. Additionally, mice do not express as many goblet cells as humans (Izbicki *et al.* 2002). Azathioprine, an immunosuppressant, was more successful when administered with prednisolone in a randomised, double-blind placebo-controlled trial. Few side effects were reported, and 43% vs 77% of patients died in the nine-year follow-up period. However, the results were not statistically significant, becoming marginally significant when adjusted for age (Raghu *et al.* 1991). Cases have been reported where Azathioprine caused pneumonia (Bir *et al.* 2006; Ishida *et al.* 2012). N-acetylcysteine (an anti-oxidant) was used in a study by Meyer *et al.* 1994 for IPF treatment and was found to be somewhat effective at augmenting lost anti-oxidants in the lungs (glutathione), potentially augmenting pulmonary anti-oxidant protection. None are very effective, as 50% of those diagnosed with IPF die within three years. Most commonly used in a trio, these three drugs are responsible for increased mortality, hospitalisation and severe adverse events (IPF Clinical Research Network 2012).

Pirfenidone, a broad-spectrum antifibrotic agent, is under clinical trials for treating IPF. A meta-analysis of Pirfenidone clinical studies has indicated a three-year survival benefit in 73% of patients that did not discontinue treatment (Margaritopoulos *et al*. 2018), indicating that pirfenidone is likely more effective than current treatments.

Nintedanib, an intracellular inhibitor of several tyrosine kinases that target growth factor receptors (VEGF, FGF, PDGF), has been used in the clinic, whereby the highest dose given to patients reduced their FVC decline, as well as reduced acute exacerbations (Raghu *et al.* 2015, Sgalla *et al*. 2018).

Ortiz *et al.* in 2003 used stem cells in a bleomycin model of injury to decrease collagen deposition, fibrosis and MMP levels. Sueblinvong *et al.* 2008 demonstrated that stem cells could express lung epithelial markers following injection into animal disease models, an avenue to restore lung architecture. Spilatieri *et al.* 2012 were able to do the same and use the cells to recover IPF induced with silica in a murine model, as found by increased weight, lung function, survivability and reduction in inflammatory and fibrotic markers. Acute hypoxia preconditioning was shown by Lan *et al.* in 2015 to increase the survival rate of engrafted MSCs by promoting the expression of genes for pro-survival, reducing inflammation and programmed cell death, and allowing the implanted cells to exert therapeutic effects in a bleomycin model of IPF.

As there is an observed reduction in SIRT3 expression in the lungs of IPF patients, a study was recently conducted in an aged mice model of IPF. Exogenous restitutions of SIRT3 levels were carried out through inhaled delivery, which reversed the persistent fibrotic phenotype via a FOXO3A-dependent mechanism in this model (Rehan *et al*. 2021).

The focus of this study is the class C G-protein coupled CaSR, whereby it has been noted in the literature that GPCR signalling promotes profibrotic signalling through $G\alpha_{i/o}$, $G\alpha_{q/11}$, $G\alpha_{12/13}$ via pathways including Rho and ROCK, which regulate the actin cytoskeleton of cells (Haak *et al*. 2021). Additionally, the study states that GPCR signalling through $G\alpha_s$ via adenylyl cyclase and cAMP, which interacts downstream with PKA and cAMP response element-binding protein (CREB), promotes antifibrotic signalling through destabilising F-actin. In-house experiments carried out by Dr Kasope Wolffs indicate that CaSR NAMs effectively block the increase in $[Ca^{2+}_i]$ in response to polyamines, which are CaSR activators and have been seen to be upregulated in PF patient saliva (Wolffs *et al.* 2020). CaSR is overexpressed in the lungs of IPF patients. This study also indicated that deletion of CaSR from SM22α+ cells reduced collagen deposition in an age-induced fibrosis model and reduced TGF-β1-induced increase in CaSR expression and pro-fibrotic changes to *in vitro* normal HLFs. These results indicate that CaSR NAMs can be a novel therapeutic for treating upstream mediators of profibrotic changes, thus attenuating chronic fibrosis in this PD and offering superior treatment to the current standard of care treatments.

1.6. CaSR, its involvement in PDs, and developing New Chemical Entity CaSR NAMs

CaSR is a pleiotropic class C heterotrimeric G-protein coupled receptor (GPCR) involved in systemic Ca^{2+}_o homeostasis (Brown and Macleod 2001), which is maintained by the secretion of parathyroid hormone (PTH) from the parathyroid gland, calcitonin release *via* the thyroid gland and renal Ca^{2+} reabsorption through vitamin $1,25(OH)_2D_3$ (Riccardi and Brown 2010). Cloned CaSR sequence revealed a 1,078 amino acid long protein ***(Figure 13)*** consisting of a large amino-terminal extracellular domain (ECD) of 612 amino acids comprised of two lobe-shaped domains (LB1 and LB2) that form the N-Terminal "Venus flytrap" (VFT) domain, which closes upon activation much like the VFT plant. The VFT domain is attached by a cysteine-rich region to a 7-transmembrane domain (7TMD) of 250 amino acids and an intracellular carboxy-terminus tail of 222 amino acids (Brown *et al.* 1993).

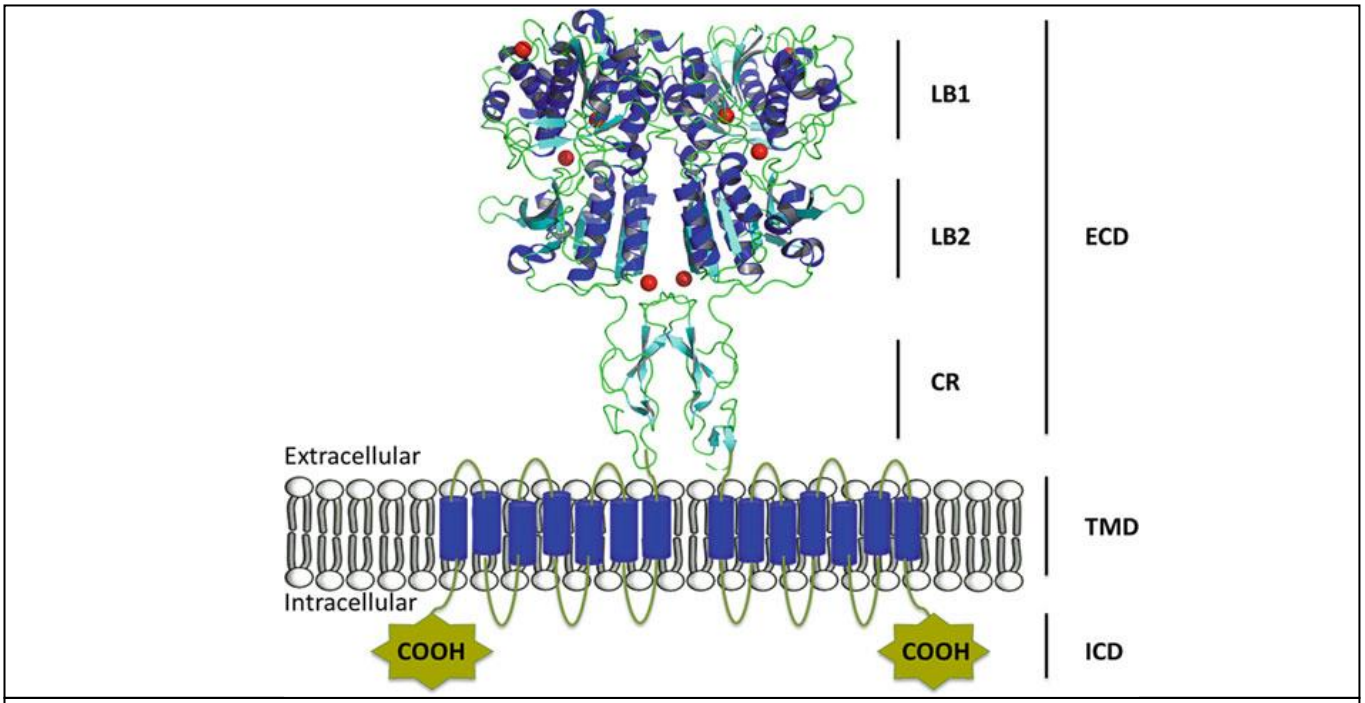

Figure 13. **CaSR homodimer structure**. Extracellular domain (ECD, 612AA), a seven transmembrane domain (TMD, 250AA) and a carboxy terminal tail (200AA). CaSR ECD exhibits a Venus-Flytrap-like domain, structure connected to the seven TMD by a cysteine rich region. In the absence of an agonist, the VFT remains open, and closes to binding of Ca^{2+}_o or L-Trp, causing conformational changes in the TMD and intracellular domains of the receptor, (Liu *et al.* 2018). There are several binding sites for calcium and other amino acids, whereby activation of different sites biases CaSR activation (Chavez-Abiega et al. 2019).

While the CaSR is highly expressed in the parathyroid gland and renal tubule, it is also found in various cell types unrelated to mineral ion metabolism (Bruce *et al*. 1999). Such tissues include the developing foetal lung (Riccardi *et al*. 2013), central nervous system (CNS) and peripheral nervous system (PNS) (Vizard *et al*. 2008), but also the liver (Canaff *et al*. 2000), gut (Riccardi *et al*. 2013), bone (Goltzman and Hendy, 2015), heart (Sun *et al*. 2017), breast, placenta (Riccardi *et al*. 2013), vasculature (Schepelmann *et al*. 2016) and adult lung (Yarova et al. 2015). CaSR activation ***(Figure 14)*** causes it to couple to several intracellular G proteins: to $G_{q/11}$, stimulating phospholipase C (PLC) to hydrolyse phosphatidylinositol 4,5-bisphosphate (PIP2) to diacylglycerol (DAG) and inositol 1,4,5- triphosphate (IP3), releasing Ca^{2+} from intracellular stores and activating protein kinase C (PKC) (Brown *et al*. 1993); to $G_{i/o}$, which inhibits adenylyl cyclase, a cyclic adenosine monophosphate (cAMP) synthesising enzyme (Chang *et al*. 1998); and to $G_{12/13}$, activating Rho-kinase.

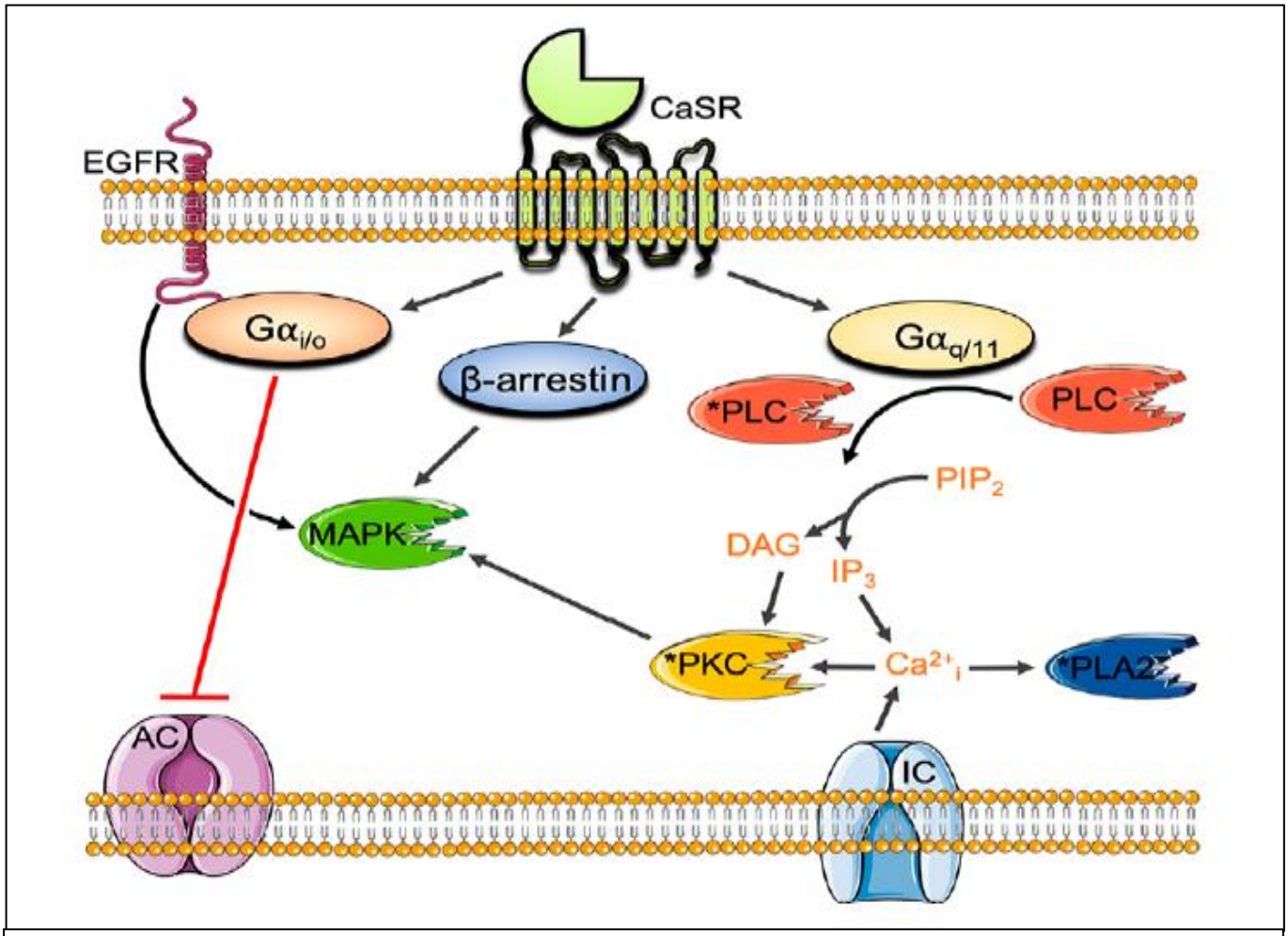

Figure 14. **CaSR signalling pathways**. CaSR activation couples with $G_{i/o}$, inhibiting adenylyl cyclase (AC), thus reducing cAMP levels; with $G_{q/11}$, activating phospholipase C (PLC), thus increasing inositol triphosphate (IP_3) and diacylglycerol (DAG), triggering the release of $Ca^{2+}{}_i$. $Ca^{2+}{}_i$ activates phospholipase A2 (PLA2) and protein kinase C (PKC), increases $Ca^{2+}{}_i$ *via* influx through L-type voltage-gated and transient receptor potential ion channels (IC).The CaSR activates MAPK signalling cascades *via* $G_{q/11}$-mediated PKC, $G_{i/o}$-mediated activation of epidermal growth factor receptor (EGFR), and β-arrestin. Figure from (Leach *et al.* 2020)

Moreover, activation of CaSR has also been found to promote cell proliferation *via* the mitogen-activated protein kinase (MAPK) signalling pathway (Brown and Macloed 2001). Additionally, it induces the deposition of tight junction (TJ) components to the epithelial cell plasma membrane (Jouret *et al*. 2013), which could account for changes in mechanical stiffness and cell-to-cell communication. CaSR activation, via the $G_{q/11}$ pathway through calmodulin and the Ca^{2+}/calmodulin-dependent protein kinase II, can also promote the phospholipase A2 (PLA2) pathway (Handlogten *et al*. 2001). CaSR-activated increase in cPLA2 is TNF-alpha-mediated, increasing TNFR1, TRAF2, ASK1, and NADPH oxidase, which ultimately activates the NF-κB path (Lin *et al*. 2016). As summarised in Leach et al. 2020, the CaSR activates several mitogen-activated protein kinase (MAPK) cascades, including extracellular signal-regulated kinase 1/2 (ERK1/2), p38 MAPK c-Jun N-terminal kinase, to regulate PTH release, proliferation, and other functions. Phosphorylation of ERK1/2 occurs *via* multiple CaSR-mediated pathways, including parallel G protein-dependent pathways, involving either G_q and PKC or G_i and EGFR transactivation. Ras and phosphatidylinositol 3-kinase (PI3K) are also involved in ERK1/2 activation by the CaSR (Hobson *et al.* 2003), but it is unclear if this pathway overlaps with G-protein- dependent pathways.

Extracellular Ca^{2+} increases the formation of CaSR–Homer1 protein complex, which binds to mTOR complex 2 (mTORC2), a protein kinase that phosphorylates serine/threonine kinase (AKT, aka protein kinase B) by 3-phosphoinositide– dependent kinase 1 (PDK1), downstream of PI3K (Rybchyn *et al*. 2019). AKT phosphorylation inhibits Glycogen synthase kinase-3 and directly phosphorylates and stabilises β-catenin, allowing its subsequent nuclear translocation, leading to cellular differentiation. AKT also suppresses apoptosis and promotes growth in the cell. The CaSR can also activate ERK1/2 through a ß-arrestin-dependent and G protein-independent pathway. In some cell types, the CaSR stimulates the opening of L-type voltage-gated channels and nonselective cation channels, including (TRPC) channels. CaSR is subject to biased agonism, where distinct ligands preferentially stimulate a subset of the CaSR's possible signalling responses to the exclusion of others. The CaSR thus serves as a model receptor to study natural bias and allostery.

Activating the CaSR on AMs triggers proteolytic cleavage of pro-IL-1b into mature IL-1b (Jäger et al. 2020). It activates the NLRP3 inflammasome, inducing airway epithelial-derived chemotactic cytokine production like TNF and monocyte chemoattractant protein-1 to be secreted from epithelial and immune cells, regulating the migration and infiltration of blood-derived monocytes, memory T lymphocytes, and natural killer cells (Gutiérrez-López *et al.* 2018). CaSR activation in ASMCs reduces cAMP, thus also reducing cAMP-dependent protein kinase A (PKA), which causes myosin light chain (MLC) phosphorylation to enable ASMC contraction and, therefore, its overactivation might facilitate AHR (Billington *et al*. 2013).

CaSR signalling activation promotes the degradation of important NLRP inflammasome regulators *via* inducing expression of Hsp70 through the chaperone-assisted ubiquitin-proteasome pathway and chaperone-assisted endosomal microautophagy. These systems are integrated by autophagosomes, as indicated by microtubule-associated protein 1 light chain 3, a classical marker for autophagy (Gutiérrez-López *et al*. 2018). Second messenger cAMP inhibits the expression of proinflammatory cytokines *via* the induction of HDACs and subsequent de-acetylation of NF-κB (Luan *et al*. 2015). Low cAMP levels dis-inhibit proinflammatory cytokines by not inducing HDACs, but ROS generation also directly causes oxidative damage to HDACs. HDACs and histone acetyltransferase (HATs) are a pair of functionally antagonistic proteases responsible for histone deacetylation and acetylation, respectively. HDACs affect chromosome structure and the activity of transcription factors by removing acetyl groups from histones (Araki and Mimura, 2017); they are involved in posttranslational modifications affecting protein activity, stability, distribution and interactions (Yoon and Eom, 2016). Non-histone proteins such as NF-κB, heat shock protein, P53, signal transducers and activators of transcription (STAT), forkhead transcription factor and mitogen-activated protein kinase (MAPK) are all modified by HDACs to regulate biological pathways (Gallinari *et al*. 2007). HDAC enzymatic activity (Brewer 2021) maintains the expression of NF-κB inhibitor, inhibitors of κB (IκBs), and the catalytic inhibitor of NF-κB (IκB) kinase (IKK) complex), which upregulates TRAF6, NLRP3 and ASC protein components of the NLRP inflammasome. A dysbalance of which enzymatic activity can cause the nuclear localisation of NF-κB and activation of its subsequent transcriptional activity.

Ogata *et al.* in 2006 indicated that CaSR activation might cause an increase in COX-2 enzyme production, upregulating PGE_2 secretion *via* the arachidonic acid pathway. PGE_2 is produced by all cell types, whereby its molecular concentration and receptor expression are crucial in controlling activation, maturation, migration, and cytokine secretion of immune cells like macrophages, neutrophils, natural killer cells, and DCs (Kalinski, 2012). As illustrated in ***Figure 15,*** upregulation of phospholipase A2 (PLA_2) enzymes releases arachidonic acid from the cell plasma membrane, whereby AA is used by housekeeping cyclooxygenases (COX) to form the precursor prostaglandin H_2 (PGH_2), which is enzymatically activated by PGE_2 synthase (PGES) to produce active PGE_2 (Park *et al*. 2006).

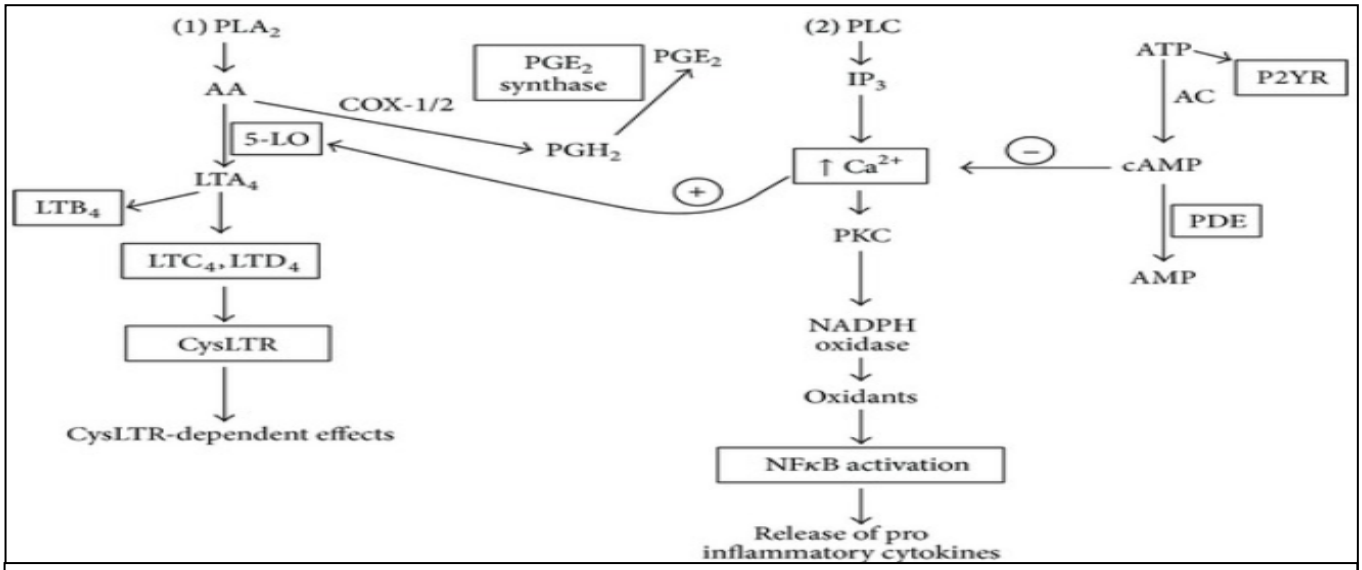

Figure 15. **Inflammatory Pathways.** (1) Phospholipase A2 (PLA2) activation converts membrane phospholipids to arachidonic acid (AA), which is subsequently metabolized to either leukotrienes (LTA_4, LTB_4, and LTC_4) or prostaglandins (PGH_2) by 5-lipoxygenase (5-LO) and COX-1/2 enzymes, respectively. PGH_2 is converted to PGE_2 by PGE_2 synthase. (2) Phospholipase C (PLC) activation generates inositol triphosphate (IP_3), causing cytosolic Ca^{2+} release from storage vesicles and downstream activation of PKC, NADPH oxidase, 5-LO, and NF-κB, releasing proinflammatory cytokines. ATP binds to purinergic receptors (P2YR) and is also converted to cyclic AMP (cAMP) by adenylyl cyclase (AC), which is degraded by intracellular phosphodiesterases (PDE). cAMP downregulates the Ca^{2+}-mediated activation of 5-LO and NADPH oxidase. **Figure** from Ogata *et al*. 2006.

PGE_2 disrupts TGFβ signalling and suppresses myofibroblast differentiation, whereby it has been discovered that a small molecule, SW033291, binds with high affinity to the PGE_2-degrading enzyme 15-hydroxyprostaglandin dehydrogenase and increases PGE_2 levels (Smith *et al*. 2020). Another small molecule, KH176m (active redox modulator metabolite of sonlicromanol), selectively inhibits mPGES-1 activity (solely expressed in diseased tissue) and the inflammatory-induced mPGES-1 feedback-loop that promotes further secretion of PGE_2 in macrophages (Jiang *et al*. 2021). PGH_2 is also a precursor for PGD_2, PGI_2, $PGF_{2\alpha}$, and prostanoid thromboxane A2 (TXA_2). PGE_2 has several receptors that it binds to (EP1, EP2, EP3 and EP4), and the duration of their respective signalling cascades and receptor binding affinities (EP3,-4 have high- and EP1,-2 have low- PGE_2 affinity) wildly vary. EP2 and EP4 are G_s-coupled receptors, which signal through the adenylyl cyclase-dependent cAMP/PKA/CREB pathways, whereas EP1 and EP3 involve cellular calcium release (Hata and Breyer, 2004) and G_i-coupled receptor signalling, which inhibit the activity of adenylate cyclase and consequently decrease levels of cAMP in the cell. Additionally, others might exist, like the recognised EP3α, EP3β, and EP3γ splice variants; thus, specific extracellular conditions and environments can cause simultaneous activation of pro-and anti-inflammatory pathways, resulting in the dual function of PGE_2 signalling.

EP2-dependant PGE_2 stimulation in macrophages, *via* the induction of immunosuppressive interleukin IL-1R-associated kinase-M (IRAK-M), causes inhibition of NADPH oxidase and nitric oxide radical release (Hubbard *et al*. 2010). Thus, PGE_2 also facilitates inflammatory resolution *via* dampening macrophage phagocytosis and promoting the secretion of anti-inflammatory mediators such as IL-10, IL-17 and TGFβ (Agard *et al*. 2013). PGE_2, acting as a ligand to activate the EP4 receptor, induces the expression of oncostatin M in wound-site macrophage cells, acting as an anti-inflammatory cytokine by attenuating pro-inflammatory cytokines TNF-α and IL-1β (Ganesh *et al*. 2012). PGE_2 additionally improves wound healing *via* promoting macrophage transition towards the alternatively activated M2 (AAMs) repair type through cooperative upregulation of STAT6 and CREB- and cAMP-regulated transcriptional coactivators 2 and 3 (CRTC 2/3)-mediated induction of Krupple-like factor 4 (Luan *et al*. 2015). Increased PGE_2 promotes AAMs that produce urea, ornithine, and other polyamines through the Arg1 pathway, promoting proliferation, wound healing, CaSR activation, and thus the inflammatory positive feedback loop. In allergic asthma, L-ornithine-derived polyamines levels are elevated, correlated with an increase in AHR to allergens *via* $Ca^{2+}{}_I$ release (Nilsson and Strand 1993), while AHR decreases with the treatment by inhibitors polyamines' synthesis (North *et al*. 2013).

Work carried out in our laboratory has shown that activation of the CaSR by asthma-associated polycations (e.g., ECP, MBP) and polyamines cause $Ca^{2+}{}_i$ mobilisation in cells that express it. In human ASM, CaSR activation leads to non-specific AHR and plays a crucial role in the pathogenesis of airway inflammation and remodelling as shown in pre-clinical models of PDs (Yarova *et al.* 2015). Inhaled CaSR NAMs prevent these effects in native and recombinant cell systems. They, therefore, have the potential to reduce ASM proliferation and abolish AHR in a corticosteroid-independent manner, targeting the root cause of the disease and not only the symptoms. CaSR NAMs also prophylactically prevent airway inflammation by inhibiting the positive feedback loops that initiate and maintain polycation influx into the lung.

Historically, the first generation of positive allosteric modulators (PAMs) of the CaSR, from which NAMs were derived, were phenylalkylamine compounds, a derivative of the voltage-gated calcium channel blocker fendiline (Nemeth et al. 1998). The first NAM of the CaSR, NPS2143, was initially trialled as a short-acting oral anabolic agent for treating osteoporosis due to its ability to stimulate serum PTH release, causing an increase in bone mass density (BMD) (Nemeth *et al.* 2001). To promote an increase in BMD, the NAMs needed to be rapid and short-acting, as a continuous high serum PTH results in catabolic conditions, such as hyperthyroidism (Gowen *et al.* 2000). Oral and intravenous administration of NAMs proved to be safe in humans ***(Table 1);*** however, they failed to show improvements in BMD in osteoporotic patients; thus, none passed Phase IIA clinical trials. For a drug to have a therapeutic effect in the targetted tissue, it must reach the cellular plasma membrane, a phospholipid bilayer with a dense hydrophobic core largely impenetrable to water-soluble molecules and ions (Lodish 2012). Generally, the rate of simple diffusion of any substance through a plasma membrane is proportional to its concentration gradient across the bilayer, as well as its hydrophobicity and size. In the case of targetting the CaSR, which is a cell surface plasma membrane-bound receptor, it is not essential to pass the membrane; instead more relevant for the pharmacological molecule to reach the surface of cells over-expressing the CaSR.

Table 1. **CaSR NAMs already tested in humans, considered for repurposing as inhaled therapeutics for the treatment of PDs**. Adapted from Yarova *et al*. 2020

CaSR NAM	COMPANY & TARGET	g/mol; IC_{50}	Clinical Development
NPSP795/SB-423562 **(amino-alcohol)** **NPSP790/SB-423557 (ester pro-drug)** **NPSP795/SHP635 (amino-alcohol)**	NPS/GSK (osteoporosis) NPS (ADH1)	436.5; 5.24 nM	Phase I (n=28; i.v.; 2 sessions, 7 days apart), (n=50; oral; > 2 sessions, 7 days apart); (Kumar *et al.* 2010) Phase II (n=7; 17 days; i.v.) (Roberts *et al.* 2019)
Ronacaleret/ SB-751689 **(amino-alcohol)**	GSK (osteoporosis)	447.5; 6.81 nM	Phase II (n=569; 12 months; oral) (Caltabiano *et al.* 2013)
JTT-305/MK-5442; **Encaleret (amino alcohol)**	JT/Merk (osteoporosis)	514; 2.71 nM	Phase II (n=526; 12 months; oral) (Cosman *et al.* 2015)
AXT914 **(quinazolin-2-one)**	Novartis (osteoporosis)	539 1.15 nM	Phase II (n=105; 4 weeks; oral) (John *et al.* 2014)

Thus, to specifically reach the cells in the lung, in-house studies were conducted on NAMs, which were repurposed from an oral to a nebulised form ***(Figure 16).*** The results indicated that nebulised NPS2143 was longer-acting than the oral version, causing no systemic changes in plasma PTH concentrations, and is, most importantly, safe for use (Yarova *et al.* 2015). The compound significantly blocks increases in Ca^{2+}_i induced by Ca^{2+}_o in the lung, shifting the response curve to the right without changing the maximum or minimum response (Nemeth *et al.* 2001). NPS2143 suppressed AHR and inflammation in our previous asthma studies when delivered in nebulised form (Yarova *et al.* 2015). CaSR NAMs also effectively reduced airway inflammation and remodelling in asthma and COPD surrogate models (Yarova *et al.* 2016).

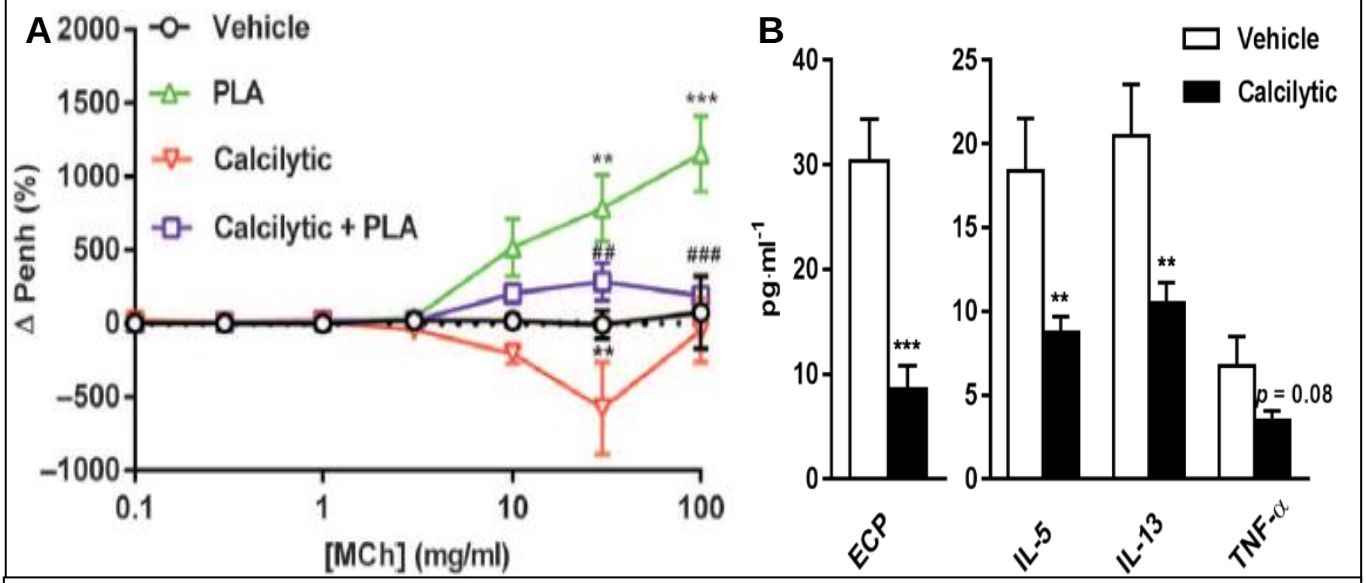

Figure 16. **Nebulized CaSR NAMs prevent AHR and inflammation in mice *in vivo*.** (**A**) CaSR NAMs prevent PLA-induced bronchoconstriction in methacholine (MCh)-challenged mice. (**B**) CaSR NAMs reduce inflammatory markers in ovalbumin-sensitized and challenged mice. Figure from Yarova *et al*. 2015.

Repeat exposure to inhaled CaSR NAMs does not evoke airway irritancy or any systemic effects in disease models ***(Figure 17)***, suggesting that lung delivery of the CaSR NAMs is safe (Yarova *et al.* 2021). However, repurposing CaSR NAMs developed to be short-acting and best suited for oral bioavailability is suboptimal, as generally inhaled drugs with a long-acting effect and lower oral bioavailability are better suited for PD therapeutics and to prevent PD prophylactically. Additionally, existing CaSR NAMs that have been tested in humans **(*Table 1*)** have freedom-to-operate (FTO) issues due to existing patents, as well as the fact that their "matter of use" patent does not cover diseases where CaSR NAMs have shown efficacy. Thus, using computer-assisted design, eight new CaSR NAMs were developed as novel therapeutics for inflammatory lung diseases like asthma and COPD and expanded to conditions like IPF, circumventing possible FTO issues. These New Chemical Entities (NCEs) are diastereomerically pure mixtures comprising complementary (R, R)// (S, S) enantiomers of substituted amino acid alcohol CaSR NAMs compound C32. In this work, the NCEs are referred to as C1 through to C8.

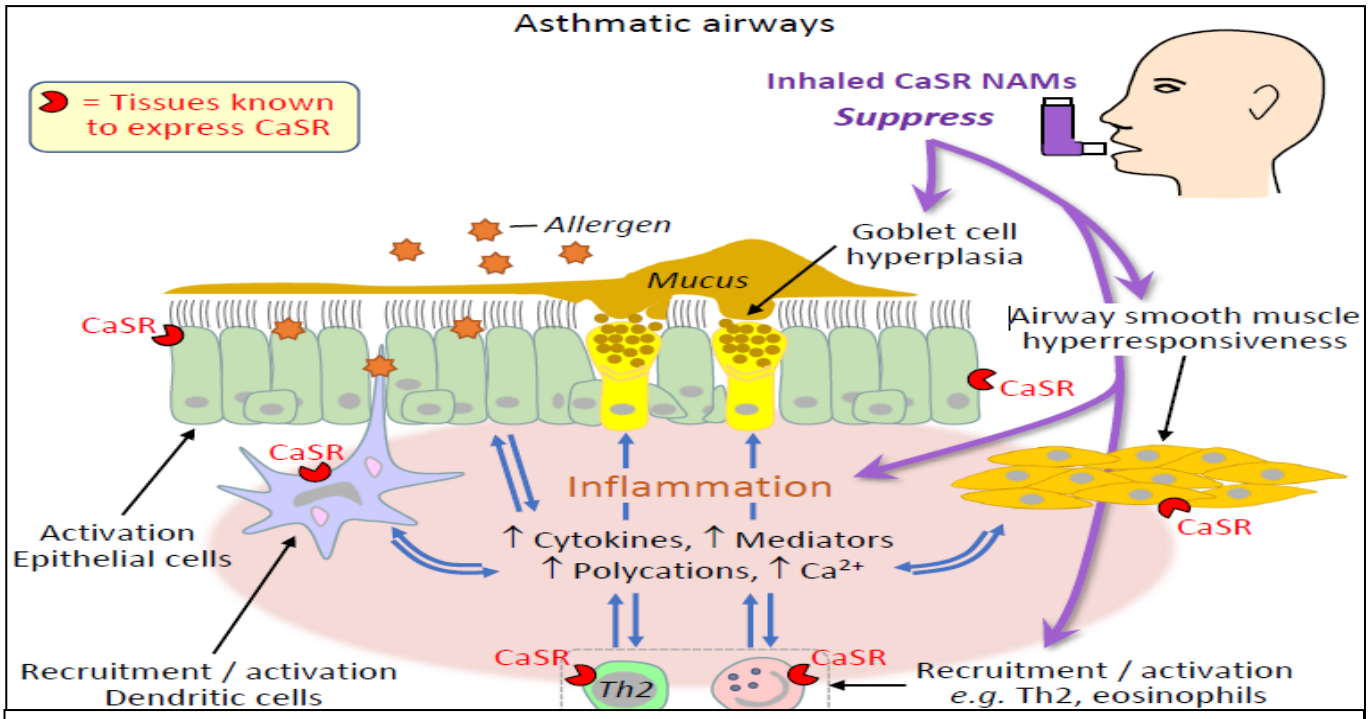

Figure 17. **Allergic asthma, the proposed involvement of the CaSR in resident cells, as well as the action of NAMs on PD**. Stimuli trigger release of polycations, which bind to pulmonary cells, leading to increased Ca^{2+}_i. This increase causes ASM contraction and airway remodelling, which feeding a feedback loop of further eosinophilic infiltration and chronic remodelling. NAMs inhibit this process upstream, abolish AHR and reduce epithelial alarmin release, possibly stopping disease progression entirely. Figure from Yarova *et al*. 2020.

The *in silico* homology model of the human CaSR AA sequence allowed our group to recognise a three-sited binding pocket common among different binding sites of known NAMs (Riccardi *et al*. 2017). As seen in **Figure 18**, NAMs are predicted to bind within a cavity located between the mid-portion and extracellular aspect of the CaSR 7TMD (Leach *et al.* 2016). Amino alcohol NAMs can bind to all three known binding sub-pockets in the active site of the intracellular CaSR. Thus, the NCE CaSR NAMs used in this project were synthesised by structurally modifying the scaffold of amino alcohol CaSR NAM. It was considered that by modifying the amino alcohol linker, further binding could be chemically reached to the sites bound by quinazolinone-type CaSR NAMs (Trp818 and Tyr825, cyan-coloured sites in ***Figure 19***).

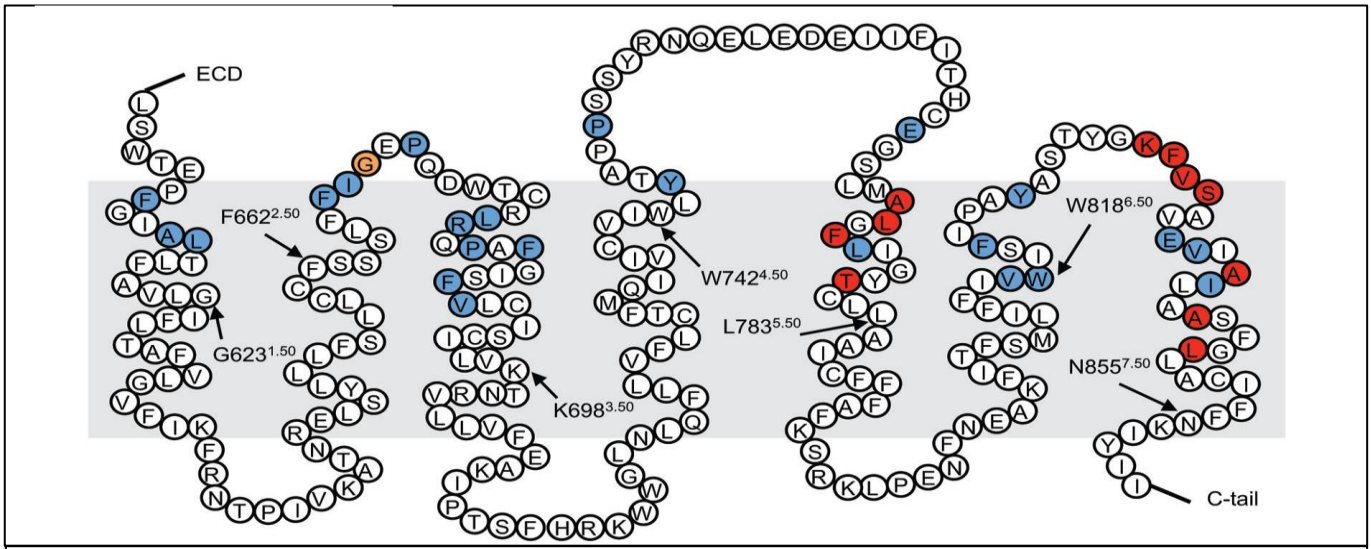

Figure 18. **Snake diagram of primary CaSR 7TM domain sequence.** The binding sites of known allosteric modulators of the CaSR are the residues coloured in blue, as mutation at these sites affects receptor binding. The grey box indicates cell plasma membrane, and the thick black arrows are pointing to conserved residues across class C GPCRs. Image from (Leach et al. 2016)

The developed NCEs exhibit similar effects to parent CaSR NAMs at inhibiting the CaSR whilst having meaningful substitutions that might confer superior lung delivery properties and potentially higher activity. Stereocentres and enantiomers of the CaSR NAM NCEs additionally have significant relevance for CaSR dimerisation as NAMs must bind both monomers of the intracellular portion of the receptor to block signalling entirely (Gregory *et al.* 2018). Patient-specific mutations for known binding sites might incur variable allosteric cooperativity, agonism and bias; thus, checking patient-specific CaSR gene structure is advisable before inhaled treatment for pulmonary disorders. NCE CaSR NAMs can be an effective prophylactic therapeutic for PDs like Asthma, IPF and COPD by preventing disease progression and alleviating symptoms. The amino alcohol scaffold used to synthesise the NCE CaSR NAMs was the lead compound for the derivation of CaSR NAM NPS-2143 (used as a positive control in most experiments in this study), C32 (Marquis *et al*. 2009). For maximum activity at CaSR, C32 requires its amino alcohol linker central hydroxyl moiety to be in R configuration (Marquis *et al*. 2009), possibly due to the binding of the OH group to the Glu837 site of the receptor.

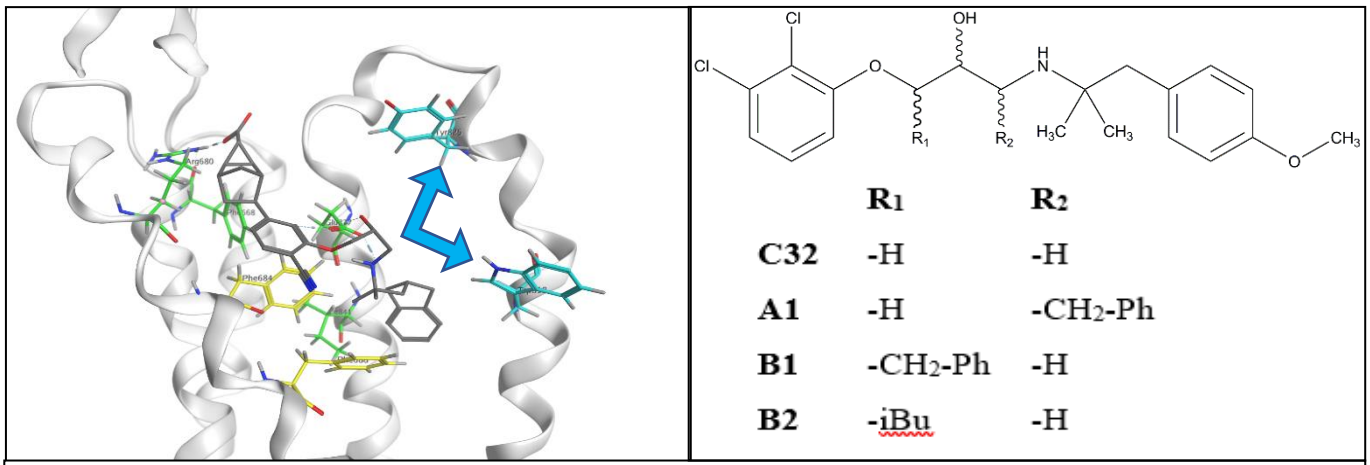

	R_1	R_2
C32	-H	-H
A1	-H	$-CH_2-Ph$
B1	$-CH_2-Ph$	-H
B2	-iBu	-H

Figure 19. **CaSR binding sites of amino alcohol NAMs and novel variant substitutions.** Two variants of novel substitutions on the amino alcohol linker moiety – isobutyl (-iBu) and benzyl (CH_2-Ph) were initially selected for synthesis. R_1 and R_2 substitutions were meant to reach the cyan quionazoline-2-ones binding sites of the intracellular portion of the CaSR. Synthesis of B2 was given priority. Patent filing (Riccardi et al. 2017).

R_1 and R_2 substitutions ***(Figure 19)*** add a second stereocentre in the target molecules, thus leading to 4 enantiomers for each of the target compounds. A1 diastereoisomers were inactive at inhibiting the CaSR, B1 synthesis did not yield the target molecule, whereas lead compound C32 and derivative B2 diastereoisomers significantly inhibited the activation of the CaSR. The most potent was separated enantiomer B2.1-E1 (a.k.a. E1) (R, R). In E1, the OH group is in the R configuration, indicating that the derivatives' stereochemical configuration is relevant to activity at the CaSR. NAM B2.1-E1 has also been tested *in vivo* for efficacy ***(Figure 20)***, showing a dose-dependent suppression in AHR and inflammation in allergen-induced mouse models of asthma.

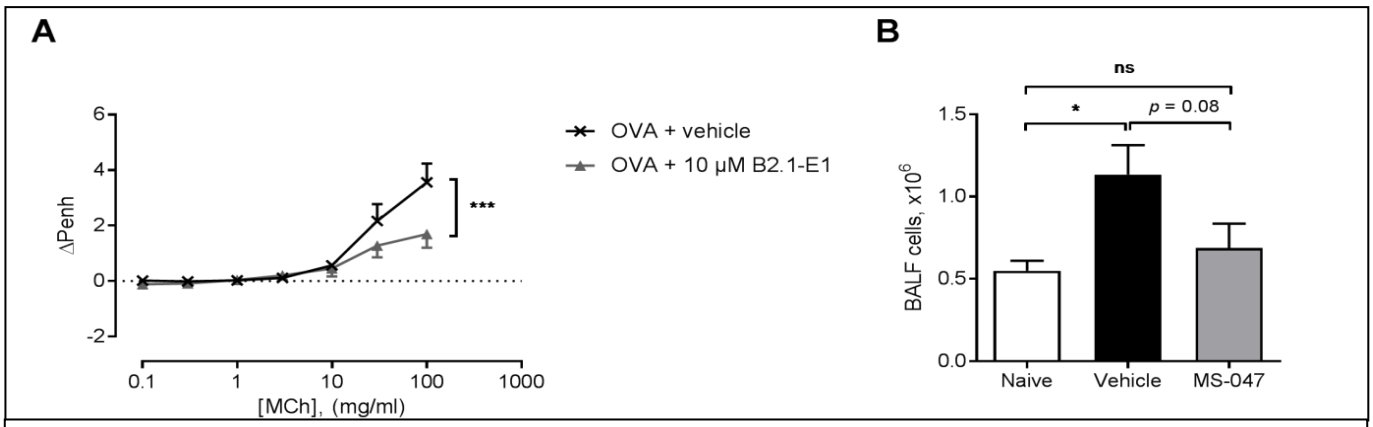

Figure 20. **Inhaled B2.1-E1 prevents AHR and inflammation in ovalbumin (OVA) sensitisation and challenge mouse model.** (**A**) ΔPenh: changes in enhanced pause calculated as a difference before and after OVA and NAM E1 (or vehicle of 0.1% DMSO) administration or (**B**) as BALF cell count. E1 was just as effective in Poly-L-Arginine (PLA)- induced AHR in mice (not shown). Patent filing (Riccardi et al. 2017)

This current study focuses on two NCE target molecules and their enantiomers, developed from substituting the R1 position of C32 with a methyl moiety and a phenyl ring, respectively. In *vitro* screens for all enantiomers ***(Figure 21)*** to determine their activity and cytotoxicity. The experimenters were blinded to the stereochemical structure of the compounds C1 through to C8. Unblinding revealed that C1 through C4 were methyl enantiomers and C5 through C8 were phenyl enantiomers.

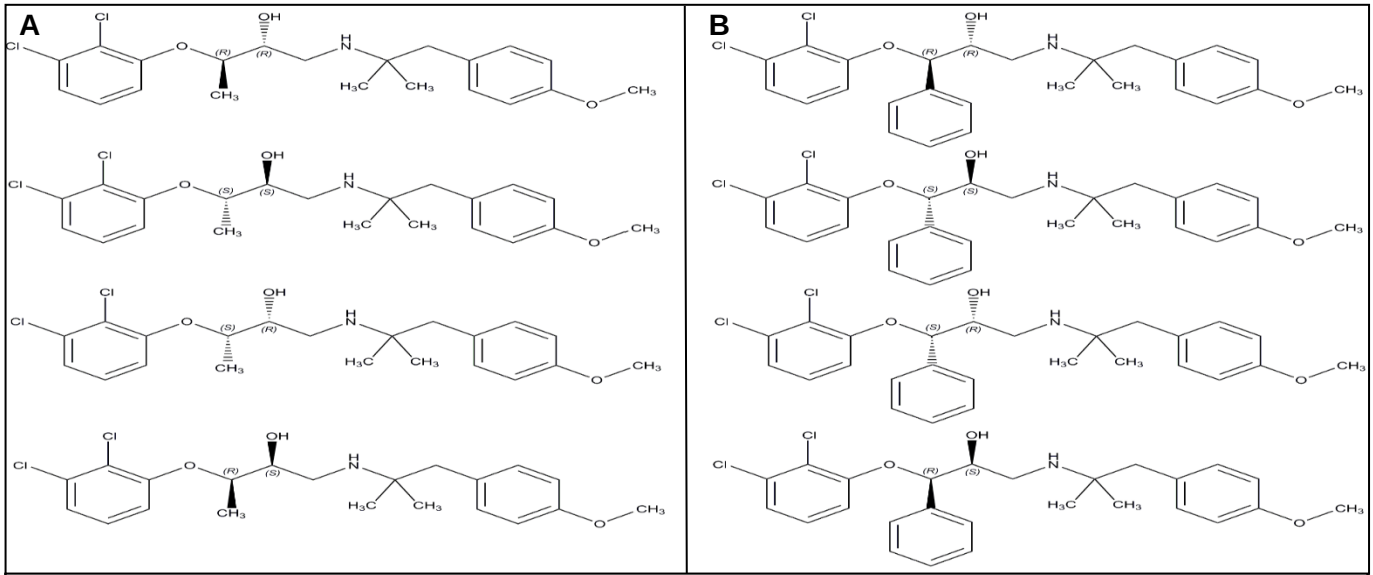

Figure 21. Confidential patent material: **the 8 separated eluting NCE CaSR NAM enantiomers.** (**A**) Methyl (CH_3) substitution diastereoisomers, termed C1 through C4; (**B**) Phenyl (C_6H_5) substitution diastereoisomers, termed C5 through C8. The experimenters remain blinded to the stereochemistry, thus **(A)** and **(B)** showcase the possible configuration of the compounds, and not the correct order of C1 through C8.

2. AIMS AND HYPOTHESIS

NCE CaSR NAMs exhibit therapeutic potential for treating asthma, COPD and IPF. Therefore, the central hypothesis of my thesis work is that:

2.1. Hypothesis:

Selected NCE CaSR NAMs exhibit safe and potent effects at the CaSR

2.2. Specific aims:

My thesis work aims to determine which of the synthesised NCEs is the optimal NAM in terms of potency, selectivity, and lack of cytotoxicity upon inhibition of the CaSR and chemicostructural properties compatible with a formulation for inhalation.

- To determine *in vitro* the potency of the NCEs to inhibit CaSR activation in Human Embryonic Kidney cells stably transfected with the human CaSR (HEK-CaSR) by comparing these synthesised NAMs to a positive control CaSR NAMs (parent compound) and vehicle-only.
- Determine cytotoxicity of the most potent NCEs *via* live-cell imaging and LDH cytotoxicity assays on primary HBECs.
- Determine the chemicostructural suitability of NCE phenyl and methyl substitutions for NAM lung delivery profile in terms of hygroscopicity, lipophilicity and receptor binding affinity.

3. MATERIALS AND METHODS

The project was split up into several stages. The bulk of the work was carried out in Cardiff University School of Biosciences laboratory of and under the direct supervision of Professor Daniela Riccardi, with the assistance of Dr Bethan Mansfield, Dr Kasope Wolffs and PhD student Richard Bruce. Primary Human Bronchial Epithelial Cells (HBEC) Live-cell imaging experiments were carried out in the UK Dementia Research Institute (UKDRI) lab in the Hadyn Ellis building of Cardiff University.

3.1. Tissue Culture of HEK293-CaSR cells

In vitro experiments described in this report were carried out on the HEK293 cell line, stably transfected with the human CaSR, referred to as HEK-CaSR cells from hereon (Ward *et al.* 2013, Roberts *et al.* 2019). Aliquots of stable transfectants were kept in liquid N_2 storage and thawed in a 37^{o}C water bath. The contents of the wholly defrosted vial were transferred in T-75 flasks with 10ml pre-warmed Dulbecco's Modified Eagle's Medium (#RNBH6732, Sigma) with 10% Foetal Bovine Serum (#A3160801, Gibco) and 1% Penicillin Streptomycin (#15140-122, Gibco). The medium was changed every two days to maintain cell proliferation, and 2 µg/ml of Hygromycin B (#10687010, Invitrogen) was added each time to retain clone selection. Before reaching confluency, the cells were subcultured into a new flask *via* the following standard procedure: the medium is removed from the T-75 flask, and the cells are washed with Phosphate

Buffered Saline (PBS) (#10010023, Gibco). PBS is then pipetted away, 3 ml of Trypsin-EDTA (0.25%) (#25200056, Gibco) is introduced, and the flask is returned to the 37ºC and 5% CO_2 incubator for two minutes so that the cells can dissociate from the plastic bottom of the flask. Then 6 ml of pre-warmed medium is added (twice the amount of trypsin), inactivating the proteolytic enzyme, whereby this cell-laden mixture is spun down on the centrifuge. The supernatant was removed, and the cell pellet was resuspended in 1 ml of fresh medium homogeneously. At that point,9 ml of fresh pre-warmed medium was added. 2 ml of this cell-laden solution is added to 8 ml of fresh medium and seeded into a T-75 Flask, 2 µg/ml Hygromycin B is added and the flask is kept in a 37°C, 5% CO^2 incubator.

3.2. Determining NCE CaSR NAMs activity in vitro

NCEs activity was determined using single-cell fluorescence Ca^{2+} Imaging experiments on an Olympus Perfusion Microscope using the fluorescent radiometric dye Fura-2 Acetoxymethyl (Fura-2AM) ester with the collaboration of Dr Martin Schepelmann. HEK-CaSR cells were subcultured using standard technique and were seeded as drops onto the middle of PDL-coated 13mm glass coverslips in wells of a 24-well plate and allowed to settle in the incubator for 30 minutes. Coverslips were examined under a microscope, and if cells were well attached, 500 µL of fresh medium was added to each well. 24-well plates were kept in an incubator until they reached 70-80% confluency and a clear cell border at around 50% of the coverslip's diameter before conducting Ca^{2+} Imaging experiments. Extracellular solution (ECS) was made fresh for each experiment, containing 135 mM NaCl, 5 mM KCl, 5 mM N-2-hydroxyethylpiperazine-N'-2-ethanesulfonic acid (HEPES), 10 mM glucose, 1.2 mM $MgCl_2$, 1.2 mM $CaCl_2$, pH adjusted to 7.4 using Mettler Toledo pH meter. Loading buffer LB was made using 0 Ca^{2+} ECS, supplemented with 1.2 mM $CaCl_2$ and a final concentration of 30 µM of Bovine Serum Albumin (BSA, dissolved overnight). Coverslips laden with HEK-CaSR cells were loaded with 3µM Fura-2AM in LB for 45 minutes at 37ºC in an incubator. After this period, Fura-2AM-containing solution was removed and replaced with LB only, and the plate was returned to the incubator for another 15 minutes. The 24-well plate (seeded with cell-laden, Fura-2AM loaded coverslips) was taken out of the incubator and kept at room temperature, away from direct light. Before transferring each coverslip onto the perfusion bath over the objective ***(Figure 22)***, coverslips were preincubated with 10 µM of NAM in ECS for 10 minutes. Cells were manually selected using the OptoFluor software from the coverslip placed over the objective, which was continually perfused with ECS containing 1.2 mM Ca^{2+} (+NAM or vehicle) to measure baseline activity for 2 minutes until the perfusion solution was changed using the Rapid Solution Changer (RSC) to 5 mM Ca^{2+} ECS solution containing 10 µM NAM. This high Ca^{2+} perfusion solution was maintained for 3 minutes, while the cells' measurements are taken by exposure to fluorescence source (Xenon lamp) light at 340 and 380 nm wavelengths. The fluorescent Fura-2AM dye emits light and is measured at 510 nm. Intracellular Ca^{2+} release is measured by calculating the fluorescent signal ratio from the two absorption wavelengths (340/380). Results are compared cells perfused with 5 mM Ca^{2+} and vehicle control of dimethyl sulfoxide (0.1% DMSO, no NAM).

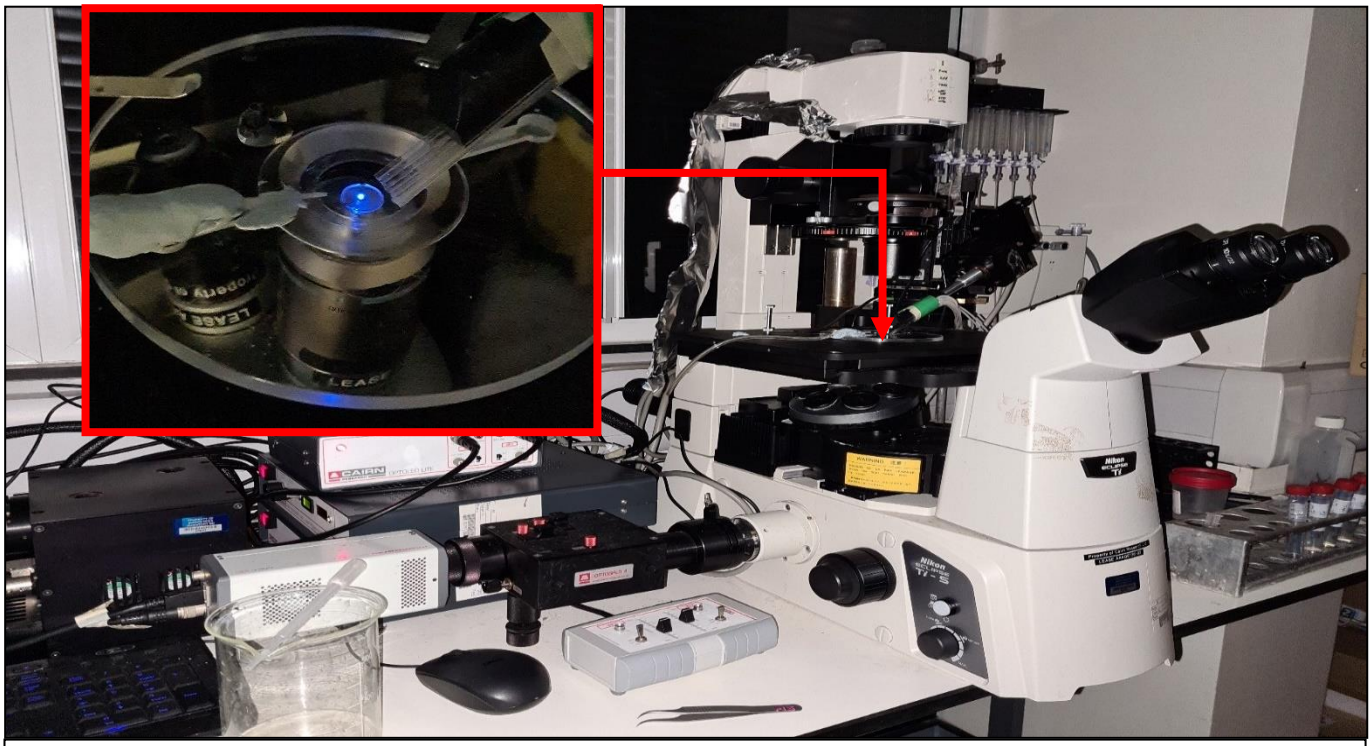

Figure 22. **Photographic images of the Rapid Solution Changer (RSC) Ca^{2+} imaging setup. (B)** Olympus Perfusion Microscope; arrow and additional image showcase the inverted microscope and rapid perfusion area, where the cell-laden coverslips are placed. The RSC system allows the different experimental buffers to be introduced from the right-hand side tubes, whereby the left-hand side has the suction tube, which intakes the constant flow, allowing rapid replacement of solutions.

3.3. Determining CaSR expression in HEK-CaSR cells using immunofluorescence

HEK-CaSR cells were fixed with 2% paraformaldehyde in PBS for 20 minutes at room temperature. Blocking buffer (1% BSA, 3% goat serum, 0.1% Triton X-100) in filter sterilised PBS (pH 7.4) was applied for 1 hour at room temperature. HEK-CaSR cells were immunostained with CaSR primary antibodies (mouse anti-human CaSR mAb, 1:200, Abcam, #ab19347) in a blocking buffer overnight at 4º. Secondary antibodies raised in goat (anti-mouse AlexaFluor-594, 1:1000, Abcam, #ab150120) were applied for 1 hour at room temperature. Slide mounting and nuclei counterstaining were carried out using Vectashield with DAPI (Vector Laboratories Ltd., Peterborough, UK) overnight at 4º. The omission of primary antibodies was used as a negative staining control. Images were captured with 20x objective using an Olympus BX61 microscope, maintaining an identical exposure time for CaSR staining and negative control.

3.4. Determining activity of NCEs using high-throughput Ca^{2+} Imaging

Following the single-cell fluorescence Ca^{2+} imaging experiment, I used the high-throughput ClarioStar Plate Reader for further experimental studies to directly compare the best performing CaSR NAMs. HEK-CaSR cells were seeded in 96-well plates to measure intracellular Ca^{2+} mobilisation, using Fura-2AM as the indicator. Fura-2AM powder was dissolved in 50 µL DMSO to make up Fura-2AM stock. The medium was removed from the plates, one row at a time not to cause cell drying, whereby each row was washed with 50-100 µL of LB. For each 96-well plate, 3 mL of LB + 9 µL Fura-2AM (2 µM) were made fresh. LB was removed from the treated row, and 30 µL Fura-2AM+LB was added to each well. The plate was kept in an incubator for 45 min – 1 hr at 37°C.

During the incubation time, the NAMs were prepared fresh from 10 µM stocks, kept at -4°C, and serial dilution was carried out in H2O until the final step, which was in ECS, for the necessary concentration being examined (1,3 or 10 µM). The Fura-2AM+LB solution was removed, one row at a time, and the wells were washed with 50-100 µL of LB only. The plate reader allowed the simultaneous reading of multiple samples in the same run, reducing experimental variability by comparing results from different tests. As detailed in ***Figure 23,*** wells were preincubated with each NAMs for 10 minutes. All 5 selected CaSR NAMs from Stage 1 could be tested in the same 96-well plate, whereby individual plates contained different NAMs at the same concentration, either 1, 3 or 10 µM. The effects of the NCEs were compared to positive control CaSR NAMs NPS2143, C32 (parent compound) and with vehicle control.

Plate Reader Setup

	E1	E1	E1	E1	E1	E1	DMSO	DMSO			
	C32	C32	C32	C32	C32	C32	DMSO	DMSO			
	C4	C4	C4	C4	C4	C4	DMSO	DMSO			
	C5	C5	C5	C5	C5	C5	DMSO	DMSO			
	C7	C7	C7	C7	C7	C7	DMSO	DMSO			
	PC	PC	PC	PC	PC	PC	DMSO	DMSO			

Labelled wells plated with **HEK-CaSR cells**, pre-incubated with NAMs E1, C32 (parent compound), C4, C5, C7 and PC= Positive Control NAM (NPS 2143) at **1, 3 or 10 µM** (separate plates for different concentration) for **10 minutes in 100 µL of 1.2 mM Ca^{2+}**

2 minutes baseline

Pump 1 injects **76 µL of 10 mM Ca^{2+}**, equating to **5mM Ca^{2+}** final concentration (176 µL total), measure for 3 minutes

DMSO= Negative Control wells, containing 0.1% DMSO in media

Control media-only wells for background fluorescence

Figure 23. ClarioStar PlateReader 96-well NAM setup. Plate reader: 20 cycles, 25 flashes per well, excitation at both 340 nm and 380 nm, emission at 510 nm. The gain was adjusted to the control well that contains cells + 5 mM Ca^{2+}, added immediately prior to placing the plate into the reader. Used adjusted gain settings for every single following plate. Each plate contains the above shown CaSR NAMs pre-treatments, where each plate contains solutions of the same concentration, either 1, 3 or 10 µM.

3.5. Tissue Culture of HBEC

While initial work to determine NCE NAM activity was carried out on HEK-CaSR cells to examine the effect NAMs might have on proliferation, cell shape and cell *via*bility, further work was carried out on Primary Human Bronchial Epithelial Cells (HBEC), as inhalation is the chosen delivery route for CaSR NAMs. These cells are isolated from the surface epithelium of human bronchi and stain positive for cytokeratin. They provide a more accurate model to determine how the NCE NAMs might affect human respiratory systems. Normal human bronchial epithelial cells (NHBECs) were purchased from Lonza (cryopreserved, cat. #CC-2450). For expansion, these cells were initially cultured in PneumaCult -Ex (Stem Cell Technologies cat. #05008) with a combination of 100 µg/ml Penicillin/Streptomycin (Gibco cat. #15140122) and 2.5 µg/ml Amphotericin B mix (Gibco, cat. #15290018). Finally, 50 µM hydrocortisone solution (Sigma cat. #H6909) was added, and this mixture of components is referred to as complete PneumaCult™-Ex Medium. Cells were incubated at a temperature of 37°C and 5% CO^2. Once the cells reached 70% confluency, cell splitting was carried out: the medium was removed, and the cells were washed with HBSS (Gibco cat. #14170-070). 0.05% Trypsin-EDTA (1X) (Gibco, cat. #25300-054) was added to the cells and Trypsin was inactivated by adding RMPI-1640 (Gibco cat. #11875-085) supplemented with 10% foetal bovine serum (FBS) (Gibco, cat. #A3160802). Cells were centrifuged and seeded into new flasks.

3.6. Measurements of cell proliferation and eccentricity using live-cell imaging

Following Ca^{2+} imaging experiments, C5 and C7 were deemed not to be active at inhibiting the CaSR; thus, long-term exposure to selected NCE NAMs was carried out to determine whether they impair cell *via*bility using the IncuCyte Live Cell Imaging incubator (Sartorius). IncuCyte is an automated microscope that resides in an incubator, allowing the experiment to take images at set periods every 2 hours. These measurements permitted plotting phase confluence and cell shape changes over time, analysed by IncuCyte computer software. This experiment was carried out on both HEK-CaSR and primary HBECs. The work with HEK-CaSR cells was carried out before Covid-19 in the Sir Martin Evans building in the laboratory of Professor Nick Allen. The primary cell work was carried out in the Hadyn Ellis Building in the UK Dementia Research Institute (UKDRI), collaborating with Dr Andrew Jefferson.

HBECs were cultured in our laboratory in Cardiff University School of Biosciences in T-25 flasks until ~80% confluence was reached, which equated to around 2.8 x 10^6 cells and the 24-well plate starting seeding density was 0.01 x 10^6 cells. The cells and required consumables were transported manually to the UKDRI. The HBECs were re-introduced to a 37°C, 5% CO_2 incubator. The cells were harvested using a standard procedure (trypsinisation, centrifugation, supernatant removal) and diluted to 10,000 cells/mL by adding 10 mL of fresh medium, then taking 1 mL of this 1:10 dilution and adding it to 27 mL fresh medium. The confluency experiment requires all wells to begin from the same initial starting density. Thus, when adding 0.5 ml of this cell suspension to each well of the two 24-well plates, the cell-containing medium was resuspended using a 1 mL pipette between seeding each row. Two 24-well plates were run simultaneously, always plated late at the work day's end, and incubated at 37°C, 5% CO_2 overnight to allow proper cell adhesion. The morning after, NAM-containing HBEC medium was made up fresh for each experiment: 1 mM stock of each NAM in water was used to make the 1 µM and 10 µM solutions in the medium. Solution preparation was as follows: add 6 µL of each 1 mM NAM to 6 ml medium for the 1 µM solutions, and 60 µL of each 1 mM stock NAM was added to 6 ml medium for 10 µM solutions. For the DMSO, vehicle control (VC) wells, 6 ml of medium containing DMSO was made, equivalent to 1 µM, and of 10 µM NAM: 10 µL DMSO in 90 µL in water was used as a stock solution, whereby 60 µL of it was added to 6 ml fresh medium for 10 µM-equivalent plates, and 6 µL of this DMSO stock was added to 6 ml medium for 1 µM-equivalent solution. The seeding medium was removed from the wells, and 0.5 mL of NAM- and VC-containing solutions were added to the following ***(Figure 24)*** setup:

The cell plates were placed into the IncuCyte® Live-Cell Analysis System incubator and allowed to warm up to 37° C for 30 minutes before scanning. The automated Imaging and Quantitative Analysis Capture was set to take images every 2 hours (10x magnification) for 72 hours total in an IncuCyte® S3 Live-Cell Analysis System using the Phase Contrast channel. Standard scan type was used, and the data were analysed using integrated software. IncuCyte readouts include confluence, eccentricity data, and movie time-lapses of regions of interest from individual wells.

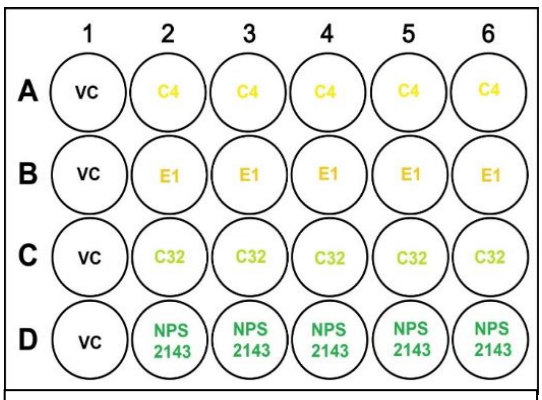

Figure 24. **IncuCyte experimental setup.** VC: vehicle control wells containing 0.1% DMSO; rest wells depict NAM-containing media.

3.7. Cytotoxicity measurements using Lactate Dehydrogenase Assay (LDH)

To determine whether the best-performing selected NCE NAMs cause direct damage to the cell plasma membrane, cytotoxicity assays were carried out on HEK-CaSR and HBECs when treated with 300 nM, 1 µM, 3 µM or 10 µM. The kit used was CyQUANT LDH (#C20300, Invitrogen) Cytotoxicity Assay; I tested two plates for 4-hour and 24-hour exposure for each experimental run. LDH is released into the cell culture medium by damage to the plasma membrane of cells, which was quantified by a coupled enzymatic reaction in which LDH catalyses the conversion of lactate to pyruvate *via* NAD^+ reduction NADH. Oxidation of NADH by diaphorase reduces tetrazolium salt to a red formazan product that can be measured spectrophotometrically at 490 nm. The level of formazan formation is directly proportional to the amount of LDH released into the medium, indicating the level of cytotoxicity. An aliquot of the cell culture medium was transferred to a new plate, and the reaction mixture was added. After a 30-minute incubation, Stop Solution stopped the reaction, and absorbance was measured using a microplate reader. We chose 96-well plates of 10,000 cells per well, as seen in ***Figure 25.***

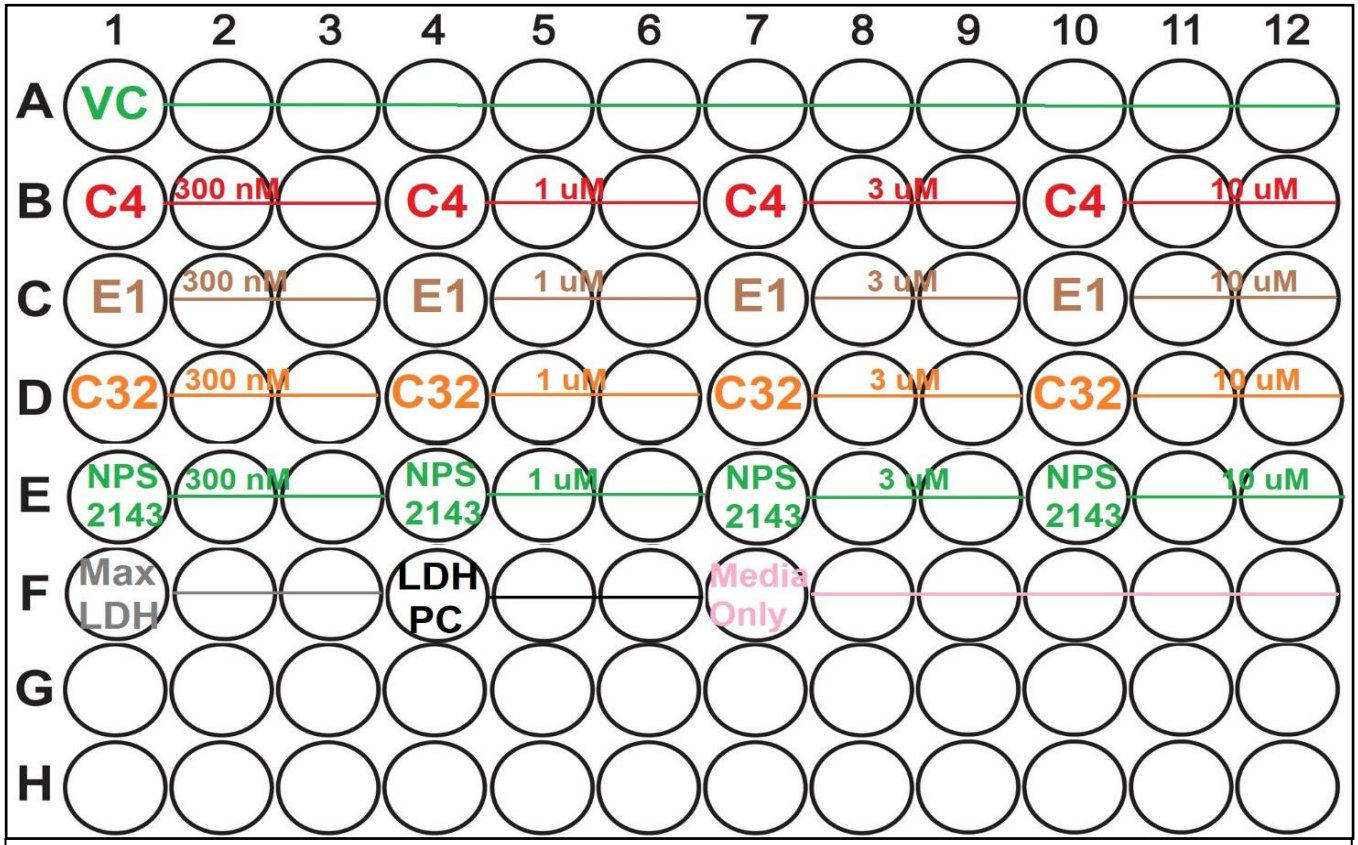

Figure 25. **LDH Experimental 96-well setup.** VC: Vehicle Control, containing 0.1% DMSO; Max LDH wells are exposed to a lysis buffer that causes cell death; LDH PC wells (no cells) of 1% BSA (bovine serum albumin) in PBS (phosphate-buffered saline) is a positive control well; Medium Only wells (no cells) contain only medium, which averaged is used as a background absorbance value.

3.8. Statistical analysis

Statistical analysis was undertaken with GraphPad Prism 9 software (GraphPad Software, USA). Data are expressed as mean and SD; Student's two-tailed, unpaired or paired t-tests were used to compare two data sets; ANOVA with an appropriate post hoc test was used for multiple comparisons.

4. RESULTS

4.1. NCEs NAMs inhibit high Ca^{2+}_o- mediated Ca^{2}_i mobilisation in HEK-CaSR cells

Ca^{2+}_i mobilisation following exposure to the CaSR agonist Ca^{2+}_o is used to indicate CaSR activation, as it is the primary physiological ligand for CaSR (Brown *et al.* 1993). Thus, the ability of NAMs to prevent Ca^{2+}_i-induced changes in CaSR was measured in HEK-CaSR cells. The exposure of HEK-CaSR to the different NAMs reduced Ca^{2+}_o- induced Ca^{2+}_i response, compared to the negative control, as seen in ***Figure 26***. It was determined that the HEK-CaSR we were carrying out this preliminary screening on had become heterogeneous in their population, as there was variability in their response to 5 mM Ca^{2+}_o – some cells had lost CaSR expression. To extract meaningful data from this experiment, Dr Schepelmann analysed the data by only including the top 20% of all responding cells. It was determined that from the NAMs tested, C4, C32, and compound B2.1-E1 significantly inhibited the CaSR.

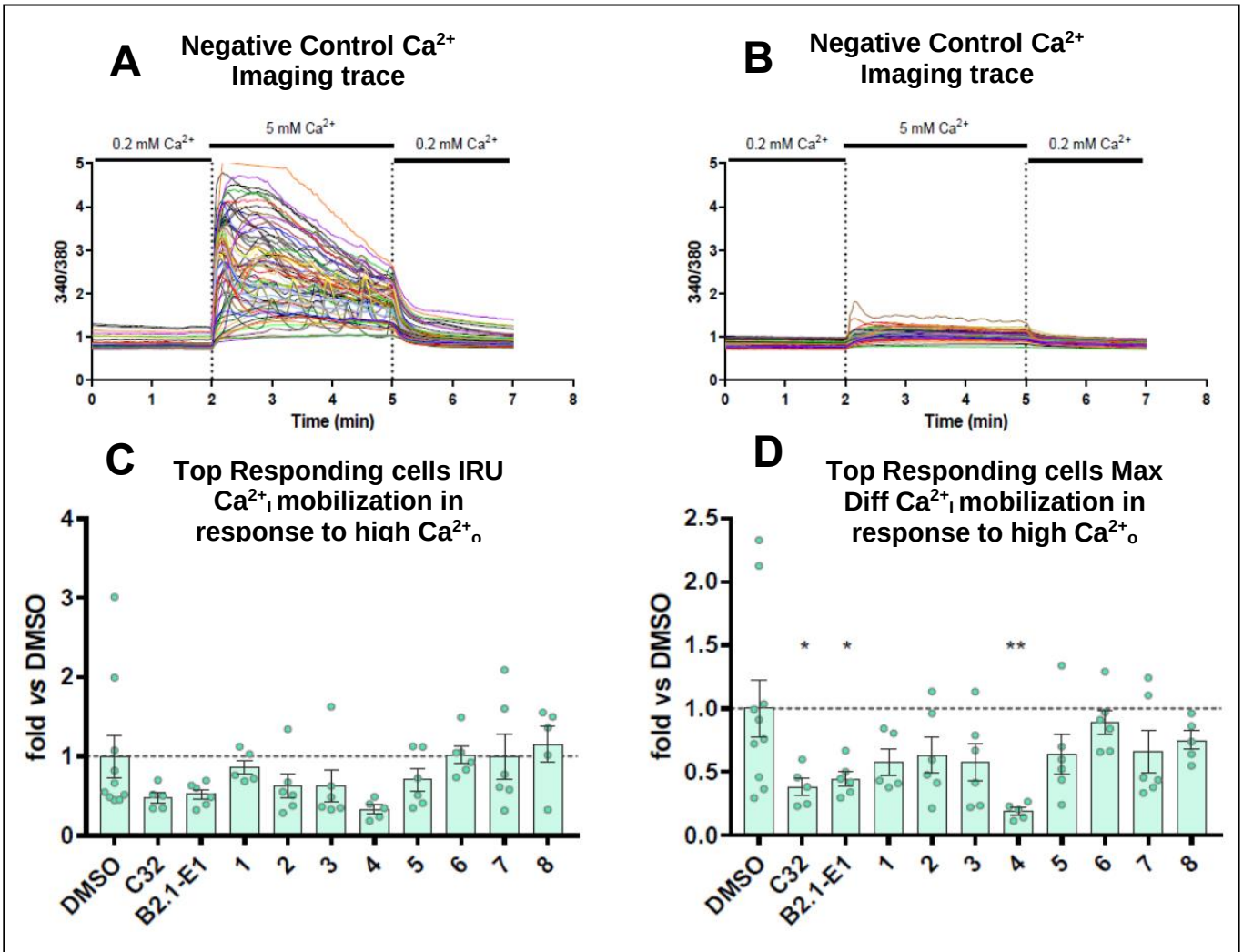

Figure 26. **Dr Martin Schepelmann analysis of preliminary Single Cell Fluorescence Calcium Imaging results.** (**A&B**) Representative traces of HEK-CaSR Ca^{2+}_i mobilization in response to high Calcium, using RSC Olympus Microscope Ca^{2+} Imaging. Coverslips A and B were exposed to the same amount of Ca^{2+}_o, however, results indicate significant variation in responses to 5mM Ca^{2+}_o. This would mean that there is a heterogenous population of HEK-CaSR cells, some of which have lost the expression of the receptor. Thus, only top responding cells were included in the analysis of NAM activity at inhibiting the CaSR activation, using Integrated Response Units (IRU) and Max Fold/Diff trapezoidal calculations of the integral or area under the curve. (**C&D**) results are represented as mean+SEM, and One-Way ANOVA with Dunnett post-test was included to compare the compounds for significant differences to DMSO control or in between groups.

4.2. Freshly thawed HEK-CaSR cells homogenously express the CaSR

Following the initial NAMs activity screening, it was decided that a different batch of HEK-CaSR cells should be used for further experiments. Immunostaining ***(Figure 27)*** of the freshly thawed culture revealed uniform expression of the CaSR and not autofluorescence (right panels), as only nuclei can be seen in the negative control (omission of the primary antibody, left panels).

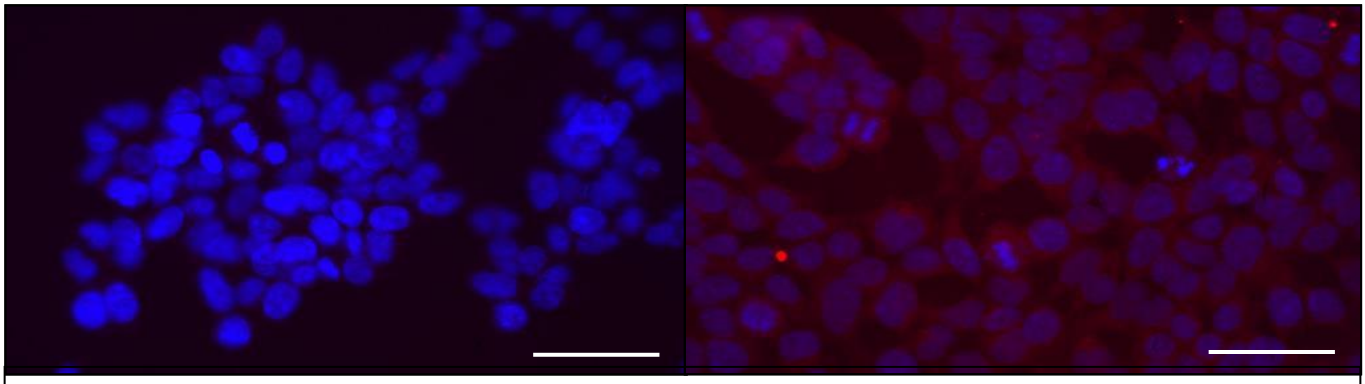

Figure 27. **Imaged Immunofluorescent slide to check for CaSR expression in HEK cells.** CaSR expression (red) and nuclei stain (blue) indicate that there is a homogenous expression of the CaSR in the freshly thawed cells. No primary antibodies were added to the negative control (left), compared to those labelled with CaSR antibodies (right). N=6. Scale bar: 100 µM.

4.3. CaSR NAMs inhibit Ca^{2+}_i mobilisation in HEK-CaSR in response to 5 mM Ca^{2+}_o

The high-throughput ClarioStar Plate Reader experiment allowed us to determine which NAMs had the highest activity at blocking Ca^{2+}_i mobilisation following exposure to 5 mM Ca^{2+}_o. ***Figure 28*** shows that C4 was the most potent, comparable to positive controls NPS2143 and parent compound C32, followed by enantiomer E1. As C5 and C7 were not active at inhibiting the CaSR, they were not included in further experiments.

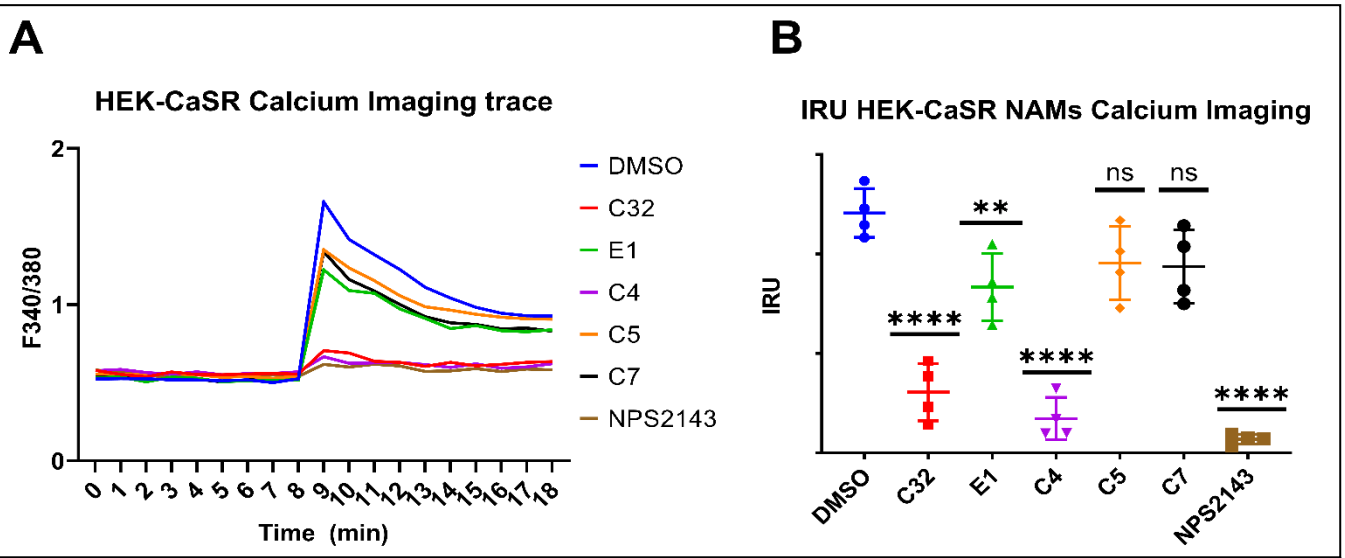

Figure 28. **NCE CaSR NAMs effectively inhibit activation of CaSR.** (**A**) representative Ca^{2+} imaging traces from plate reader; 10 µM NAM activity measured as inhibiting of HEK-CaSR response to the CaSR activator, 5mM Ca^{2+}_o. (**B**) IRU: Integrated Response Units, derived from the trapezoidal integrals under the curve of the trace. Data are presented as Mean+SD. Statistical comparisons: One-way ANOVA. Significance level indicated on graphs using *, N=4 plates.

4.4. CaSR NAMs (10 μM) impair HBEC proliferation and morphology

Prolonged exposure to 10 μM NPS2143 and E1 in HBECs arrests cell proliferation ***(Figure 29)***. 1 μM NAMs did not significantly affect proliferation or cell shape. In total, two plates for each concentration were run.

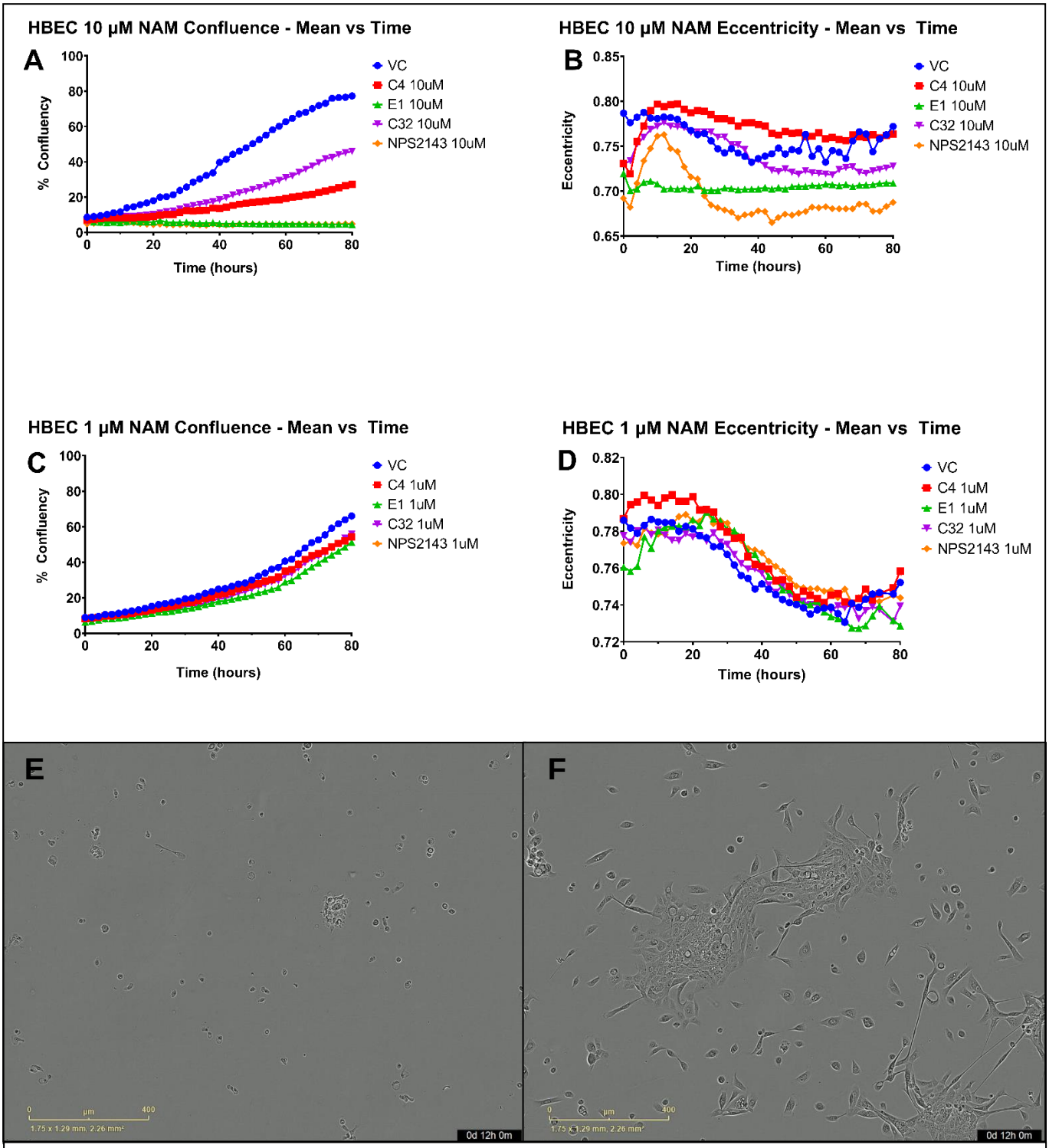

Figure 29. Exposure to 10 μM NAMs E1 and NPS2143 arrests HBEC proliferation. Graphs **A** and **C** indicate phase confluence, which shows complete inhibition of cell proliferation in wells treated with 10 μM NPS2143 and E1, as seen in **E**, movie generated from IncuCyte - HBECs have rounded up, detached, and stopped proliferating. **B and D** are graphs showing the shape changes to the HBECs over the period of NAM exposure, whereby the closer the value is to 1, the “spikier” the cells are, and the closer the value is to 0, the more round they are. **F** is HBEC VC. N=2, n=4.

4.5. Preliminary LDH assay indicates prolonged exposure to NAM E1 at 10 μM causes cell death

24- and 4-hour exposure experiments using LDH assay suggest that while most NAMs do not seem to cause direct plasma membrane damage, NAM E1 does. As seen in ***Figure 30***, this effect is concentration- and exposure time-dependent, as no other concentrations of E1 besides 10 μM caused cell death and 4-hour exposure to E1 caused significantly less cell death than 24-hour exposure.

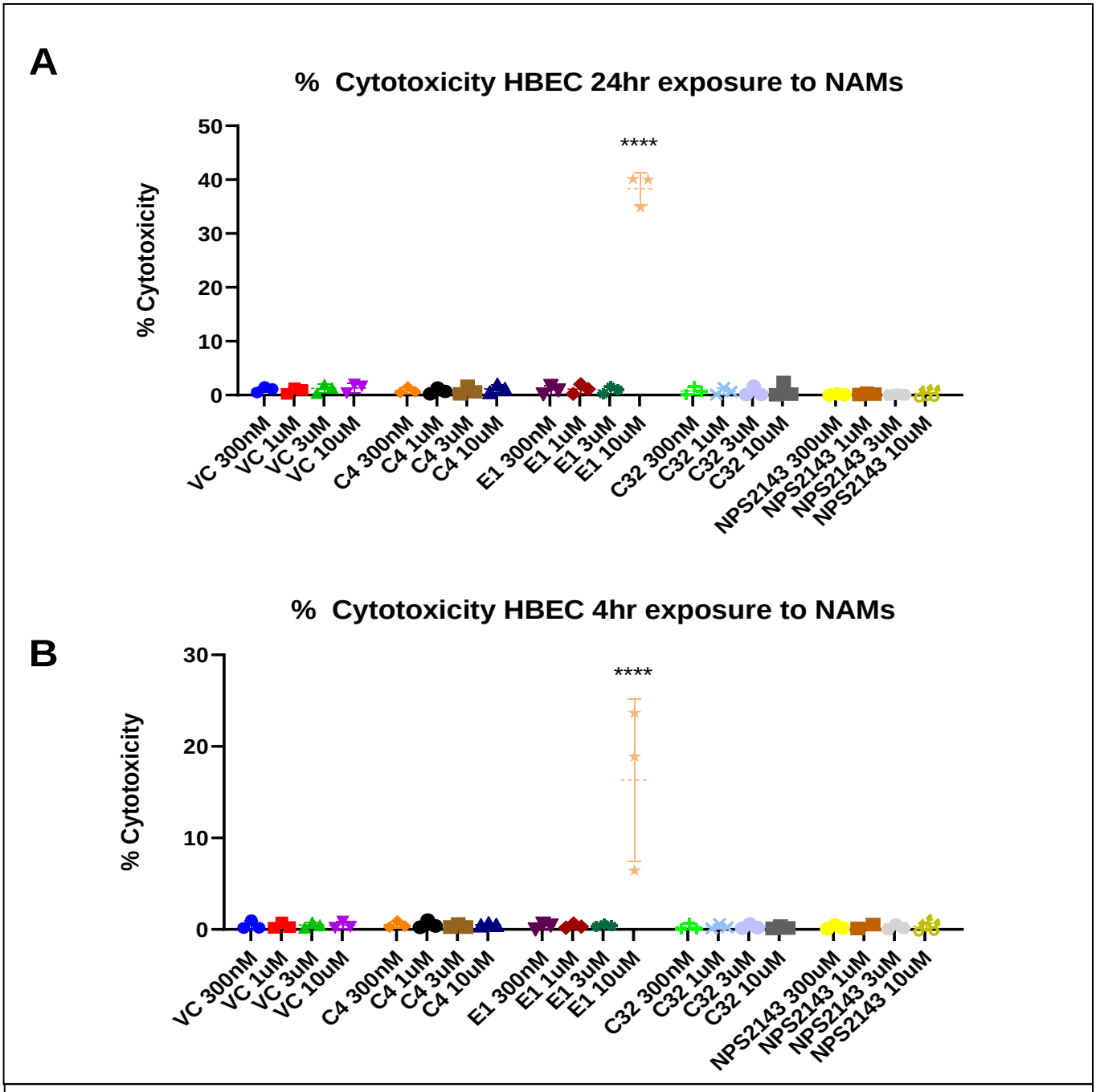

Figure 30. LDH Assay indicates that compound E1 at concentration of 10 μM causes cell death in primary HBEC. (A&B) LDH assay results from 24-hour and 4-hour, respectively, exposure to various concentrations of NAMs. VC groups had equivalent quantities of the solvent DMSO (used to dissolve the NAMs) as the gradient of concentrations for the NAMs. One-way ANOVA indicates that there is no significant difference between any of the groups when compared to any other groups, besides a significant difference in group E1 10 μM to all other groups (p=0.0001), N=3, n=3.

4.6. Optimal concentration for safe inhibition of CaSR is 3 μM of NCEs C4 and E1

Additional Ca^{2+} imaging experiments ***(Figure 31)*** were carried out individually on the best NCE NAMs, E1 and C4, to determine optimal concentrations for activity and lack of cytotoxicity. At 3 μM, E1 and C4 are equipotent at inhibiting the CaSR, both non-cytotoxic at this concentration. 10 μM of E1 confers reduced inhibition of the CaSR compared to equimolar C4, possibly inferring cell damage at that concentration. 100 μM ATP was used at the end of the experiment to confirm cell *via*bility.

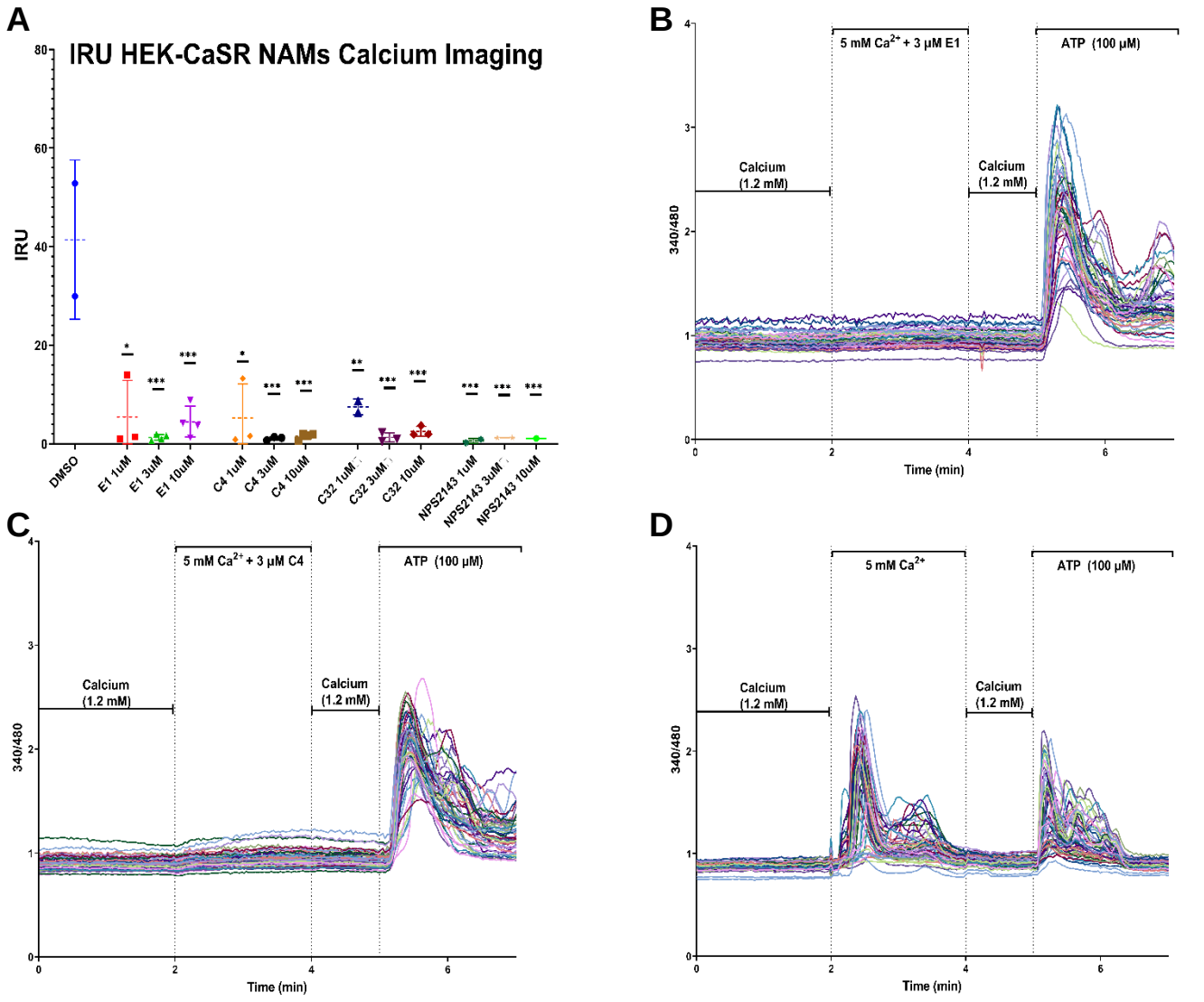

Figure 31. **NAMs C4 and E1 most optimally inhibit CaSR activation at 3uM concentration**. (**A**) IRU analysis of all NAMs and concentrations tested, indicating C4 is more potent and effective at inhibiting the CaSR than E1 at doses higher than 1 μM. (**B:D**) Individual traces of 3 μM E1 and C4, compared to DMSO. 100 μM ATP was introduced at the end of the experiment to confirm cell *via*bility. N=3 per condition.

5. DISCUSSION

5.1. Main Findings

My data show that NCE NAMs effectively block Ca^{2+}_i mobilisation in response to high Ca^{2+}_o. Of all the NCE CaSR NAM tested, the best NCE NAMs are C4 and E1, with optimal concentrations of 1-3 μM. This conclusion is consistent with *in vivo* data gathered from mouse models of airway hyperresponsiveness and allergic asthma, in which the NAM E1 was administered by inhalation, and from studies of PTH release in rats, in which E1 was administered by gavage (Yarova et al, unpublished observations, and data for patent application). *In vitro*, CaSR NAMs significantly reduce proliferation in primary HBECs, with a 10 μM concentration of NPS2143 and E1 completely arresting cell proliferation. In preliminary cytotoxicity LDH assays, 10 μM concentration of the E1 compound appears toxic in HBEC following 24-hour exposure to this compound.

5.2. Chemicostructural suitability of NCE NAMs for inhaled treatment of PDs

As seen in the results section of this work, the most active NCE NAM of the CaSR were C4 and E1, whereby the remaining compounds showed a lack of efficacy or were toxic.

For C5 through to C8, the phenyl at R_1 might be causing conformational instability of the molecule, increasing steric hindrance due to -Ph size and distance to the dichlorobenzene. However, the -Ph substitution in enantiomers C5:C8 could be favourable for lung delivery, as C-Ph substitutions generally confer electronegativity and increase the molecule's hydrophobicity, thus lowering solubility and hygroscopicity (Hansch et al. 1991).

Substituting a methyl group at R_1 increases the molecule's hydrophobicity. It has also been linked with a significant increase in the potency effect of a drug, termed the “magic methyl” effect, sometimes enhancing target binding affinity 100- to 1000-fold (Aynetdinova *et al*. 2021). Methyl groups additionally increase lipophilicity, but the most significant improvements in activity have arisen from coupling the conformational gain with the burial of the methyl group in a hydrophobic region of the protein (Leung *et al*. 2012). Methyl substitutions ortho to an aryl ring can improve activity by inducing a substantial torsional twist, which leads to a favourable conformational change if strategically placed. Methyl groups do not necessarily have to be added at the beginning of synthesis, as late-stage installation can be carried out by oxidative C-H methylation (Feng *et al*. 2020).

There was no significant difference between the inhibitory potency of the CaSR between C32 and E1; thus, presumably, the R_1 substitution of the isobutyl moiety of E1 might not confer superior negative CaSR allostery directly. The isobutyl chain might not be extended/ polar enough to allow NAM binding to the Trp818 or Tyr825 sites of the CaSR (cyan-coloured sites in ***Figure 19***). It is unclear whether, in NCE C4, the C-Me substitution confers any superior binding to the active site of the intracellular portion of the CaSR; however, it might be that the isobutyl substitution in E1 is causing structural instability or poor selectivity for the CaSR.

As summarised by Collingwood *et al*. in 2009, the ideal lung delivery drug *via* dry-powder inhalation would have properties ***(Table 2)*** that allow it to be micronised to the size range of 1-5 μM for appropriate aerodynamic diameter, high potency in the low nanomolar range, low in solubility and dissolution rate, pH-independent, high in crystallinity, low in hygroscopicity (to not form solid bridge aggregations and increase in particle size) and low to moderate in lipophilicity (to not be cleared by cilia-propelled mucous). The micronised drug is blended with an excipient, usually a larger carrier, commonly lactose, and delivered with an inhaler.

Table 2. **Mean physicochemical properties of marketed small molecule oral inhalation drugs**

Physicochemical Property	10^{th} to 90^{th} P_r
The logarithm of octanol/water distribution coefficient (cLogD) (pH 7.4)	-6.3-3.8
Molecular weight (Da)	225-482
Polar surface area (Å) (MWt/logP)	65-178
The logarithm of octanol/water partition coefficient (cLogP)	-1.0-4.1
Hydrogen bond donors	2-6
Hydrogen bond acceptors	4-11

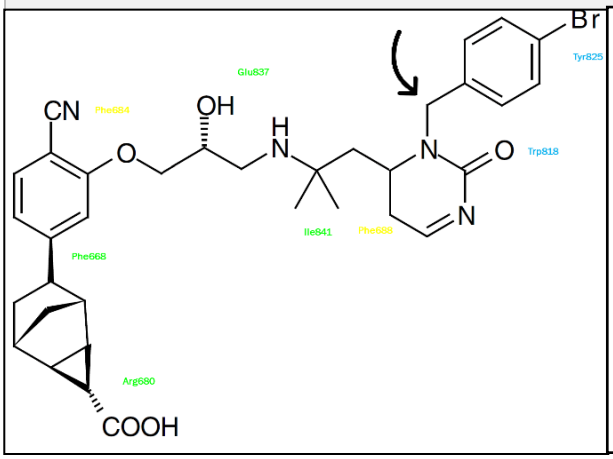

Figure 32. **"Designer" most active CaSR NAM?** Combined amino alcohol CaSR NAMs JTT-355 enantiomer 3b and qinazoline-2-one CaSR NAM AXT914; can be realized; COOH component is bridged to the aromatic ring with a bulky and greasy ring system (which increases potency and reduces oral bioavailability). Green and yellow: amino alcohol binding sites; yellow and blue: Quinazoline-2-ones; R_1 and R_2 positions free, potential to further optimise properties for inhaled lung delivery. Substituting methyl to arrow position might incur torsional twist, which could tilt the molecule so that the charged bromine binds Quinazoline-2-ones sites. Empirical formula: $C_{35}O_5N_4H_{37}Br_1$; MW: 673.59

5.3. CaSR in PDs, and their treatment with inhaled CaSR NAMs

AM-derived pro-inflammatory IL-1β has been shown to drastically decrease 15-PGDH, the enzyme that degrades PGE_2 (Arima *et al*. 2018), which would increase PGE_2, and, if inflammation is sustained, could be a first step towards locking the chronic inflammatory-driven pathologic wound healing. PNECs respond to hypoxia and several environmental stimuli and mechanical forces (Cutz *et al*. 2013). NEB O_2-sensing complex consists of an NADPH oxidase coupled to an O_2-sensitive K^+ channel in the plasma membrane. Potassium channels on PNECs close in hypoxic or inflammatory conditions, while voltage-sensitive Ca^{2+} channels open up to facilitate the influx of extracellular Ca^{2+}, leading to Calcium-dependent exocytosis of dense-core vesicles (DCVs) (Cutz *et al*. 2013). The release of DCV affects the physiological functions of lung tissues through direct or indirect interaction *via* vagal afferent and central nerve fibres. PNECs express prolyl hydroxylase domain enzymes (PHDs) which respond to hypoxia by catalysing the hydroxylation of hypoxia-inducible factor 1 (HIF-1), thus stabilising it (Semenza, 2009). Importantly, loss of PHDs provokes a PNEC hyperplasia phenotype (Pan *et al*. 2012, 2016). Histologically, PNEC hyperplasia, often associated with increased sensitivity to chemical stimuli (Tashkin *et al*. 1996), has been observed in asthmatic patients' lungs (Adriaensen and Sui *et al*. 2018). In addition, allergen challenges

increase PNECs in animal models (Bousbaa and Fleury-Feith, 1991). The progressively worsening oxygen conditions and mechanically differentiating (gradient) environment thus cause NEBs overactivation and proliferation. NEB increased presence and activity could potentially be driving total lung hyperplasia, as well as CaSR overexpression and overactivation, activating and recruiting further innate and extrapulmonary immune cells. Furthermore, mechanical stretch activates the CaSR (Wells *et al*. 2020) and enhances 5-HT release from NEBs in rabbit models, suggesting that PNECs transduce mechanical information into neurotransmission (Pan *et al*. 2006). PNECs are shown to be the cell type that contains most CaSR expression within the lung (Lembrechts *et al*. 2013). The CGRP (rodent equivalent of bombesin) produced by PNECs stimulates ILC2s, enriched at airway branching points, triggering immune responses to allergens. Sui *et al*. in 2018 demonstrated that endodermal Ascl1-knockout mice, which are PNEC deficient, lack the allergen-induced asthmatic response. Intratracheal administration of CGRP and gamma-aminobutyric acid (GABA) to these mutants recovered the immune response, including goblet cell hyperplasia. NEBs thus directly promote neuroendocrine-dependent increased inflammatory influx through vagal parasympathetic and sympathetic innervation.

In asthma, AHR generally leads to progressive airway remodelling and airway wall thickening, ever-increasing overall airflow obstruction (Hogg and Timens 2009). Human PNECs express OR2W1, a member of the olfactory receptor family, and respond to inhaled volatile chemicals, eventually releasing 5-HT to induce ASMC contraction (Gu *et al*. 2014). The naphthalene-induced acute epithelial injury repair model revealed that epithelial recovery preferentially occurs around nodal NEBs, whereby club cells and PNECs proliferate in NEBs during regeneration *via* transient-amplifying variant club (vClub) cells (Reynolds *et al*. 2000). The application of extracellular potassium rapidly mobilises intracellular Ca^{2+} in PNECs, followed by a delayed increase of intracellular Ca^{2+} in neighbouring vClub cells (De Proost *et al*. 2008). PNEC depolarisation evokes Calcium-mediated ATP release and activates them *via* P2Y purinergic receptors, suggesting a functional coupling between PNECs and vClub cells (Schnorbusch *et al*. 2013). Thus, NEBs may supply niche factors like GABA and bombesin, promoting CC differentiation into goblet cells (Sui *et al*. 2018). BEC hyperplasia stimulates mucous hyperproduction, leading to obstruction of the small airway lumen. AMs in PDs have reduced phagocytotic qualities and exhibit 10-fold increased secretion of inflammatory and fibrotic cytokines. An environment of chronic PRR activation would cause M1 macrophage activity through inflammasome activation whilst simultaneously promoting AAM polarisation due to the over-expression and overactivation of the CaSR and reduced cAMP levels. The polarisation from M2 to M1 could also be directly mediated by low oxygen availability during foetal hypoxia or chronic injury-induced hypoxia (Rudloff *et al*. 2021). This hypoxia-mediated shift from anti-inflammatory M2 to pro-inflammatory M1 macrophages was even more prominent in fetuin-A KO mice (Rudloff *et al*. 2021). Levels of serum protein fetuin-A were seen to have an inverse relation with disease progression, whereby more severe COPD patients had lower levels of fetuin-A (Minas *et al*. 2012). Fetuin-A stabilises Ca^{2+} and phosphate into 70-100 nm-sized colloidal calciprotein particles (CPPs), which are taken up by monocytes and macrophages through CaSR-dependent constitutive macropinocytosis, triggered by increases in Ca^{2+}_o (Canton *et al*. 2016). Enhanced constitutive micropinocytosis of CPPs, which exceeds fetuin-A-binding capacity, results in increased NLRP3 inflammasome activation, IL-1β release and thus

increased lysosomal activity (Jäger *et al*. 2020). This feedback is exacerbated in genetic predispositions that might bias AM populations into the alternatively activated phenotype, synergistically with ongoing chronic inflammation tilts the total pulmonary homeostasis *via* numerous positive feedback loops into chronic dysfunctional repair and extracellular matrix deposition **(Figure 33)**.

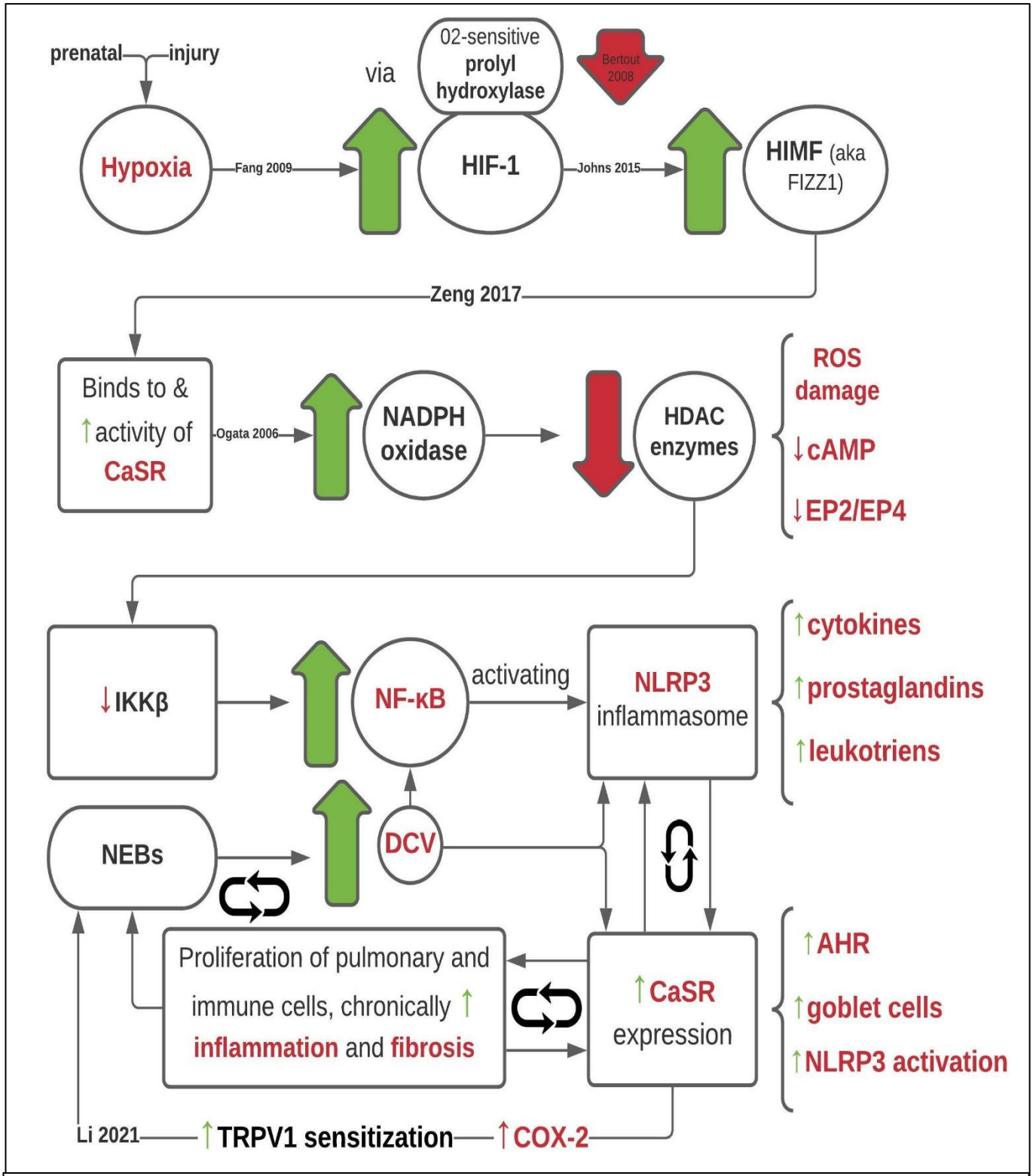

Figure 33. **Diagrammatic representation of CaSR involvement in PDs.** Direct damage to lung epithelium or chronic hypoxia activates the CaSR, which activates the NLRP3 inflammasome, increasing the expression of CaSR in the lung in a positive feedback loop, which further activates the NLRP3 inflammasome. Increased CaSR expression and activation causes pulmonary and immune cell activation, importantly causing NEBs to release dense-core vesicles (DCV) containing neuropeptides and other inflammatory agents, sealing the positive feedback loop. CaSR NAMs inhibit **these** effects.

Pulmonary resident cells that express the CaSR include airway smooth muscle cells (ASM), neuroepithelial bodies (Lembrechts *et al.* 2013), bronchial epithelial cells (Yarova *et al.* 2015), fibroblasts (Wolffs *et al.* 2020), eosinophils, neutrophils, macrophages (Rossol *et al*. 2012), dendritic cells (Mansfield *et al.* 2019), ILC2s (Mansfield *et al*. unpublished), and potentially others, or all other pulmonary cells. Ca^{2+} (together with L-Trp) is the primary endogenous and orthosteric agonist of the CaSR. However, CaSR functions as a multimodal extracellular cation sensor (Riccardi and Kemp 2012). Its activators include, but are not limited to, eosinophilic polyamines, allergens, and urban particulate matter (UPM) (Mansfield *et al.* 2019). The higher the ligand charge, the more potent, quicker binding effect to the orthosteric sites of CaSR. The CaSR is the master controller for serum ionised Ca^{2+} levels (Brown *et al.* 1993) activated by various polyvalent cations (especially the trivalent Ca^{2+}, but also Mg^{2+}) (Brown *et al*. 1990) eosinophil cationic protein and major basic protein (well-established asthma markers).

The receptor is overexpressed in ASM cells from asthmatic patients (Yarova *et al.* 2015), and its activation *via* agonists may be presented in the airway in the form of smoke, car fumes or bacterial/ viral infections. It may cause the reduced threshold/ increased airway sensitisation to Ca^{2+} ions (Yarova *et al.* 2015) that is seen in asthma. In asthma, for example, irritants, allergens or polycations (Kurosawa *et al.* 1992) bind to the CaSR of pulmonary, causing a rapid increase in cytoplasmic Ca^{2+}, followed by a much slower recovery rate to baseline levels, as well as an increased arginase activity, which diverts L-arginine towards productions of spermine, spermidine and putrescine (Maarsingh *et al.* 2008). These polyamines have anti-inflammatory properties in normal physiology but seem to drive disease progression *via* CaSR over-activation. In eosinophils, the CaSR overactivation and subsequent Ca^{2+}_i mobilisation cause a further release of polycations, which recruits more eosinophils to the airway, inducing a positive feedback loop that progressively furthers inflammation and airway remodelling. Increased inflammation and altered Ca^{2+} homeostasis increase cationic properties that drive further CaSR activation and increase of Ca^{2+}, thus increasing bronchoconstriction *via* indirect inhibition due to low levels of cAMP and recruitment of more inflammatory cells, creating a positive-feedback loop.

In-house experiment results can be seen in ***Figure 34***, summarising so-far proven benefits of NAM treatment for PDs. Our group has shown that inhibition of the CaSR can disrupt this positive feedback loop by topical CaSR NAM therapy and reduce inflammation, receptor expression and AHR (Yarova *et al.* 2015). Leach *et al.* (2016) indicate that NAMs hold the CaSR in an inactive state through hydrogen bond interactions – NAM binding to CaSR restricts movement in 7TMD, possibly adhering the NAM onto cells. In-house HBEC *in vitro* studies by Dr Bethan Mansfield also indicate that NAMs reduce UPM-induced CaSR activation of DC, thus inhibiting their maturation and cytokine release (Mansfield *et al.* 2020). Other in-house experiments by Dr Kasope Wolffs have also indicated that TGF-B treatment increased the baseline expression of CaSR in HLFs and that NAM treatment significantly reduces TGF-B-induced collagen secretion, proliferation, and αSMA expression (Wolffs *et al*. 2020). In arterial smooth muscle of pulmonary vessels, CaSR activation causes vasoconstriction and proliferation of these cells, whereby CaSR NAMs prevent this and the progression of models of pulmonary hypertension (Tang *et al*. 2016). *In vivo* experiments indicated that inhaled NAMs directly decrease eosinophilic infiltration, remodelling, and AHR without having a significant systemic effect on serum PTH (Yarova *et al*. 2021).

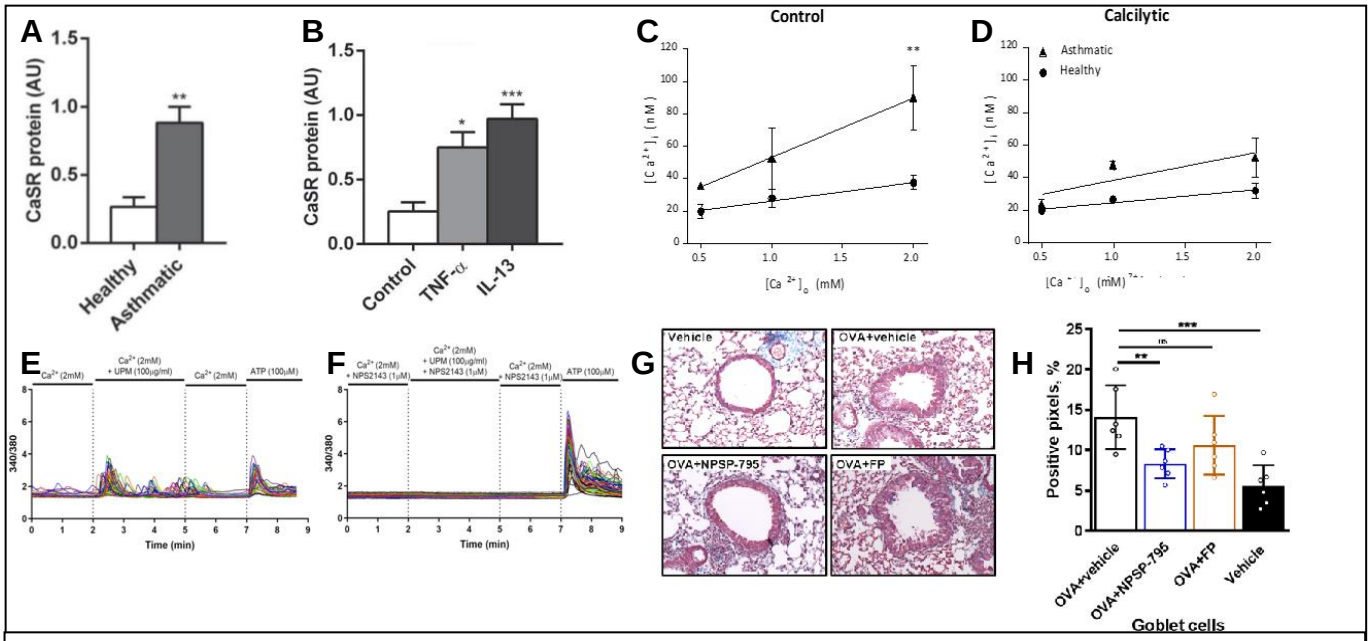

Figure 34. Summary of results from in-house experiments. (**A**) Analysis indicating increased CaSR expression in human ASM from asthmatics in comparison to healthy control. (**B**) Exposing healthy cells to asthma-related cytokines causes an increase in CaSR expression. (**C&D**) CaSR NAMs subdue pathologically increased $Ca^{2+}{}_i$ response to $Ca^{2+}{}_o$ in asthmatic ASMs cells to healthy physiological levels, ameliorating AHR (**A:D** Yarova *et al.* 2015). (**E&F**) UPM acts on the CaSR and exposure to 1 μM NAM NPS2143 abolishing response to UPM (Mansfield *et al.* 2019). (**G&H**) Inhaled NAMs reduce inflammatory markers in OVA sensitised and challenged BalbC mice as effectively as the current standard of care (corticosteroid fluticasone propionate), but also additionally reduce aspects of remodelling, whereas CS do not. The analysis includes Masson's trichrome-stained lung sections, whereby the StrataQuest image analysis software allowed us to semi-quantitatively measure differences in total lung area and differences in goblet cells, both of which NAMs reduce (Yarova *et al*. 2021).

6. Conclusions

NCE NAMs effectively block CaSR-mediated $Ca^{2+}{}_i$ mobilisation in response to high $Ca^{2+}{}_o$. My data show that from the NCE CaSR NAM tested, the best NCE NAMs are C4 and E1, with optimal concentrations of 1-3 μM. This conclusion is consistent with extensive *in vivo* data, which indicates the efficacy and safety of E1 when administered by inhalation in murine models of airway hyperresponsiveness and asthma. By potentially targeting some of the root causes of disease, CaSR NAMs provide an alternative (and possibly superior) replacement therapy for asthma and other pulmonary conditions, such as COPD and IPF.

7. Future Directions

Constraints brought about by the COVID-19 pandemic caused this study to be cut short – our team wanted to investigate the long-term storage of NCE CaSR NAMs, the pharmacokinetic profile of NCE CaSR NAMs, delivered by intra-tracheal administration (Penn Century devise), and to determine the physicochemical properties of micronised drugs and their compatibility with inhaled use. Additionally, using a next-generation lung impactor device in collaboration with Professor James Birchall at Cardiff University School of Pharmacy, we wanted to study the deposition of the best-performing micronised NCE CaSR NAM to determine whether this formulation would have optimal pharmacodynamic properties for inhaled lung delivery. Additionally, *in vivo* drug absorption, metabolism and disposition studies will have to be performed to determine the effects of long-term NAM exposure in healthy and diseased cells.

8. Limitations

As aforementioned, COVID-19 placed constraints on conducting experiments; thus, this study would benefit from a higher sample size for every test. We only trialled the NCE CaSR NAMs *in vitro* on healthy HBECs. Testing this drug in asthmatic cells, which are innately more “leaky”, could determine whether the NAMs might cause irritancy.

Acknowledgements

I cannot thank Professor Riccardi enough for accepting me for this role in her laboratory. This position has been a life-changing opportunity that has made me grow in more ways than I could imagine. I have received stellar attention, direction, laboratory training and cooperation from our team: Professor Daniela Riccardi, Dr Martin Schepelmann, Dr Bethan Mansfield, Dr Kasope Wolffs and Richard Bruce. I also want to thank Dr Mark Young for helping me troubleshoot and assisting me with the high-throughput ClarioStar PlateReader instrument. I thank Professor Nick Allen for allowing our team to use the IncuCyte Live-Cell imaging system when it was in BIOSCI, Dr Andrew Jefferson when it was in the Hayden Ellis building, and PhD student Emily Maguire, who assisted me with the IncuCyte. Last but not least, I thank the team that synthesised the NCEs, formulated in collaboration with Cardiff University School of Pharmacy, whereby the co-creators are Professor Andrea Brancale, Dr Martin Schepelmann and Dr Salvatore Ferla.

Thank you, Cardiff University! I hope to have been helpful and continue contributing to this stellar institution's life and research.

References

Adenuga, D., Caito, S., Yao, H., Sundar, I.K., Hwang, J.-W., Chung, S. and Rahman, I. 2010. Nrf2 Deficiency Influences Susceptibility to Steroid Resistance via HDAC2 Reduction. *Biochemical and Biophysical Research Communications* 403(3-4), pp. 452–456. doi: 10.1016/j.bbrc.2010.11.054.

Agard, M., Asakrah, S. and Morici, L.A. 2013. PGE2 Suppression of Innate Immunity during Mucosal Bacterial Infection. *Frontiers in Cellular and Infection Microbiology* 3(45), pp. 1–45. Available at: https://www.frontiersin.org/article/10.3389/fcimb.2013.00045.

Aktan, F. 2004. iNOS-mediated Nitric Oxide Production and Its Regulation. *Life Sciences* 75(6), pp. 639–653. doi: 10.1016/j.lfs.2003.10.042.

Allard, B., Panariti, A. and Martin, J.G. 2018. Alveolar Macrophages in the Resolution of Inflammation, Tissue Repair, and Tolerance to Infection. *Frontiers in Immunology* 9(1777). doi: 10.3389/fimmu.2018.01777.

Arima, K. et al. 2018. Downregulation of 15-hydroxyprostaglandin Dehydrogenase by interleukin-1β from Activated Macrophages Leads to Poor Prognosis in Pancreatic Cancer. *Cancer Science* 109(2), pp. 462–470. doi: 10.1111/cas.13467.

ATS 2000. Idiopathic Pulmonary Fibrosis: Diagnosis and Treatment. *American Journal of Respiratory and Critical Care Medicine* 161(2), pp. 646–664. doi: 10.1164/ajrccm.161.2.ats3-00.

Aynetdinova, D. et al. 2021. Installing the “Magic Methyl” – C–H Methylation in Synthesis. *Chemical Society Reviews* 50(9), pp. 5517–5563. doi: 10.1039/d0cs00973c.

Balakrishna, S. et al. 2014. TRPV4 Inhibition Counteracts Edema and Inflammation and Improves Pulmonary Function and Oxygen Saturation in Chemically Induced Acute Lung Injury. *American Journal of Physiology-Lung Cellular and Molecular Physiology* 307(2), pp. L158–L172. doi: 10.1152/ajplung.00065.2014.

Ballantyne, S.J. et al. 2007. Blocking IL-25 Prevents Airway Hyperresponsiveness in Allergic Asthma. *Journal of Allergy and Clinical Immunology* 120(6), pp. 1324–1331. doi: 10.1016/j.jaci.2007.07.051.

Barkauskas, C.E. et al. 2013. Type 2 Alveolar Cells Are Stem Cells in Adult Lung. *Journal of Clinical Investigation* 123(7), pp. 3025–3036. doi: 10.1172/jci68782.

Barnes, P.J. 2001. Th2 Cytokines and asthma: an Introduction. *Respiratory Research* 2(2), p. 64. doi: 10.1186/rr39.

Barr, R.G., Rowe, B.H. and Camargo, C.A. 2003. Methylxanthines for Exacerbations of Chronic Obstructive Pulmonary Disease. *Cochrane Database of Systematic Reviews* 2(CD002168). doi: 10.1002/14651858.cd002168.

Baum, P.R. et al. 1994. Molecular Characterization of Murine and Human OX40/OX40 Ligand systems: Identification of a Human OX40 Ligand as the HTLV-1-regulated Protein gp34. *The EMBO Journal* 13(17), pp. 3992–4001. doi: 10.1002/j.1460-2075.1994.tb06715.x.

Bertout, J.A., Patel, S.A. and Simon, M.C. 2008. The Impact of O2 Availability on Human Cancer. *Nature Reviews Cancer* 8(12), pp. 967–975. Available at: https://www.ncbi.nlm.nih.gov/pmc/articles/PMC3140692/ [Accessed: 8 December 2019].

BéruBé, K. 2009. In Vitro Models of Inhalation Toxicity and Disease. *ATLA* 37(89-141)

Billington, C.K., Ojo, O.O., Penn, R.B. and Ito, S. 2013. cAMP Regulation of Airway Smooth Muscle Function. *Pulmonary Pharmacology & Therapeutics* 26(1), pp. 112–120. doi: 10.1016/j.pupt.2012.05.007.

Boser, S.R. et al. 2017. Myofibroblasts Are Increased in the Lung Parenchyma in Asthma. Loukides, S. ed. *PLOS ONE* 12(8), p. e0182378. doi: 10.1371/journal.pone.0182378.

Boulet, L.-P., Turcotte, Hé., Laviolette, M., Naud, F., Bernier, M.-C., Martel, S. and Chakir, J. 2000. Airway Hyperresponsiveness, Inflammation, and Subepithelial Collagen Deposition in Recently Diagnosed versus Long-standing Mild Asthma. *American Journal of Respiratory and Critical Care*

Medicine 162(4), pp. 1308–1313. doi: 10.1164/ajrccm.162.4.9910051.

Brand, P., Schulte, M., Wencker, M., Herpich, C.H., Klein, G., Hanna, K. and Meyer, T. 2009. Lung Deposition of Inhaled 1-proteinase Inhibitor in Cystic Fibrosis and 1-antitrypsin Deficiency. *European Respiratory Journal* 34(2), pp. 354–360. doi: 10.1183/09031936.00118408.

Brannan, J.D. and Lougheed, M.D. 2012. Airway Hyperresponsiveness in Asthma: Mechanisms, Clinical Significance, and Treatment. *Frontiers in Physiology* 3(460). doi: 10.3389/fphys.2012.00460.

Brennan, S.C. et al. 2013. Calcium Sensing Receptor Signalling in Physiology and Cancer. *Biochimica Et Biophysica Acta (BBA) - Molecular Cell Research* 1833(7), pp. 1732–1744. doi: 10.1016/j.bbamcr.2012.12.011.

Brewer, A.C. 2021. Physiological Interrelationships between NADPH Oxidases and Chromatin Remodelling. *Free Radical Biology and Medicine* 170((2021)), pp. 109–115. doi: 10.1016/j.freeradbiomed.2021.01.052.

Brown, E.M. et al. 1993. Cloning and Characterization of an Extracellular Ca2+-sensing Receptor from Bovine Parathyroid. *Nature* 366(6455), pp. 575–580. doi: 10.1038/366575a0.

Buchman, A.L. 2001. Side Effects of Corticosteroid Therapy. *Journal of Clinical Gastroenterology* 33(4), pp. 289–294. doi: 10.1097/00004836-200110000-00006.

Caceres, A.I. et al. 2009. A Sensory Neuronal Ion Channel Essential for Airway Inflammation and Hyperreactivity in Asthma. *Proceedings of the National Academy of Sciences* 106(22), pp. 9099–9104. doi: 10.1073/pnas.0900591106.

Cai, L.-M. et al. 2019. Thymic Stromal Lymphopoietin Induced Early Stage of epithelial-mesenchymal Transition in Human Bronchial Epithelial Cells through Upregulation of Transforming Growth Factor Beta 1. *Experimental Lung Research* 45(8), pp. 221–235. doi: 10.1080/01902148.2019.1646841.

Caltabiano, S. et al. 2013. Characterization of the Effect of Chronic Administration of a calcium-sensing Receptor antagonist, ronacaleret, on Renal Calcium Excretion and Serum Calcium in Postmenopausal Women. *Bone* 56(1), pp. 154–162. doi: 10.1016/j.bone.2013.05.021.

Camelo, A., Dunmore, R., Sleeman, M.A. and Clarke, D.L. 2014. The epithelium in idiopathic pulmonary fibrosis: breaking the barrier. *Frontiers in Pharmacology* 4(173). doi: 10.3389/fphar.2013.00173.

Canning, B.J. and Fischer, A. 2001. Neural Regulation of Airway Smooth Muscle Tone. *Respiration Physiology* 125(1-2), pp. 113–127. doi: 10.1016/s0034-5687(00)00208-5.

Canton, J., Schlam, D., Breuer, C., Gütschow, M., Glogauer, M. and Grinstein, S. 2016. Calcium-sensing Receptors Signal Constitutive Macropinocytosis and Facilitate the Uptake of NOD2 Ligands in Macrophages. *Nature Communications* 7(1). doi: 10.1038/ncomms11284.

Caramori, G. 2003. Nuclear Localisation of p65 in Sputum Macrophages but Not in Sputum Neutrophils during COPD Exacerbations. *Thorax* 58(4), pp. 348–351. doi: 10.1136/thorax.58.4.348.

Carrell, R.W. and Lomas, D.A. 2002. Alpha1-Antitrypsin Deficiency — A Model for Conformational Diseases. *New England Journal of Medicine* 346(1), pp. 45–53. doi: 10.1056/nejmra010772.

Cazzola, M. and Donner, C.F. 2000. Long-Acting β2 Agonists in the Management of Stable Chronic Obstructive Pulmonary Disease. *Drugs* 60(2), pp. 307–320. doi: 10.2165/00003495-200060020-00005.

Chang, W., Pratt, S., Chen, T.-H., Nemeth, E., Huang, Z. and Shoback, D. 1998. Coupling of Calcium Receptors to Inositol Phosphate and Cyclic AMP Generation in Mammalian Cells and Xenopus laevis Oocytes and Immunodetection of Receptor Protein by Region-Specific Antipeptide Antisera. *Journal of Bone and Mineral Research* 13(4), pp. 570–580. doi: 10.1359/jbmr.1998.13.4.570.

Chavez-Abiega, S. et al. 2019. Sensing Extracellular Calcium – an Insight into the Structure and Function of the Calcium-Sensing Receptor (CaSR). *Advances in Experimental Medicine and Biology* 1131, pp. 1031–1063. doi: 10.1007/978-3-030-12457-1_41.

Chi, Y.S., Jong, H.G., Son, K.H., Chang, H.W., Kang, S.S. and Kim, H.P. 2001. Effects of Naturally Occurring Prenylated Flavonoids on Enzymes Metabolizing Arachidonic acid: Cyclooxygenases and Lipoxygenases. *Biochemical Pharmacology* 62(9), pp. 1185–1191. doi: 10.1016/s0006-2952(01)00773-0.

Cho, K.-A. et al. 2012. IL-33 Induces Th17-mediated Airway Inflammation via Mast Cells in ovalbumin-challenged Mice. *American Journal of Physiology-Lung Cellular and Molecular Physiology* 302(4), pp. L429–L440. doi: 10.1152/ajplung.00252.2011.

Choi, J.Y., Lee, H.Y., Hur, J., Kim, K.H., Kang, J.Y., Rhee, C.K. and Lee, S.Y. 2018. TRPV1 Blocking Alleviates Airway Inflammation and Remodeling in a Chronic Asthma Murine Model. *Allergy, Asthma & Immunology Research* 10(3), p. 216. doi: 10.4168/aair.2018.10.3.216.

Coffman, R.L. et al. 1988. The Role of Helper T Cell Products in Mouse B Cell Differentiation and Isotype Regulation. *Immunological Reviews* 102(1), pp. 5–28. doi: 10.1111/j.1600-065x.1988.tb00739.x.

Cohn, L., Tepper, J.S. and Bottomly, K. 1998. Cutting Edge: IL-4-Independent Induction of Airway Hyperresponsiveness by Th2, but Not Th1, Cells. *The Journal of Immunology* 161(8), pp. 3813–3816. Available at: http://www.jimmunol.org/content/161/8/3813.

Coll, R., O'Neill, L. and Schroder, K. 2016. Questions and Controversies in Innate Immune research: What Is the Physiological Role of NLRP3? *Cell Death Discovery* 2(1). doi: 10.1038/cddiscovery.2016.19.

Collingwood, S., Lock, R. and Searcey, M. 2009. Optimizing Drugs for Local Delivery. *Drug News & Perspectives* 22(10), p. 627. doi: 10.1358/dnp.2009.22.10.1443395.

Corrigan, C.J. 2020. Calcilytics: a non-steroidal Replacement for Inhaled Steroid and SABA/LABA Therapy of Human asthma? *Expert Review of Respiratory Medicine* 14(8), pp. 807–816. doi: 10.1080/17476348.2020.1756779.

Cosman, F. et al. 2015. A Phase 2 Study of MK-5442, a calcium-sensing Receptor antagonist, in Postmenopausal Women with Osteoporosis after long-term Use of Oral Bisphosphonates. *Osteoporosis International* 27(1), pp. 377–386. doi: 10.1007/s00198-015-3392-7.

Costanzo, L.S. 2013. *Physiology.* Philadelphia, Pa: Saunders/Elsevier.

Crapo, J.D., Barry, B.E., Gehr, P., Bachofen, M. and Weibel, E.R. 1982. Cell Number and Cell Characteristics of the Normal Human Lung. *The American Review of Respiratory Disease* 126(2), pp. 332–7. doi: DOI: 10.1164/arrd.1982.126.2.332.

Croston, G.E., Cao, Z. and Goeddel, D.V. 1995. NF-κB Activation by Interleukin-1 (IL-1) Requires an IL-1 Receptor-associated Protein Kinase Activity. *Journal of Biological Chemistry* 270(28), pp. 16514–16517. doi: 10.1074/jbc.270.28.16514.

Crystal, R.G., Randell, S.H., Engelhardt, J.F., Voynow, J. and Sunday, M.E. 2008. Airway Epithelial Cells: Current Concepts and Challenges. *Proceedings of the American Thoracic Society* 5(7), pp. 772–777. doi: 10.1513/pats.200805-041hr.

Damann, N., Owsianik, G., Li, S., Poll, C. and Nilius, B. 2009. The calcium-conducting Ion Channel Transient Receptor Potential Canonical 6 Is Involved in Macrophage Inflammatory protein-2-induced Migration of Mouse Neutrophils. *Acta Physiologica* 195(1), pp. 3–11. doi: 10.1111/j.1748-1716.2008.01918.x.

Davis, J., Burr, Adam R., Davis, Gregory F., Birnbaumer, L. and Molkentin, Jeffery D. 2012. A TRPC6-Dependent Pathway for Myofibroblast Transdifferentiation and Wound Healing In Vivo. *Developmental Cell* 23(4), pp. 705–715. doi: 10.1016/j.devcel.2012.08.017.

de Oliveira, M.V. 2016. Animal Models of Chronic Obstructive Pulmonary Disease Exacerbations: A Review of the Current Status. *Journal of Biomedical Sciencies* 05(01). doi: 10.4172/2254-609x.100022.

Denney, L. et al. 2015. Pulmonary Epithelial Cell-Derived Cytokine TGF-β1 Is a Critical Cofactor for Enhanced Innate Lymphoid Cell Function. *Immunity* 43(5), pp. 945–958. doi: 10.1016/j.immuni.2015.10.012.

Deshmane, S.L., Kremlev, S., Amini, S. and Sawaya, B.E. 2009. Monocyte Chemoattractant Protein-1 (MCP-1): An Overview. *Journal of Interferon & Cytokine Research* 29(6), pp. 313–326. doi: 10.1089/jir.2008.0027.

Dettmer, P. 2021. Sources - The Immune System Explained. Available at: https://sites.google.com/view/sources-immunesystemexplained/.

Dietrich, A. 2019. Modulators of Transient Receptor Potential (TRP) Channels as Therapeutic Options in Lung Disease. *Pharmaceuticals* 12(1), p. 23. doi: 10.3390/ph12010023.

Diette, G.B. et al. 2012. Obstructive Lung Disease and Exposure to Burning Biomass Fuel in the Indoor Environment. *Global Heart* 7(3), pp. 265–270. Available at: https://www.ncbi.nlm.nih.gov/pmc/articles/PMC3489498/.

Duan, Z. and Luo, Y. 2021. Targeting Macrophages in Cancer Immunotherapy. *Signal Transduction and Targeted Therapy* 6(1), pp. 1–21. Available at: https://www.nature.com/articles/s41392-021-00506-6.

Esquivel, A.L., Pérez-Ramos, J., Cisneros, J., Herrera, I., Rivera-Rosales, R., Montaño, M. and Ramos, C. 2014. The Effect of Obesity and Tobacco Smoke Exposure on Inflammatory Mediators and Matrix Metalloproteinases in Rat Model. *Toxicology Mechanisms and Methods* 24(9), pp. 633–643. doi: 10.3109/15376516.2014.956911.

Fadok, V.A., Bratton, D.L., Konowal, A., Freed, P.W., Westcott, J.Y. and Henson, P.M. 1998. Macrophages That Have Ingested Apoptotic Cells in Vitro Inhibit Proinflammatory Cytokine Production through autocrine/paracrine Mechanisms Involving TGF-beta, PGE2, and PAF. *Journal of Clinical Investigation* 101(4), pp. 890–898. doi: 10.1172/jci1112.

Fang, H.-Y. et al. 2009. Hypoxia-inducible Factors 1 and 2 Are Important Transcriptional Effectors in Primary Macrophages Experiencing Hypoxia. *Blood* 114(4), pp. 844–859. doi: 10.1182/blood-2008-12-195941.

Feng, K., Quevedo, R.E., Kohrt, J.T., Oderinde, M.S., Reilly, U. and White, M.C. 2020. Late-stage Oxidative C(Sp 3)–H Methylation. *Nature* 580(7805), pp. 621–627. Available at: https://www.nature.com/articles/s41586-020-2137-8.

Fernandes, D., Bonacci, J. and Stewart, A. 2006. Extracellular Matrix, Integrins, and Mesenchymal Cell Function in the Airways. *Current Drug Targets* 7(5), pp. 567–577. doi: 10.2174/138945006776818700.

Finney-Hayward, T.K. et al. 2010. Expression of Transient Receptor Potential C6 Channels in Human Lung Macrophages. *American Journal of Respiratory Cell and Molecular Biology* 43(3), pp. 296–304. doi: 10.1165/rcmb.2008-0373oc.

Fraga Righetti, R. 2014. New Pharmacological Targets for Asthma Drug Development. *Journal of Allergy & Therapy* 05(02). doi: 10.4172/2155-6121.1000170.

Gaidt, M.M. and Hornung, V. 2017. Alternative Inflammasome Activation Enables IL-1β Release from Living Cells. *Current Opinion in Immunology* 44(PMC 2018), pp. 7–13. doi: 10.1016/j.coi.2016.10.007.

Gallinari, P., Marco, S.D., Jones, P., Pallaoro, M. and Steinkühler, C. 2007. HDACs, Histone Deacetylation and Gene transcription: from Molecular Biology to Cancer Therapeutics. *Cell Research* 17(3), pp. 195–211. Available at: https://www.nature.com/articles/7310149.

Ganesh, K. et al. 2012. Prostaglandin E2 Induces Oncostatin M Expression in Human Chronic Wound Macrophages through Axl Receptor Tyrosine Kinase Pathway. *The Journal of Immunology* 189(5), pp. 2563–2573. doi: 10.4049/jimmunol.1102762.

Ge, T., Yang, J., Zhou, S., Wang, Y., Li, Y. and Tong, X. 2020. The Role of the Pentose Phosphate Pathway in Diabetes and Cancer. *Frontiers in Endocrinology* 11(365). doi: 10.3389/fendo.2020.00365.

Geng, Y. et al. 2016. Structural Mechanism of Ligand Activation in Human calcium-sensing Receptor. *eLife* 5(e13662). Available at: https://www.ncbi.nlm.nih.gov/pmc/articles/PMC4977154/.

Ginguay, A., Cynober, L., Curis, E. and Nicolis, I. 2017. Ornithine Aminotransferase, an Important Glutamate-Metabolizing Enzyme at the Crossroads of Multiple Metabolic Pathways. *Biology* 6(4), p. 18. doi: 10.3390/biology6010018.

Gowen, M. et al. 2000. Antagonizing the Parathyroid Calcium Receptor Stimulates Parathyroid Hormone Secretion and Bone Formation in Osteopenic Rats. *Journal of Clinical Investigation* 105(11), pp. 1595–1604. doi: 10.1172/jci9038.

Gregory, K.J. et al. 2018. Dual Action Calcium-Sensing Receptor Modulator Unmasks Novel Mode-Switching Mechanism. *ACS Pharmacology & Translational Science* 1(2), pp. 96–109. doi: 10.1021/acsptsci.8b00021.

Gregory, L.G. et al. 2012. IL-25 Drives Remodelling in Allergic Airways Disease Induced by House Dust Mite. *Thorax* 68(1), pp. 82–90. doi: 10.1136/thoraxjnl-2012-202003.

Griesenauer, B. and Paczesny, S. 2017. The ST2/IL-33 Axis in Immune Cells during Inflammatory Diseases. *Frontiers in Immunology* 8(475). doi: 10.3389/fimmu.2017.00475.

Guilliams, M. et al. 2013. Alveolar Macrophages Develop from Fetal Monocytes That Differentiate into long-lived Cells in the First Week of Life via GM-CSF. *The Journal of Experimental Medicine* 210(10), pp. 1977–1992. doi: 10.1084/jem.20131199.

Gutiérrez-López, T.Y., Orduña-Castillo, L.B., Hernández-Vásquez, M.N., Vázquez-Prado, J. and Reyes-Cruz, G. 2018. Calcium Sensing Receptor Activates the NLRP3 Inflammasome via a chaperone-assisted Degradative Pathway Involving Hsp70 and LC3-II. *Biochemical and Biophysical Research Communications* 505(4), pp. 1121–1127. doi: 10.1016/j.bbrc.2018.10.028.

Haak, A.J., Ducharme, M.T., Diaz Espinosa, A.M. and Tschumperlin, D.J. 2020. Targeting GPCR Signaling for Idiopathic Pulmonary Fibrosis Therapies. *Trends in Pharmacological Sciences* 41(3), pp. 172–182. doi: 10.1016/j.tips.2019.12.008.

Halse, J. et al. 2014. A Phase 2, Randomized, Placebo-Controlled, Dose-Ranging Study of the Calcium-Sensing Receptor Antagonist MK-5442 in the Treatment of Postmenopausal Women With Osteoporosis. *The Journal of Clinical Endocrinology & Metabolism* 99(11), pp. E2207–E2215. doi: 10.1210/jc.2013-

4009.

Hammad, H., Chieppa, M., Perros, F., Willart, M.A., Germain, R.N. and Lambrecht, B.N. 2009. House Dust Mite Allergen Induces Asthma via Toll-like Receptor 4 Triggering of Airway Structural Cells. *Nature Medicine* 15(4), pp. 410–416. doi: 10.1038/nm.1946.

Handlogten, M.E., Huang, C., Shiraishi, N., Awata, H. and Miller, R.T. 2001. The Ca2+-sensing Receptor Activates Cytosolic Phospholipase A2 via a Gqα-dependent ERK-independent Pathway. *Journal of Biological Chemistry* 276(17), pp. 13941–13948. doi: 10.1074/jbc.m007306200.

Hansch, Corwin., Leo, A. and Taft, R.W. 1991. A Survey of Hammett Substituent Constants and Resonance and Field Parameters. *Chemical Reviews* 91(2), pp. 165–195. doi: 10.1021/cr00002a004.

Hart, S., Trawinska, M. and Rupesinghe, R. 2016. Patient Considerations and Drug Selection in the Treatment of Idiopathic Pulmonary Fibrosis. *Therapeutics and Clinical Risk Management* 12(PMC4833375), p. 563. doi: 10.2147/tcrm.s81144.

Hedström, U., Hallgren, O., Öberg, L., DeMicco, A., Vaarala, O., Westergren-Thorsson, G. and Zhou, X. 2018. Bronchial Extracellular Matrix from COPD Patients Induces Altered Gene Expression in Repopulated Primary Human Bronchial Epithelial Cells. *Scientific Reports* 8(1). doi: 10.1038/s41598-018-21727-w.

Heijink, I.H., Kuchibhotla, V.N.S., Roffel, M.P., Maes, T., Knight, D.A., Sayers, I. and Nawijn, M.C. 2020. Epithelial Cell dysfunction, a Major Driver of Asthma Development. *Allergy* 75(8), pp. 1902–1917. doi: 10.1111/all.14421.

Hernández-Ramírez, G. et al. 2020. Group 1 allergens, Transported by Mold spores, Induce Asthma Exacerbation in a Mouse Model. *Allergy* 75(9). doi: 10.1111/all.14347.

Higham, A., Quinn, A.M., Cançado, J.E.D. and Singh, D. 2019. The Pathology of Small Airways Disease in COPD: Historical Aspects and Future Directions. *Respiratory Research* 20(1). doi: 10.1186/s12931-019-1017-y.

Hinz, B. 2007. Formation and Function of the Myofibroblast during Tissue Repair. *Journal of Investigative Dermatology* 127(3), pp. 526–537. Available at: https://www.jidonline.org/article/S0022-202X(15)33286-3/fulltext#s0020.

Hodge, S., Hodge, G., Scicchitano, R., Reynolds, P.N. and Holmes, M. 2003. Alveolar Macrophages from Subjects with Chronic Obstructive Pulmonary Disease Are Deficient in Their Ability to Phagocytose Apoptotic Airway Epithelial Cells. *Immunology & Cell Biology* 81(4), pp. 289–296. doi: 10.1046/j.1440-1711.2003.t01-1-01170.x.

Hogan, B.L.M. et al. 2014. Repair and Regeneration of the Respiratory system: complexity, plasticity, and Mechanisms of Lung Stem Cell Function. *Cell Stem Cell* 15(2), pp. 123–38. Available at:

https://www.ncbi.nlm.nih.gov/pubmed/25105578.

Hogg, J.C. and Timens, W. 2009. The Pathology of Chronic Obstructive Pulmonary Disease. *Annual review of pathology* 4(PMID: 18954287), pp. 435–59. Available at: https://www.ncbi.nlm.nih.gov/pubmed/18954287.

Holgate, S.T. 2012. Innate and Adaptive Immune Responses in Asthma. *Nature Medicine* 18(5), pp. 673–683. doi: 10.1038/nm.2731.

Hsia, C.C.W., Hyde, D.M. and Weibel, E.R. 2016. Lung Structure and the Intrinsic Challenges of Gas Exchange. *Comprehensive Physiology* 6(2), pp. 827–895. Available at: https://www.ncbi.nlm.nih.gov/pmc/articles/PMC5026132/.

Huang, Q. et al. 2021. Role of the IL-33/ST2 Axis in Cigarette smoke-induced Airways Remodelling in Chronic Obstructive Pulmonary Disease. *Thorax* 76(8), pp. 750–762. doi: 10.1136/thoraxjnl-2020-214712.

Huang, Y. et al. 2007. Identification and Dissection of Ca2+-binding Sites in the Extracellular Domain of Ca2+-sensing Receptor. *Journal of Biological Chemistry* 282(26), pp. 19000–19010. doi: 10.1074/jbc.m701096200.

Hubbard, L.L.N. et al. 2010. A Role for IL-1 Receptor-Associated Kinase-M in Prostaglandin E2-Induced Immunosuppression Post-Bone Marrow Transplantation. *The Journal of Immunology* 184(11), pp. 6299–6308. doi: 10.4049/jimmunol.0902828.

Hung, C.-H. et al. 2018. Altered Pattern of Monocyte Differentiation and monocyte-derived TGF-β1 in Severe Asthma. *Scientific Reports* 8(1). doi: 10.1038/s41598-017-19105-z.

Hussell, T. and Bell, T.J. 2014. Alveolar macrophages: Plasticity in a tissue-specific Context. *Nature Reviews Immunology* 14(2), pp. 81–93. doi: 10.1038/nri3600.

Huynh, M.-L.N., Malcolm, K.C., Kotaru, C., Tilstra, J.A., Westcott, J.Y., Fadok, V.A. and Wenzel, S.E. 2005. Defective Apoptotic Cell Phagocytosis Attenuates Prostaglandin E2and 15-Hydroxyeicosatetraenoic Acid in Severe Asthma Alveolar Macrophages. *American Journal of Respiratory and Critical Care Medicine* 172(8), pp. 972–979. doi: 10.1164/rccm.200501-035oc.

Ito, T. et al. 2005. TSLP-activated Dendritic Cells Induce an Inflammatory T Helper Type 2 Cell Response through OX40 Ligand. *The Journal of Experimental Medicine* 202(9), pp. 1213–1223. Available at: https://www.ncbi.nlm.nih.gov/pmc/articles/PMC2213234/.

Jäger, E. et al. 2020. Calcium-sensing receptor-mediated NLRP3 Inflammasome Response to Calciprotein Particles Drives Inflammation in Rheumatoid Arthritis. *Nature Communications* 11(1). doi: 10.1038/s41467-020-17749-6.

Jaiswal, A.K. 2004. Nrf2 Signaling in Coordinated Activation of Antioxidant Gene Expression. *Free Radical Biology and Medicine* 36(10), pp. 1199–1207. doi: 10.1016/j.freeradbiomed.2004.02.074.

Jiang, X. et al. 2021. Mechanism of Action and Potential Applications of Selective Inhibition of Microsomal Prostaglandin E synthase-1-mediated PGE2 Biosynthesis by Sonlicromanol's Metabolite KH176m. *Scientific Reports* 11(1). doi: 10.1038/s41598-020-79466-w.

John, M.R. et al. 2014. AXT914 a novel, orally-active Parathyroid hormone-releasing Drug in Two Early Studies of Healthy Volunteers and Postmenopausal Women. *Bone* 64((2014)), pp. 204–210. Available at: https://reader.elsevier.com/reader/sd/pii/S8756328214001501?token=A63E50E5F171974C51AE32A2697B07F638C624924DD1263373D2C1E0D40AEBFE5D000D11DE985B83942F269009CCDCA5&originRegion=eu-west-1&originCreation=20210812061030.

Johnson, P.R.A., Burgess, J.K., Ge, Q., Poniris, M., Boustany, S., Twigg, S.M. and Black, J.L. 2006. Connective Tissue Growth Factor Induces Extracellular Matrix in Asthmatic Airway Smooth Muscle. *American Journal of Respiratory and Critical Care Medicine* 173(1), pp. 32–41. doi: 10.1164/rccm.200406-703oc.

JOHNSON, PETER R. A. et al. 2001. Airway Smooth Muscle Cell Proliferation Is Increased in Asthma. *American Journal of Respiratory and Critical Care Medicine* 164(3), pp. 474–477. doi: 10.1164/ajrccm.164.3.2010109.

Jouret, F. et al. 2013. Activation of the calcium-sensing Receptor Induces Deposition of Tight Junction Components to the Epithelial Cell Plasma Membrane. *Journal of Cell Science* 126(22), pp. 5132–5142. doi: 10.1242/jcs.127555.

Kamiide, Y., Inomata, N., Furuya, M. and Yada, T. 2015. Ghrelin Ameliorates Catabolic Conditions and Respiratory Dysfunction in a Chronic Obstructive Pulmonary Disease Model of Chronic Cigarette smoke-exposed Rats. *European Journal of Pharmacology* 755((2015)), pp. 88–94. Available at: https://reader.elsevier.com/reader/sd/pii/S0014299915001727?token=E9362F1F4F3E3A745CB69B77FC66BE09BD78BA61CB89E1A38E30BAE50C294D85AB6A133F3032180376EE0F678BB4006A&originRegion=eu-west-1&originCreation=20210812060923.

Kardas, G., Daszyńska-Kardas, A., Marynowski, M., Brząkalska, O., Kuna, P. and Panek, M. 2020. Role of Platelet-Derived Growth Factor (PDGF) in Asthma as an Immunoregulatory Factor Mediating Airway Remodeling and Possible Pharmacological Target. *Frontiers in Pharmacology* 11(1663-9812), p. 47. doi: 10.3389/fphar.2020.00047.

Kay, A.B. 2005. The Role of Eosinophils in the Pathogenesis of Asthma. *Trends in Molecular Medicine* 11(4), pp. 148–152. doi: 10.1016/j.molmed.2005.02.002.

Kolli, D., Gupta, M.R., Sbrana, E., Velayutham, T.S., Chao, H., Casola, A. and Garofalo, R.P. 2014.

Alveolar Macrophages Contribute to the Pathogenesis of Human Metapneumovirus Infection while Protecting against Respiratory Syncytial Virus Infection. *American Journal of Respiratory Cell and Molecular Biology* 51(4), pp. 502–515. doi: 10.1165/rcmb.2013-0414oc.

Kraneveld, A.D., Folkerts, G., Van Oosterhout, A.J.M. and Nijkamp, F.P. 1997. Airway hyperresponsiveness: First Eosinophils and Then Neuropeptides. *International Journal of Immunopharmacology* 19(9-10), pp. 517–527. doi: 10.1016/s0192-0561(97)00085-4.

Krüger, K., Dischereit, G., Seimetz, M., Wilhelm, J., Weissmann, N. and Mooren, F.C. 2015. Time Course of Cigarette smoke-induced Changes of Systemic Inflammation and Muscle Structure. *American Journal of Physiology-Lung Cellular and Molecular Physiology* 309(2), pp. L119–L128. doi: 10.1152/ajplung.00074.2015.

Kumar, S. et al. 2010. An Orally Active calcium-sensing Receptor Antagonist That Transiently Increases Plasma Concentrations of PTH and Stimulates Bone Formation. *Bone* 46(2), pp. 534–542. doi: 10.1016/j.bone.2009.09.028.

Kurosawa, M., Shimizu, Y., Tsukagoshi, H. and Ueki, M. 1992. Elevated Levels of peripheral-blood, Naturally Occurring Aliphatic Polyamines in Bronchial Asthmatic Patients with Active Symptoms. *Allergy* 47(6), pp. 638–643. doi: 10.1111/j.1398-9995.1992.tb02388.x.

LaRock, C.N. and Cookson, B.T. 2013. Burning Down the House: Cellular Actions during Pyroptosis. Miller, V. ed. *PLoS Pathogens* 9(12), p. e1003793. doi: 10.1371/journal.ppat.1003793.

Lauweryns, J.M., Van Lommel, A.T. and Dom, R.J. 1985. Innervation of Rabbit Intrapulmonary Neuroepithelial Bodies. *Journal of the Neurological Sciences* 67(1), pp. 81–92. doi: 10.1016/0022-510x(85)90024-3.

Leach, K. et al. 2016. Towards a Structural Understanding of Allosteric Drugs at the Human calcium-sensing Receptor. *Cell Research* 26(5), pp. 574–592. doi: 10.1038/cr.2016.36.

Leach, K. et al. 2020. International Union of Basic and Clinical Pharmacology. CVIII. Calcium-Sensing Receptor Nomenclature, Pharmacology, and Function. Ohlstein, E. H. ed. *Pharmacological Reviews* 72(3), pp. 558–604. doi: 10.1124/pr.119.018531.

Lee, J.-W. et al. 2016. NPS2143 Inhibits MUC5AC and Proinflammatory Mediators in Cigarette Smoke Extract (CSE)-Stimulated Human Airway Epithelial Cells. *Inflammation* 40(1), pp. 184–194. doi: 10.1007/s10753-016-0468-2.

Lee, S.-H. et al. 2007. Antielastin Autoimmunity in Tobacco Smoking–induced Emphysema. *Nature Medicine* 13(5), pp. 567–569. doi: 10.1038/nm1583.

Lembrechts, R. et al. 2013. Functional Expression of the Multimodal Extracellular calcium-sensing Receptor in Pulmonary Neuroendocrine Cells. *Journal of Cell Science* 126(19), pp. 4490–4501. doi:

10.1242/jcs.131656.

Leung, C.S., Leung, S.S.F., Tirado-Rives, J. and Jorgensen, W.L. 2012. Methyl Effects on Protein–Ligand Binding. *Journal of Medicinal Chemistry* 55(9), pp. 4489–4500. doi: 10.1021/jm3003697.

Li, C. et al. 2019. miR-429 and miR-424-5p Inhibit Cell Proliferation and Ca2+ Influx by Downregulating CaSR in Pulmonary Artery Smooth Muscle Cells. *American Journal of Physiology-Cell Physiology* 316(1), pp. C111–C120. doi: 10.1152/ajpcell.00219.2018.

Li, T., Wang, G., Hui, V.C.C., Saad, D., de Sousa Valente, J., La Montanara, P. and Nagy, I. 2021. TRPV1 feed-forward Sensitisation Depends on COX2 Upregulation in Primary Sensory Neurons. *Scientific Reports* 11(1). doi: 10.1038/s41598-021-82829-6.

Liao, X. et al. 2011. Krüppel-like Factor 4 Regulates Macrophage Polarization. *Journal of Clinical Investigation* 121(7), pp. 2736–2749. doi: 10.1172/jci45444.

Licona-Limón, P., Kim, L.K., Palm, N.W. and Flavell, R.A. 2013. TH2, Allergy and Group 2 Innate Lymphoid Cells. *Nature Immunology* 14(6), pp. 536–542. doi: 10.1038/ni.2617.

Lin, C.-C., Lin, W.-N., Cho, R.-L., Wang, C., Hsiao, L.-D. and Yang, C.-M. 2016. TNF-α-Induced cPLA2 Expression via NADPH Oxidase/Reactive Oxygen Species-Dependent NF-κB Cascade on Human Pulmonary Alveolar Epithelial Cells. *Frontiers in Pharmacology* 7(447). doi: 10.3389/fphar.2016.00447.

Lin, K.-M. . et al. 2013. IRAK-1 Bypasses Priming and Directly Links TLRs to Rapid NLRP3 Inflammasome Activation. *Proceedings of the National Academy of Sciences* 111(2), pp. 775–780. doi: 10.1073/pnas.1320294111.

Lindemann, O. et al. 2013. TRPC6 Regulates CXCR2-Mediated Chemotaxis of Murine Neutrophils. *The Journal of Immunology* 190(11), pp. 5496–5505. doi: 10.4049/jimmunol.1201502.

Lindskog, C. 2019. Normal: Lung - The Human Protein Atlas. Available at: https://www.proteinatlas.org/learn/dictionary/normal/lung.

Liu, G., Cao, W., Jia, G., Zhao, H., Chen, X. and Wang, J. 2018. Calcium-sensing Receptor in Nutrient sensing: an Insight into the Modulation of Intestinal Homoeostasis. *British Journal of Nutrition* 120(8), pp. 881–890. doi: 10.1017/s0007114518002088.

Lodish, H.F. 2012. *Molecular Cell Biology*. 7th ed. New York: W.H. Freeman-Macmillan Learning.

Lorenz, R.J. 1966. Weibel, E. R.: Morphometry of the Human Lung. Springer Verlag, Berlin-Göttingen-Heidelberg 1963; 151 S., 109 Abb., DM 36,-. *Biometrische Zeitschrift* 8(1-2), pp. 143–144. doi: 10.1002/bimj.19660080155.

Louahed, J. et al. 2001. Interleukin 9 Promotes Influx and Local Maturation of Eosinophils. *Blood* 97(4),

pp. 1035–1042. doi: 10.1182/blood.v97.4.1035.

Luan, B., Yoon, Y.-S., Le Lay, J., Kaestner, K.H., Hedrick, S. and Montminy, M. 2015. CREB Pathway Links PGE2 Signaling with Macrophage Polarization. *Proceedings of the National Academy of Sciences* 112(51), pp. 15642–15647. doi: 10.1073/pnas.1519644112.

Lumsden, A.B., McLean, A. and Lamb, D. 1984. Goblet and Clara Cells of Human Distal airways: Evidence for Smoking Induced Changes in Their numbers. *Thorax* 39(11), pp. 844–849. doi: 10.1136/thx.39.11.844.

Lv, J. et al. 2018. Airway Epithelial TSLP Production of TLR2 Drives Type 2 Immunity in Allergic Airway Inflammation. *European Journal of Immunology* 48(11), pp. 1838–1850. doi: 10.1002/eji.201847663.

Maarsingh, H., Zaagsma, J. and Meurs, H. 2008. Arginine Homeostasis in Allergic Asthma. *European Journal of Pharmacology* 585(2-3), pp. 375–384. doi: 10.1016/j.ejphar.2008.02.096.

Mansfield, B. et al. 2019. Calcium-sensing Receptor (CaSR) Antagonists (calcilytics) Prevent Urban Particulate Matter (UPM)-induced Dendritic Cell Activation. *Airway Cell Biology and Immunopathology* 54(63). doi: 10.1183/13993003.congress-2019.pa2401.

Mansfield, B. et al. 2020. Calcium-sensing Receptor antagonists, calcilytics, Prevent Activation of Human Dendritic and Epithelial Cells by Urban Particulate Matter. *Airway Cell Biology and Immunopathology* 56(Suppl. 64, 1970). doi: 10.1183/13993003.congress-2020.1970.

Marciniuk, D., Schraufnagel, D., Ferkol, T., Fong, K., Joos, G., López Varela, V. and Zar, H. 2017. *The Global Impact of Respiratory Disease*. Second Edition: Forum of International Respiratory Societies. Available at: https://www.who.int/gard/publications/The_Global_Impact_of_Respiratory_Disease.pdf.

Margaritopoulos, G.A. et al. 2018. Pirfenidone Improves Survival in IPF: Results from a real-life Study. *BMC Pulmonary Medicine* 18(1). doi: 10.1186/s12890-018-0736-z.

Marquis, R.W. et al. 2009. Antagonists of the Calcium Receptor I. Amino Alcohol-Based Parathyroid Hormone Secretagogues. *Journal of Medicinal Chemistry* 52(13), pp. 3982–3993. doi: 10.1021/jm900364m.

Martin, L.D., Krunkosky, T.M., Voynow, J.A. and Adler, K.B. 1998. The Role of Reactive Oxygen and Nitrogen Species in Airway Epithelial Gene Expression. *Environmental Health Perspectives* 106(Suppl. 5), pp. 1197–1203. doi: 10.2307/3433986.

Matthews, N.C., Pfeffer, P.E., Mann, E.H., Kelly, F.J., Corrigan, C.J., Hawrylowicz, C.M. and Lee, T.H. 2016. Urban Particulate Matter–Activated Human Dendritic Cells Induce the Expansion of Potent Inflammatory Th1, Th2, and Th17 Effector Cells. *American Journal of Respiratory Cell and Molecular Biology* 54(2), pp. 250–262. doi: 10.1165/rcmb.2015-0084oc.

Mills, C.D., Kincaid, K., Alt, J.M., Heilman, M.J. and Hill, A.M. 2000. M-1/M-2 Macrophages and the Th1/Th2 Paradigm. *Journal of Immunology* 164(12), pp. 6166–73. Available at: https://www.ncbi.nlm.nih.gov/pubmed/10843666.

Minas, M., Mystridou, P., Georgoulias, P., Pournaras, S., Kostikas, K. and Gourgoulianis, K.I. 2012. Fetuin-A is Associated with Disease Severity and Exacerbation Frequency in Patients with COPD. *COPD: Journal of Chronic Obstructive Pulmonary Disease* 10(1), pp. 28–34. doi: 10.3109/15412555.2012.727922.

Monie, T.P. and Bryant, C.E. 2015. Caspase-8 Functions as a Key Mediator of Inflammation and pro-IL-1β Processing via Both Canonical and non-canonical Pathways. *Immunological Reviews* 265(1), pp. 181–193. doi: 10.1111/imr.12284.

Morimoto, K., Janssen, W.J. and Terada, M. 2012. Defective Efferocytosis by Alveolar Macrophages in IPF Patients. *Respiratory Medicine* 106(12), pp. 1800–1803. doi: 10.1016/j.rmed.2012.08.020.

Neergaard, K. 1929. Neue Auffassungen über einen Grundbegriff der Atemmechanik. *Zeitschrift für Die Gesamte Experimentelle Medizin* 66(1), pp. 373–394. doi: 10.1007/bf02621963.

Nemeth, E. et al. 2001. Calcilytic Compounds: Potent and Selective Ca2+Receptor Antagonists That Stimulate Secretion of Parathyroid Hormone. *Journal of Pharmacology and Experimental Therapeutics* 299(1), pp. 323–331.

Nemeth, E.F., Steffey, M.E., Hammerland, L.G., Hung, B.C.P., Van Wagenen, B.C., DelMar, E.G. and Balandrin, M.F. 1998. Calcimimetics with Potent and Selective Activity on the Parathyroid Calcium Receptor. *Proceedings of the National Academy of Sciences* 95(7), pp. 4040–4045. doi: 10.1073/pnas.95.7.4040.

Niederman, M.S. 2018. Pneumonia Complicating COPD: Are Corticosteroids a Help or a Hindrance? *Chronic Obstructive Pulmonary Diseases: Journal of the COPD Foundation* 5(1), pp. 1–4. doi: 10.15326/jcopdf.5.1.2018.0162.

Nilsson, B.O. and Strand, P.H. 1993. Effects of Polyamines on Intracellular Calcium and Mechanical Activity in Smooth Muscle of guinea-pig Taenia Coli. *Acta Physiologica Scandinavica* 148(1), pp. 37–43. doi: 10.1111/j.1748-1716.1993.tb09529.x.

Noguchi, M., Furukawa, K.T. and Morimoto, M. 2020. Pulmonary Neuroendocrine cells: physiology, Tissue Homeostasis and Disease. *Disease Models & Mechanisms* 13(12), p. dmm046920. doi: 10.1242/dmm.046920.

North, M.L., Grasemann, H., Khanna, N., Inman, M.D., Gauvreau, G.M. and Scott, J.A. 2013. Increased Ornithine-Derived Polyamines Cause Airway Hyperresponsiveness in a Mouse Model of Asthma. *American Journal of Respiratory Cell and Molecular Biology* 48(6), pp. 694–702. doi:

10.1165/rcmb.2012-0323oc.

Oberacker, P. et al. 2019. Bio-On-Magnetic-Beads (BOMB): Open platform for high-throughput nucleic acid extraction and manipulation. *PLOS Biology* 17(1), p. e3000107. doi: 10.1371/journal.pbio.3000107.

Ogata, S., Kubota, Y., Satoh, S., Ito, S., Takeuchi, H., Ashizuka, M. and Shirasuna, K. 2006. Ca2+ stimulates COX-2 expression through calcium-sensing receptor in fibroblasts. *Biochemical and Biophysical Research Communications* 351(4), pp. 808–814. doi: 10.1016/j.bbrc.2006.10.098.

Ohta, Y., Hayashi, M., Kanemaru, T., Abe, K., Ito, Y. and Oike, M. 2008. Dual Modulation of Airway Smooth Muscle Contraction by Th2 Cytokines via Matrix Metalloproteinase-1 Production. *The Journal of Immunology* 180(6), pp. 4191–4199. doi: 10.4049/jimmunol.180.6.4191.

Ordoñez, C.L. et al. 2001. Mild and Moderate Asthma Is Associated with Airway Goblet Cell Hyperplasia and Abnormalities in Mucin Gene Expression. *American Journal of Respiratory and Critical Care Medicine* 163(2), pp. 517–523. Available at: https://www.ncbi.nlm.nih.gov/pubmed/11179133.

Palmans, E., Pauwels, R.A. and Kips, J.C. 2002. Repeated Allergen Exposure Changes Collagen Composition in Airways of Sensitised Brown Norway Rats. *European Respiratory Journal* 20(2), pp. 280–285. doi: 10.1183/09031936.02.00255402.

Park, J.Y., Pillinger, M.H. and Abramson, S.B. 2006. Prostaglandin E2 Synthesis and secretion: the Role of PGE2 Synthases. *Clinical Immunology* 119(3), pp. 229–240. Available at: https://www.sciencedirect.com/science/article/abs/pii/S1521661606000453?via%3Dihub.

Pilcer, G. and Amighi, K. 2010. Formulation Strategy and Use of Excipients in Pulmonary Drug Delivery. *International Journal of Pharmaceutics* 392(1-2), pp. 1–19. doi: 10.1016/j.ijpharm.2010.03.017.

Pilcer, G., Wauthoz, N. and Amighi, K. 2012. Lactose Characteristics and the Generation of the Aerosol. *Advanced Drug Delivery Reviews* 64(3), pp. 233–256. doi: 10.1016/j.addr.2011.05.003.

Porsbjerg, C.M., Sverrild, A., Lloyd, C.M., Menzies-Gow, A.N. and Bel, E.H. 2020. Anti-alarmins in asthma: Targeting the Airway Epithelium with next-generation Biologics. *European Respiratory Journal* 56(5), p. 2000260. doi: 10.1183/13993003.00260-2020.

Possa, S.S., Leick, E.A., Prado, C.M., Martins, M.A. and Tibério, I.F.L.C. 2013. Eosinophilic Inflammation in Allergic Asthma. *Frontiers in Pharmacology* 4(46). doi: 10.3389/fphar.2013.00046.

Quinn, S.J., Ye, C.-P., Diaz, R., Kifor, O., Bai, M., Vassilev, P. and Brown, E. 1997. The Ca2+-sensing receptor: a Target for Polyamines. *American Journal of Physiology-Cell Physiology* 273(4), pp. C1315–C1323. doi: 10.1152/ajpcell.1997.273.4.c1315.

Raghu, G. et al. 2015. An Official ATS/ERS/JRS/ALAT Clinical Practice Guideline: Treatment of Idiopathic Pulmonary Fibrosis. An Update of the 2011 Clinical Practice Guideline. *American Journal of*

Respiratory and Critical Care Medicine 192(2), pp. e3–e19. doi: 10.1164/rccm.201506-1063st.

Rehan, M. et al. 2021. Restoration of SIRT3 Gene Expression by Airway Delivery Resolves age-associated Persistent Lung Fibrosis in Mice. *Nature Aging* 1(2), pp. 205–217. doi: 10.1038/s43587-021-00027-5.

Riccardi, D. 2016. *Inhaled calcilytics: Effects on Airway Inflammation and remodeling. Respiratory Drug Delivery 1*., pp. 1–12. Available at: http://orca.cf.ac.uk/106160/1/Inhaled%20Calcilytics-%20Effects%20on%20Airway%20Inflammation%20and%20Remodeling%20%20.pdf.

Riccardi, D., Brancale, A., Ferla, S., Schepelmann, M. and Yarova, P. 2017. *Discovery and Development of a Novel Therapeutic for the Treatment of Inflammatory Lung Disorders*.

Riccardi, D., Brennan, S.C. and Chang, W. 2013. The Extracellular calcium-sensing receptor, CaSR, in Fetal Development. *Best Practice & Research Clinical Endocrinology & Metabolism* 27(3), pp. 443–453. doi: 10.1016/j.beem.2013.02.010.

Riccardi, D. and Brown, E.M. 2010. Physiology and Pathophysiology of the calcium-sensing Receptor in the Kidney. *American Journal of Physiology-Renal Physiology* 298(3), pp. F485–F499. doi: 10.1152/ajprenal.00608.2009.

Riccardi, D. and Kemp, P.J. 2012. The Calcium-Sensing Receptor Beyond Extracellular Calcium Homeostasis: Conception, Development, Adult Physiology, and Disease. *Annual Review of Physiology* 74(1), pp. 271–297. doi: 10.1146/annurev-physiol-020911-153318.

Riley, C.M. and Sciurba, F.C. 2019. Diagnosis and Outpatient Management of Chronic Obstructive Pulmonary Disease. *JAMA* 321(8), p. 786. doi: 10.1001/jama.2019.0131.

Risse, P.-A. et al. 2011. Interleukin-13 Inhibits Proliferation and Enhances Contractility of Human Airway Smooth Muscle Cells without Change in Contractile Phenotype. *American Journal of Physiology-Lung Cellular and Molecular Physiology* 300(6), pp. L958–L966. doi: 10.1152/ajplung.00247.2010.

Roberts, M.S. et al. 2019. Treatment of Autosomal Dominant Hypocalcemia Type 1 With the Calcilytic NPSP795 (SHP635). *Journal of Bone and Mineral Research* 34(9), pp. 1609–1618. doi: 10.1002/jbmr.3747.

Robins, A.G. 1983. Pathophysiology of Emphysema. *Clinics in Chest Medicine* 4(3), pp. 413–420. doi: 10.1016/s0272-5231(21)00217-3.

Roesler, A.M. et al. 2021. Calcium-Sensing Receptor Contributes to Hyperoxia Effects on Human Fetal Airway Smooth Muscle. *Frontiers in Physiology* 12(585895). doi: 10.3389/fphys.2021.585895.

Rossol, M. et al. 2012. Extracellular Ca2+ Is a Danger Signal Activating the NLRP3 Inflammasome through G protein-coupled Calcium Sensing Receptors. *Nature Communications* 3(1). doi:

10.1038/ncomms2339.

Roth, F.D., Quintar, A.A., Leimgruber, C., García, L., Uribe Echevarría, E.M., Torres, A.I. and Maldonado, C.A. 2013. Restoration of the Normal Clara Cell Phenotype after Chronic Allergic Inflammation. *International Journal of Experimental Pathology* 94(6), pp. 399–411. doi: 10.1111/iep.12041.

Rudloff, S., Janot, M., Rodriguez, S., Dessalle, K., Jahnen-Dechent, W. and Huynh-Do, U. 2021. Fetuin-A Is a HIF Target That Safeguards Tissue Integrity during Hypoxic Stress. *Nature Communications* 12(1). doi: 10.1038/s41467-020-20832-7.

Rybchyn, M.S. et al. 2019. Homer1 Mediates CaSR-dependent Activation of mTOR Complex 2 and Initiates a Novel Pathway for AKT-dependent β-catenin Stabilization in Osteoblasts. *Journal of Biological Chemistry* 294(44), pp. 16337–16350. doi: 10.1074/jbc.ra118.006587.

Sadowska, A.M., Verbraecken, J., Darquennes, K. and Backer, W.D. 2006. Role of N-acetylcysteine in the Management of COPD. *International Journal of COPD* 1(4), pp. 425–434. doi: 10.2147/copd.2006.1.4.425.

Saito, A., Horie, M. and Nagase, T. 2018. TGF-β Signaling in Lung Health and Disease. *International Journal of Molecular Sciences* 19(8), p. 2460. Available at: https://www.mdpi.com/1422-0067/19/8/2460.

Scaffidi, A.K., Moodley, Y.P., Weichselbaum, M., Thompson, P.J. and Knight, D.A. 2001. Regulation of Human Lung Fibroblast Phenotype and Function by Vitronectin and Vitronectin Integrins. *Journal of Cell Science* 114(19), pp. 3507–3516. Available at: http://jcs.biologists.org/content/114/19/3507.long.

Schepelmann, M. et al. 2016. The Vascular Ca2+-sensing Receptor Regulates Blood Vessel Tone and Blood Pressure. *American Journal of Physiology-Cell Physiology* 310(3), pp. C193–C204. doi: 10.1152/ajpcell.00248.2015.

Schmitz, J. et al. 2005. IL-33, an Interleukin-1-like Cytokine that Signals via the IL-1 Receptor-Related Protein ST2 and Induces T Helper Type 2-Associated Cytokines. *Immunity* 23(5), pp. 479–490. doi: 10.1016/j.immuni.2005.09.015.

Sehnal, D. et al. 2021. Mol* Viewer: Modern Web App for 3D Visualization and Analysis of Large Biomolecular Structures. *Nucleic Acids Research* 49(W1). doi: 10.1093/nar/gkab314.

Sekiguchi, R. and Yamada, K.M. 2018. Basement Membranes in Development and Disease. *Current Topics in Developmental Biology* 130(PMC 2019), pp. 143–191. Available at: https://www.ncbi.nlm.nih.gov/pmc/articles/PMC6701859/.

Sgalla, G., Iovene, B., Calvello, M., Ori, M., Varone, F. and Richeldi, L. 2018. Idiopathic Pulmonary fibrosis: Pathogenesis and Management. *Respiratory Research* 19(1). doi: 10.1186/s12931-018-0730-2.

Sirianni, F.E., Chu, F.S.F. and Walker, D.C. 2003. Human Alveolar Wall Fibroblasts Directly Link Epithelial Type 2 Cells to Capillary Endothelium. *American Journal of Respiratory and Critical Care Medicine* 168(12), pp. 1532–1537. doi: 10.1164/rccm.200303-371oc.

Smith, J.N.P., Witkin, M.D., Jogasuria, A.P., Christo, K.F., Raffay, T.M., Markowitz, S.D. and Desai, A.B. 2020. Therapeutic targeting of 15-PGDH in murine pulmonary fibrosis. *Scientific Reports* 10(1). doi: 10.1038/s41598-020-68336-0.

Smith, M., Dalurzo, M., Panse, P., Parish, J. and Leslie, K. 2013. Usual Interstitial pneumonia-patternfibrosis in Surgical Lung biopsies. Clinical, Radiological and Histopathological Clues to Aetiology. *Journal of Clinical Pathology* 66(10), pp. 896–903. Available at: https://www.ncbi.nlm.nih.gov/pmc/articles/PMC3786616/.

Stewart, J.P., Usherwood, E.J., Ross, A., Dyson, H. and Nash, T. 1998. Lung Epithelial Cells Are a Major Site of Murine Gammaherpesvirus Persistence. *Journal of Experimental Medicine* 187(12), pp. 1941–1951. doi: 10.1084/jem.187.12.1941.

Sugiura, H. et al. 2007. Cultured Lung Fibroblasts from Ovalbumin-Challenged “Asthmatic” Mice Differ Functionally from Normal. *American Journal of Respiratory Cell and Molecular Biology* 37(4), pp. 424–430. doi: 10.1165/rcmb.2007-0089oc.

Sui, P. et al. 2018. Pulmonary Neuroendocrine Cells Amplify Allergic Asthma Responses. *Science* 360(6393), p. eaan8546. doi: 10.1126/science.aan8546.

Suissa, S., Patenaude, V., Lapi, F. and Ernst, P. 2013. Inhaled Corticosteroids in COPD and the Risk of Serious Pneumonia. *Thorax* 68(11), pp. 1029–1036. doi: 10.1136/thoraxjnl-2012-202872.

Tang, H. et al. 2010. The T Helper Type 2 Response to Cysteine Proteases Requires Dendritic Cell–basophil Cooperation via ROS-mediated Signaling. *Nature Immunology* 11(7), pp. 608–617. doi: 10.1038/ni.1883.

Tang, H. et al. 2016. Pathogenic Role of calcium-sensing Receptors in the Development and Progression of Pulmonary Hypertension. *American Journal of Physiology-Lung Cellular and Molecular Physiology* 310(9), pp. L846–L859. doi: 10.1152/ajplung.00050.2016.

Taraseviciene-Stewart, L. 2006. Mechanisms of Autoimmune Emphysema. *Proceedings of the American Thoracic Society* 3(6), pp. 486a487. doi: 10.1513/pats.200603-063ms.

Temann, U.-A., Geba, G.P., Rankin, J.A. and Flavell, R.A. 1998. Expression of Interleukin 9 in the Lungs of Transgenic Mice Causes Airway Inflammation, Mast Cell Hyperplasia, and Bronchial Hyperresponsiveness. *Journal of Experimental Medicine* 188(7), pp. 1307–1320. doi: 10.1084/jem.188.7.1307.

Van Heeke, G., Allosery, K., De Brabandere, V., De Smedt, T., Detalle, L. and de Fougerolles, A. 2017.

Nanobodies® Nanobody Is a Registered Trademark of Ablynx NV. as Inhaled Biotherapeutics for Lung Diseases. *Pharmacology & Therapeutics* 169((2017)), pp. 47–56. doi: 10.1016/j.pharmthera.2016.06.012.

van Panhuys, N., Prout, M., Forbes, E., Min, B., Paul, W.E. and Le Gros, G. 2011. Basophils Are the Major Producers of IL-4 during Primary Helminth Infection. *The Journal of Immunology* 186(5), pp. 2719–2728. doi: 10.4049/jimmunol.1000940.

Vancheri, C., Failla, M., Crimi, N. and Raghu, G. 2010. Idiopathic pulmonary fibrosis: a disease with similarities and links to cancer biology. *European Respiratory Journal* 35(3), pp. 496–504. doi: 10.1183/09031936.00077309.

Vareille, M., Kieninger, E., Edwards, M.R. and Regamey, N. 2011. The Airway Epithelium: Soldier in the Fight against Respiratory Viruses. *Clinical Microbiology Reviews* 24(3), pp. 631–631. doi: 10.1128/cmr.00012-11.

Venkayya, R., Lam, M., Willkom, M., Grünig, G., Corry, D.B. and Erle, D.J. 2002. The Th2 Lymphocyte Products IL-4 and IL-13 Rapidly Induce Airway Hyperresponsiveness Through Direct Effects on Resident Airway Cells. *American Journal of Respiratory Cell and Molecular Biology* 26(2), pp. 202–208. doi: 10.1165/ajrcmb.26.2.4600.

Vlahos, R. and Bozinovski, S. 2014. Recent Advances in pre-clinical Mouse Models of COPD. *Clinical Science* 126(4), pp. 253–265. Available at: http://www.clinsci.org/content/126/4/253.full.

Wadsworth, S., Sin, D. and Dorscheid, D. 2011. Clinical Update on the Use of Biomarkers of Airway Inflammation in the Management of Asthma. *Journal of Asthma and Allergy* 4(77-86), p. 77. doi: 10.2147/jaa.s15081.

Walter, D.M., McIntire, J.J., Berry, G., McKenzie, A.N.J., Donaldson, D.D., DeKruyff, R.H. and Umetsu, D.T. 2001. Critical Role for IL-13 in the Development of Allergen-Induced Airway Hyperreactivity. *The Journal of Immunology* 167(8), pp. 4668–4675. doi: 10.4049/jimmunol.167.8.4668.

Wang, A. et al. 2021. Inhibition of GABRP Reduces the Differentiation of Airway Epithelial Progenitor Cells into Goblet Cells. *Experimental and Therapeutic Medicine* 22(1). doi: 10.3892/etm.2021.10152.

Wark, P.A.B., Johnston, S.L., Moric, I., Simpson, J.L., Hensley, M.J. and Gibson, P.G. 2001. Neutrophil Degranulation and Cell Lysis Is Associated with Clinical Severity in virus-induced Asthma. *European Respiratory Journal* 19(1), pp. 68–75. doi: 10.1183/09031936.02.00226302.

Weissmann, N. et al. 2012. Activation of TRPC6 Channels Is Essential for Lung Ischaemia–reperfusion Induced Oedema in Mice. *Nature Communications* 3(1). Available at: https://www.ncbi.nlm.nih.gov/pmc/articles/PMC3272568/.

Wells, N., Roesler, A., Ravix, J., Teske, J., Pabelick, C. and Prakash, Y. 2020. Mechanical Stretch

Contributes to Airway Hyperresponsiveness and Remodeling in Human Fetal Airway Smooth Muscle Cells via the Calcium Sensing Receptor. *Am J Respir Crit Care Med* 201(A1254)

Widler, L. et al. 2010. 1-Alkyl-4-phenyl-6-alkoxy-1H-quinazolin-2-ones: A Novel Series of Potent Calcium-Sensing Receptor Antagonists. *Journal of Medicinal Chemistry* 53(5), pp. 2250–2263. doi: 10.1021/jm901811v.

Wolffs, K. et al. 2020. Calcium-sensing Receptor Antagonism as a Novel Therapeutic for Pulmonary Fibrosis. *medRxiv* . Available at: https://www.medrxiv.org/content/medrxiv/early/2020/03/16/2020.03.12.20034751.full.pdf.

Yamaguchi, M. et al. 1997. IgE Enhances Mouse Mast Cell FcεRI Expression in Vitro and in Vivo: Evidence for a Novel Amplification Mechanism in IgE-dependent Reactions. *Journal of Experimental Medicine* 185(4), pp. 663–672. Available at: https://rupress.org/jem/article-pdf/185/4/663/1110857/5422.pdf.

Yarova, P.L. et al. 2015. Calcium-sensing Receptor Antagonists Abrogate Airway Hyperresponsiveness and Inflammation in Allergic Asthma. *Science Translational Medicine* 7(284), pp. 284ra60–284ra60. doi: 10.1126/scitranslmed.aaa0282.

Yarova, P.L. et al. 2016. Inhaled calcilytics: Effects on Airway Inflammation and Remodeling. *Respiratory Drug Delivery* 1, pp. 1–12. Available at: https://docplayer.net/205052600-Inhaled-calcilytics-effects-on-airway-inflammation-and-remodeling.html.

Yarova, P.L. et al. 2021. Characterisation of Negative Allosteric Modulators of the calcium-sensing receptor, CaSR, for Repurposing as a Treatment for Asthma. *Journal of Pharmacology and Experimental Therapeutics* 376(1), pp. 51–63. doi: 10.1124/jpet.120.000281.

Yeretssian, G., Labbé, K. and Saleh, M. 2008. Molecular Regulation of Inflammation and Cell Death. *Cytokine* 43(3), pp. 380–390. doi: 10.1016/j.cyto.2008.07.015.

Yoshimoto, T., Yasuda, K., Tanaka, H., Nakahira, M., Imai, Y., Fujimori, Y. and Nakanishi, K. 2009. Basophils Contribute to TH2-IgE Responses in Vivo via IL-4 Production and Presentation of peptide–MHC Class II Complexes to CD4+ T Cells. *Nature Immunology* 10(7), pp. 706–712. doi: 10.1038/ni.1737.

Yurchenco, P.D. 2010. Basement Membranes: Cell Scaffoldings and Signaling Platforms. *Cold Spring Harbor Perspectives in Biology* 3(2), pp. a004911–a004911. doi: 10.1101/cshperspect.a004911.

Zeng, X. et al. 2017. Hypoxia-Induced Mitogenic Factor Acts as a Nonclassical Ligand of Calcium-Sensing Receptor, Therapeutically Exploitable for Intermittent Hypoxia-Induced Pulmonary Hypertension. *Hypertension* 69(5), pp. 844–854. doi: 10.1161/hypertensionaha.116.08743.

Zhang, L., Wang, Y., Wu, G., Xiong, W., Gu, W. and Wang, C.-Y. 2018. Macrophages: Friend or Foe in

Idiopathic Pulmonary fibrosis? *Respiratory Research* 19(1). Available at: https://www.ncbi.nlm.nih.gov/pmc/articles/PMC6127991/.